DEPARTMENT OF MECHANICAL ENGINEERING AND MECHANICS
SCHOOL OF ENGINEERING
OLD DOMINION UNIVERSITY
NORFOLK, VIRGINIA

ACCURATE EVALUATION OF HOMOGENEOUS AND NONHOMOGENEOUS GAS EMISSIVITIES

By

S. N. Tiwari, Principal Investigator

and

K. P. Lee

A Supplement to the Final Report
For the period ending July 31, 1983

Prepared for the
National Aeronautics and Space Administration
Langley Research Center
Hampton, Virginia 23665

Under
Research Grant NAG-1-21
John T. Suttles, Technical Monitor

January 1984

DEPARTMENT OF MECHANICAL ENGINEERING AND MECHANICS
SCHOOL OF ENGINEERING
OLD DOMINION UNIVERSITY
NORFOLK, VIRGINIA

ACCURATE EVALUATION OF HOMOGENEOUS AND NONHOMOGENEOUS GAS EMISSIVITIES

By

S. N. Tiwari, Principal Investigator

and

K. P. Lee

A Supplement to the Final Report
For the period ending July 31, 1983

Prepared for the
National Aeronautics and Space Administration
Langley Research Center
Hampton, Virginia 23665

Under
Research Grant NAG-1-21
John T. Suttles, Technical Monitor

Submitted by the
Old Dominion University Research Foundation
P. O. Box 6369
Norfolk, Virginia 23508

January 1984

FOREWORD

This is a supplement to the report "Analysis of Longwave Radiation for the Earth-Atmosphere System." The work was done under the project "Radiative Transfer Models for the Earth Radiation Budget Studies." The work was supported by the NASA/Langley Research Center through the grant NAG-1-21. The grant was monitored by Dr. John T. Suttles of the Radiation Sciences Branch (Atmospheric Sciences Division), Mail Stop 420.

TABLE OF CONTENTS

	Page
LIST OF TABLES	v
LIST OF FIGURES	vii
LIST OF SYMBOLS	x
Chapter	
1. INTRODUCTION	1
2. THEORETICAL FORMULATION	4
2.1 Homogeneous Gas Emissivities	4
2.2 Nonhomogeneous Gas Emissivities	6
3. BAND MODELS AND CORRELATIONS	9
3.1 Direct Integration Model	9
3.2 Narrow Band Models	10
3.3 Wide Band Models	18
3.4 Band Model Correlations	19
4. PHYSICAL CONDITIONS AND DATA SOURCES	27
5. RESULTS AND DISCUSSIONS	31
5.1 Homogeneous Results for CO_2	31
5.2 Homogeneous Results for H_2O	61
5.3 Homogeneous Results for $CO_2 + H_2O$	90
5.4 Nonhomogeneous Results	100
6. CONCLUSION	105
REFERENCES	107
APPENDICES	
A. EXPLANATION OF SYMBOLS USED IN COMPUTER PROGRAMS	112
B. QUASI-RANDOM BAND MODEL COMPUTER PROGRAM	116

TABLE OF CONTENTS - CONCLUDED

Page

APPENDICES (Concluded)

C. COMPUTER PROGRAM TO CALCULATE NONHOMOGENEOUS BAND ABSORPTION AND BAND EMISSION..... 121

LIST OF TABLES

Table		Page
3.1	Band absorption correlation by Edwards and Menard for isothermal gas	20
3.2	Band absorption correlation by Edwards and Balakrishnan for isothermal gas	21
4.1	Significant band regions	28
4.2	Exponential wide-band parameters	30
5.1	Comparison of total band absorptance for the 15μ CO_2 band at T=300 K	34
5.2	Comparison of total band absorptance for the 15μ CO_2 band at T=555 K	35
5.3	Comparison of total band absorptance for the 15μ CO_2 band at T=833 K	36
5.4	Comparison of total band absorptance for the 15μ CO_2 band at T=1110 K	37
5.5	Comparison of total band absorptance for the 4.3μ CO_2 band at T=300 K	42
5.6	Comparison of total band absorptance for the 4.3μ CO_2 band at T=555 K	43
5.7	Comparison of total band absorptance for the 4.3μ CO_2 band at T=830 K	44
5.8	Comparison of total band absorptance for the 4.3μ CO_2 band at T=1110 K	45
5.9	Comparison of total band absorptance for the 2.7μ CO_2 band at T=300 K	49
5.10	Comparison of total band absorptance for the 2.7μ CO_2 band at T=555 K	50
5.11	Comparison of total band absorptance for the 2.7μ CO_2 band at T=830 K	51
5.12	Comparison of total band absorptance for the 2.7μ CO_2 band at T=1110 K	52

LIST OF TABLES - CONCLUDED

Table		Page
5.13	Comparison of total band absorptance for the 6.3μ H_2O band at T=300 K	72
5.14	Comparison of total band absorptance for the 6.3μ H_2O band at T=555 K	73
5.15	Comparison of total band absorptance for the 6.3μ H_2O band at T=833 K	74
5.16	Comparison of total band absorptance for the 6.3μ H_2O band at T=1111 K	75
5.17	Comparison of total band absorptance for the 2.7μ H_2O and at T=300 K	79
5.18	Comparison of total band absorptance for the 2.7μ H_2O band at T=555 K	80
5.19	Comparison of total band absorptance for the 2.7μ H_2O band at T=833 K	81
5.20	Comparison of total band absorptance for the 2.7μ H_2O band at T=1111 K	82
5.21	Comparison of total band absorptance for the 1.87μ H_2O band at T=300 K	86
5.22	Comparison of total band absorptance for the 1.87μ H_2O band at T=555 K	87
5.23	Comparison of total band absorptance for the 1.87μ H_2O band at T=833 K	88
5.24	Comparison of total band absorptance for the 1.87μ H_2O band at T=1111 K	89
5.25	Comparison of total gas emissivities for mixtures of water vapor, carbon dioxide and nitrogen	99
5.26	Comparison of nonisothermal band absorptance for CO_2 gas	101
5.27	Comparison of nonisothermal band absorptance for H_2O gas	102
5.28	Comparison of nonisothermal band emission for 2.7μ H_2O band	103

LIST OF FIGURES

Figure		Page
5.1	Comparison of transmittances of 15μ CO_2 band.....	32
5.2	Comparison of transmittances of 10μ CO_2 band (P_e=798 mm Hg, X=625 atm-cm).....	38
5.3	Comparison of transmittances of 10μ CO_2 band (P_e=1780 mm Hg, X=2945 atm-cm).....	39
5.4	Comparison of transmittances of 4.3μ CO_2 band.....	41
5.5	Comparison of transmittances of 2.7μ CO_2 band (P_e=980 mm Hg, X=6.08 atm-cm).....	46
5.6	Comparison of transmittances of 2.7μ CO_2 band (P_e=542 mm Hg, X=0.759 atm-cm).....	47
5.7	Comparison of total emissivity of carbon dioxide at T=300 K.....	53
5.8	Comparison of results of total emissivity by using wide band correlations at 300 K.....	54
5.9	Comparison of total emissivity of carbon dioxide at T=600 K.....	55
5.10	Comparison of results of total emissivity by using wide band correlations at 600 K.....	56
5.11	Comparison of total emissivity of carbon dioxide at T=1000 K.....	57
5.12	Comparison of results of total emissivity by using wide band correlations at 1000 K.....	58
5.13	Comparison of total emissivity of carbon dioxide at T=2000 K.....	59
5.14	Comparison of results of total emissivity by using wide band correlations at 2000 K.....	60
5.15	Comparison of spectral emissivities of the rotational band of H_2O at T=590 K.....	63

LIST OF FIGURES - CONTINUED

Figure		Page
5.16	Comparison of spectral emissivities of the rotational band of H_2O at T=850 K.....	64
5.17	Comparison of spectral emissivities of the rotational band of H_2O at T=1040 K.....	65
5.18	Comparison of spectral emissivities of the rotational band of H_2O at T=1640 K.....	66
5.19	Comparison of spectral emissivities of the rotational band of H_2O at T=1830 K.....	67
5.20	Comparison of spectral emissivities of the rotational band of H_2O at T=2200 K.....	68
5.21a	Comparison of transmittances of 6.3μ H_2O band in the spectral range 1200-1500 cm.....	69
5.21b	Comparison of transmittances of 6.3μ H_2O band in the spectral range 1500-1800 cm.....	70
5.21c	Comparison of transmittances of 6.3μ H_2O band in the spectral range 1800-2100 cm.....	71
5.22	Comparison of transmittances of 2.7μ H_2O band (P_e=782 mm Hg, X=0.0033 pr. cm).....	77
5.23	Comparison of transmittances of 2.7μ H_2O band (P_e=113 mm Hg, X=0.109 pr. cm).....	78
5.24	Comparison of transmittances of 1.87μ H_2O band (P_e= 765 mm Hg, X=0.007 pr. cm).....	84
5.25	Comparison of transmittances of 1.87μ H_2O band (P_e= 765 mm Hg, X=0.0483 pr. cm).....	85
5.26	Comparison of total emissivity of water vapor at T=300 K.....	91
5.27	Comparison of results of total emissivity by using wide band correlations at 300 K.....	92

LIST OF FIGURES - CONCLUDED

Figure		Page
5.28	Comparison of total emissivity of water vapor at T=600 K.....	93
5.29	Comparison of results of total emissivity by using wide band correlations at 600 K.....	94
5.30	Comparison of total emissivity of water vapor at T=1000 K.....	95
5.31	Comparison of results of total emissivity by using wide band correlations at 1000 K.....	96
5.32	Comparison of total emissivity of water vapor at T=2000 K.....	97
5.33	Comparison of results of total emissivity by using wide band correlations at 2000 K.....	98

LIST OF SYMBOLS

A_ω	spectral absorptance
A	total band absorptance, cm^{-1}
$\bar{A}$	dimensionless total band absorptance
B	Planck's function
c	velocity of light, cm/s
d	line spacing, cm^{-1}
E	band emission, W/m^2
E_1, E_3	exponential integral of the first and third order, respectively
$f(\omega, \omega_n)$	line shape factor
g	statistical weighting factor for degeneracy
h	Planck constant
I_0, I_1	Bessel function of imaginary arguments of the zeroth and first order, respectively
k	Boltzmann constant
$L(x)$	Ladenberg-Reiche function
P	pressure, atm
P_e	effective broadening pressure, atm
$P_E(S, S_0)$	line intensity distribution function
S	line intensity
T	temperature, K
u	nondimensional path length
v	vibrational quantum number
X	pressure path length, atm-cm
x	mass path length, g/m^2; optical path
α	integrated intensity, $cm^{-1}/g\ m^{-2}$

β	line width to spacing parameter
γ	line half-width; Euler's constant, 0.5772156
δ	spectral interval
δ_K	change in vibrational quantum number of kth mode
ϵ_ω, ϵ_n, ϵ_T	spectral, band and total emissivities, respectively
K_ω	spectral absorption coefficient
K^D, K^W	direct and wing contributions of absorption coefficient, respectively
ν	wavenumber of band center, cm^{-1}
ρ	density, g/m^3
σ	Stefan-Boltzmann constant
τ_ω	spectral transmittance
$\Phi(T)$	line-width-to-spacing temperature-variation parameter
$\Psi(T)$	band-intensity temperature-variation parameter
ω	wavenumber, cm^{-1}; band width parameter, cm^{-1}

SUBSCRIPTS

E	experimental value
h	scaling parameter for nonhomogeneous path
ω	value of quantity at particular wavenumber

ACCURATE EVALUATION OF HOMOGENEOUS AND NONHOMOGENEOUS GAS EMISSIVITIES

By

S. N. Tiwari[1] and K. P. Lee[2]

SUMMARY

Spectral transmittance and total band absorptance of selected infrared bands of carbon dioxide and water vapor are calculated by using the line-by-line and quasi-random band models and these are compared with available experimental results to establish the validity of the quasi-random band model. Various wide-band model correlations (such as Edwards and Balakrishnan, Tien and Lowder, and Felske and Tien) are employed to calculate the total band absorptance and total emissivity of these two gases under homogeneous and nonhomogeneous conditions. These results are compared with available experimental results under identical conditions. From these comparisons, it is found that the quasi-random band model can provide quite accurate results and is quite suitable for most atmospheric applications. Edwards and Balakrishnan, and Tien and Lowder correlations can provide reasonable results for homogeneous and nonhomogeneous conditions and, therefore, are useful for most engineering applications.

---

[1]Eminent Professor, Department of Mechanical Engineering and Mechanics, Old Dominion University, Norfolk, Virginia 23508.

[2]Graduate Research Assistant, Department of Mechanical Engineering and Mechanics, Old Dominion University, Norfolk, Virginia 23508.

Chapter 1

INTRODUCTION

The concept of total emissivity has proven to be very important in many radiative transfer analyses. It is useful in calculating atmospheric radiation fluxes and cooling rates [1-3]*, and predicting the emission and absorption of infrared radiation by hot gases in the heat transfer within high temperature furnaces, combustion chambers, heat engines, and chemical reactors [4-8]. Moreover, it is very convenient to use the emissivity charts of Hottel and co-workers [9] to estimate heat transfer from homogeneous, as well as nonhomogeneous, gases quite accurately. But, in the extrapolated portions of the emissivity charts, especially for water vapor, a discrepancy exists [10, 11]. In order to examine the usefulness of Hottel's data, a number of investigators calculate the emissivities which are based on spectral data or acquire them from experiments to make a comparison [4, 5, 10, 12-17].

The most accurate theoretical procedure to compute the spectral gas properties of a vibration-rotation band is probably the direct integration (line-by-line) method, which calculates the monochromatic absorption spectrum by numerically summing the contributions of the individual molecular absorption lines. Although this method is of high spectral

---

*The numbers in the brackets indicate references.

resolution, it is time-consuming and requires knowledge of individual line parameters. If one wants to save computational time and does not require high resolution, one can use narrow band models to evaluate the spectral absorptance within a narrow frequency interval of a vibration-rotation band. The commonly used narrow band models are Elsasser, statistical, random-Elsasser, and quasi-random models. The quasi-random band model is probably the best one to represent emission of a vibration-rotation band accurately.

Although the computational time required when using the narrow band model is much less than the time required when using the line-by-line method, it still requires a large amount of computer time, as well as a massive amount of input data, which makes it impractical for engineering applications. Therefore, it is desirable to make use of the so-called "wide band models" [11, 15, 18-21] which represent absorption from an actual band with reasonable accuracy. As these models are based on various narrow band model relations for absorption by assuming that the line intensjty is an exponentially decaying function of the wavenumber, they are called the exponential wide band models. In addition to reducing the mathematical complexities in radiative transport calculations and saving the computational time, it is convenient to express the total band absorptance or the band emissivity by fairly accurate continuous correlations [22-25].

Assuming the real optical paths of combustion chambers, furnaces, or the atmosphere to be homogeneous can lead to considerable errors when an estimate is made of the total radiative flux. Since optical paths

usually are nonhomogeneous, actual radiative flux calculations are very complicated and time-consuming. In order to save a considerable amount of computational time and make the problems more simple and suitable for engineering applications, one can apply the Curtis-Godson scaling approximation to predict the band emission from the nonhomogeneous gases.

The purpose of this study is to calculate the spectral and total emissivity of carbon dioxide and water vapor by using band models and band model correlations. We specify these two gases because they are the most effective in the emission and absorption of infrared radiation. The spectral transmittance and total band absorptance of different bands of these two gases, as obtained by using the quasi-random band model and several band model correlations, are compared with available experimental results [26-28] in order to establish the validity of a particular formulation to specific applications.

The basic theoretical formulations of emissivity for homogeneous and nonhomogeneous gases are presented in Chap. 2. A brief review of line and band models, and band model correlations are given in Chap. 3. Physical conditions and data sources for this study are presented in Chap. 4. Results are presented and discussed in Chap. 5.

Chapter 2

THEORETICAL FORMULATION

A large amount of information concerning various relations for emissivity of different gases is available in the literature [1-8, 10-15, 29-31]. In this section, we only review the basic formulations for calculating the emissivity for homogeneous and nonhomogeneous paths briefly.

2.1 Homogeneous Gas Emissivities

For a homogeneous path of absorbing-emitting gases, the spectral emissivity, ε_ω, at wavenumber ω is defined as

$$\varepsilon_\omega = A_\omega = 1-\tau_\omega = 1-\exp(-K_\omega X) \tag{2.1}$$

where A_ω is the spectral absorptance, τ_ω is the spectral transmittance, K_ω is the volumetric absorption coefficient and $X=py$ is the pressure path length. The total emissivity, ε_T, is obtained by integrating over the entire energy spectrum; it is defined by

$$\varepsilon_T(X,P,T) = \frac{\pi}{\sigma T^4} \int_0^\infty \varepsilon_\omega(X,P,T) B_\omega(T) d\omega \tag{2.2}$$

where σ is the Stefan-Boltzmann constant and B_ω is the Planck function evaluated at wavenumber ω. If one considers only the band emissivity, ε_n, of the nth band, Eq. (2.2) is integrated over the band region only.

For a single gas, where the absorption spectrum consists of vibrational-rotational bands, the total emissivity may be expressed as

$$\varepsilon_T(X,P,T) = \frac{\pi}{\sigma T^4} \sum_i B_i(T) A_i(X,P,T) \tag{2.3}$$

where $B_i(T)$ is the Planck function evaluated at the band center, and A_i is the integrated (total) band absorptance of the ith band and is given by

$$A = \int_{\Delta\omega} A_\omega d\omega = \int_{\Delta\omega} [1-\exp(-K_\omega X)] d\omega \tag{2.4}$$

By using an appropriate band absorptance relation, the total emissivity can be calculated with Eq. (2.2) and Eq. (2.3). Especially, one can obtain the emissivity without the integration by employing the band model correlations; these are extremely convenient and useful for engineering applications.

The spectral emissivity for a two component mixture of radiating gases denoted by subscripts 1 and 2 is given by

$$\varepsilon_{\omega,12} = 1 - \tau_{\omega,1}\, \tau_{\omega,2} = 1-\exp[-(K_{\omega,1}X_1 + K_{\omega,2}X_2)] \tag{2.5}$$

Thus, the total emissivity is expressed as

$$\varepsilon_{T,12} = \frac{\pi}{\sigma T^4} \int_0^\infty \varepsilon_{\omega,12}(X,P,T) B_\omega(T) d\omega$$

or

$$\varepsilon_{T,12} = \frac{\pi}{\sigma T^4} \int_0^\infty B_\omega(T)\{1-\exp[-(K_{\omega,1}X_1 + K_{\omega,2}X_2)]\} d\omega \qquad (2.6)$$

Equation (2.6) may be rewritten in the following form:

$$\varepsilon_{T,12} = \varepsilon_{T,1} + \varepsilon_{T,2} -$$

$$\frac{\pi}{\sigma T^4} \int_0^\infty B_\omega(T)[1-\exp(-K_{\omega,1}X_1)][1-\exp(-K_{\omega,2}X_2)] d\omega \qquad (2.7)$$

where $\varepsilon_{T,1}$ and $\varepsilon_{T,2}$ are the total emissivities of the pure components 1 and 2, respectively. The last term of Eq. (2.7) is called the correction for partial overlapping which is discussed in detail by Penner and Varanasi [32].

2.2 Nonhomogeneous Gas Emissivities

For a nonhomogeneous path, temperature, pressure and concentration of gas vary along the path and this affects the absorption of the gas; and, therefore, the emissivity relation should be modified appropriate-

ly. Corresponding to Eq. (2.2), the emissivity for a nonhomogeneous path for the path between level x and x' can be expressed by

$$\varepsilon(x,x') = \int_0^\infty A_\omega(x,x') \frac{B_\omega(x')}{B(x')} d\omega \tag{2.8}$$

where $A_\omega(x,x')$ is spectral absorptance between x and x', and $B(x') = \int B_\omega(x')d\omega = \sigma T^4/\pi$. Thus, it is necessary to acquire the spectral absorption $A_\omega(x,x')$ before evaluating the emissivity.

Nonhomogeneous behavior can be considered by employing the Curtis-Godson approximation [1], which appropriately averages the mean line intensity and line spacing over the nonhomogeneous path. For nonisothermal gases, this approximation, by using narrow band models, is not suitable for most engineering applications because of the complexity of the models and the large amount of computational time required. It is, therefore, desirable to use wide band models. Several investigators [19, 33-36] have applied the Curtis-Godson approximation to wide band models by obtaining three scaled parameters for the entire band. These are: a scaled integrated intensity, a scaled line width to spacing ratio, and a scaled band width parameter related to the rotational constant.

The simplest and most accurate model is the one suggested by Chan and Tien [33]. For this model, the scaling parameters can be expressed as

$$(\alpha)_h = (1/x) \int_0^L \alpha\rho dy \tag{2.9}$$

$$(\beta P_e)_h = (1/\alpha_h x) \int_0^L \beta P_e \alpha\rho dy \tag{2.10}$$

$$(\omega)_h = (1/\alpha_h x) \int_0^L \alpha\omega\rho dy \tag{2.11}$$

where $x = \int_0^L \rho\, dy$, L is the thickness of the gas layer, ρ is the density, y is the distance along the optical path; α, ω and β are integrated intensity, line width to spacing ratio parameter and band width parameter respectively; and P_e is the effective broadening pressure. By using these three scaled parameters in an available band model correlation, one can determine the nonisothermal band absorptance and band emission which is given by

$$E = \int_0^{x_L} B_\omega[T(x)] \frac{d}{dx} A[T(x'),x]dx \tag{2.12}$$

By employing Eq. (2.12), one may obtain the nonhomogeneous gas emissivity.

Chapter 3

BAND MODELS AND CORRELATIONS

Various theoretical formulations of spectral, narrow and wide band models, as well as band models correlations, are available in the literature [1, 11, 18, 20-25, 37-43]. In this section, these models and correlations are described briefly.

3.1 Direct Integration (Line-By-Line) Model

In this method, the entire spectral range of interest is first divided into a large number of narrow intervals. Each interval is then divided into a variable number of subintervals depending upon the number of lines within the interval. Two very narrow subintervals are created on each side of a line center. The transmittance, and then the spectral emissivity, is computed at four frequency locations in each subinterval and is finally averaged over each interval.

The total absorption coefficient in Eq. (2.1) at wavenumber ω is computed into two parts as

$$K(\omega) = K^D(\omega) + K^W(\omega) \qquad (3.1)$$

where $K^D(\omega)$ and $K^W(\omega)$ are called the direct and wing contributions respectively. Direct contribution originates from lines in very close vicinity (on both sides) and is obtained from

$$K^D(\omega) = \sum_n S_n\gamma_n/\{\pi[(\omega-\omega_n)^2 + \gamma_n^2]\} \qquad (3.2)$$

where ω_n refers to the nth contributing line, S_n and γ_n are the intensity and the Lorentz line half-width respectively. The wing contribution arises from lines which are further from ω than the range of direct contribution and is obtained from

$$K^W(\omega) = \sum_n S_n\gamma_n/[\pi(\omega-\omega_n)^2] \qquad (3.3)$$

Both Eq. (3.2) and Eq. (3.3) are based on the assumption that the line shape is Lorentzian. For a complete discussion on the direct integration procedure, one should refer to [38-40].

3.2 Narrow Band Models

The mean spectral emissivity within a narrow frequency interval can be represented with reasonable accuracy by the so-called "narrow band model." Four commonly used narrow band models are Elsasser, statistical, random Elsasser, and quasi-random. The application of any model to a particular case depends upon the nature of the absorbing-emitting molecule. Complete information on these models are available in the literature [1, 11, 24].

3.2.1 Elsasser (Regular) Band Model

The regular Elsasser band model consists of equally spaced Lorentz lines of equal half-width and intensity [44]. The absorption coeffi-

cient is a periodic function (with the period of the line spacing) and is given by

$$K_\omega = \sum_{n=-\infty}^{\infty} \frac{S_j}{\pi} \frac{\gamma_j}{(\omega-nd)^2 + \gamma_j^2} \tag{3.4}$$

where ω is the distance from the center of any line and d is the distance between adjacent lines. Elsasser [44] showed that Eq. (3.4) can be expressed in an alternate form as

$$K_\omega = \frac{S_j}{d} \frac{\sinh\beta}{\cosh\beta - \cos Z} \tag{3.5}$$

where

$$\beta = 2\pi\gamma_j/d, \qquad \text{and} \qquad Z = 2\pi(\omega-\omega_o)/d \tag{3.6}$$

The mean spectral emissivity of the periodic line pattern over the line spacing d is obtained by combining Eqs. (3.5) and (2.1) as

$$\varepsilon = 1 - \frac{1}{2\pi} \int_{-\pi}^{\pi} \exp\left[\frac{-\beta x \sinh\beta}{\cosh\beta - \cos Z} \right] dZ \tag{3.7}$$

where

$$x = S_j X/2\pi\gamma_j \tag{3.8}$$

The approximate forms of the Elsasser model can be expressed as:

1. The weak-line approximation

$$\varepsilon = 1-\exp(-\beta x) \qquad \beta \to \infty,\ x<<1 \tag{3.9}$$

2. The strong-line approximation

$$\varepsilon = \mathrm{erf}\left[\left(\frac{1}{2}\beta^2 x\right)^{1/2}\right] \qquad x>>1 \tag{3.10}$$

where erf(t) denotes the error function.

3. The nonoverlapping-line approximation

$$\varepsilon = \beta L(x) \qquad \beta<<1,\ \beta^2 x<<1 \tag{3.11}$$

where L(x) is Ladenberg-Reiche function defined as

$$L(x) = x\exp(-x)(I_0(x) + I_1(x)] \tag{3.12}$$

where I_0 and I_1 are the Bessel functions of imaginary arguments.

4. The strong nonoverlapping-line approximation

$$\varepsilon = \beta(2x/\pi)^{1/2} \qquad x>>1,\ \beta<<1,\ \beta^2 x<<1 \tag{3.13}$$

3.2.2 Statistical (Mayer-Goody) Model

The statistical band model is based upon the assumption that, in a

given wavenumber interval, the spectral lines are spaced randomly, and the intensity of these lines can be specified by some distribution function [1].

For uniform statistical model, which assumes all spectral lines in a narrow spectral interval to be equally intense, the mean spectral emissivity for lines of the Lorentz profile is expressed as

$$\varepsilon = 1-\exp[-\beta x e^{-x}(I_0(x) + I_1(x))] \qquad (3.14)$$

The line spacing d in the expression $\beta = (2\pi\ \gamma_j/d)$ refers to average spacing over the narrow band. The approximate forms of this model are the same as that of the Elsasser model except the strong-line approximation which is expressed as

$$\varepsilon = 1-\exp[-(2\beta^2 x/\pi)^{1/2}] \qquad x>>1 \qquad (3.15)$$

These should be expected because the particular arrangement of the spectral lines in the band does not influence the emission in the weak-line approximation and only intensity distribution function influences the emission in the nonoverlapping-line approximation.

The general statistical model assumes the distribution of line intensities to be, generally, represented by an exponential distribution (i.e., in a band, the probability of finding a spectral line of intensity S_j in a given intensity range decreases exponentially). Then the mean spectral emissivity by this model consisting of Lorentz lines is

given by

$$\varepsilon = 1-\exp[-\beta x/(1 + 2x)^{1/2}] \qquad (3.16)$$

Now the line spacing d and line intensity S in β and x should be replaced with the average value over the narrow spectral interval. The weak-line and strong-line approximation are the same as that in the uniform statistical model, but the nonoverlapping-line approximation for this model is expressed as

$$\varepsilon + \beta x/(1 + 2x)^{1/2} \qquad \beta<<1, \quad \beta^2 x<<1 \qquad (3.17)$$

Other line intensity distributions also have been suggested for the statistical band formulation; for detailed discussion on this, one should refer to [24, 25].

3.2.3 Random Elsasser Band Model

The random Elsasser band model assumes the random superposition of several different Elsasser bands. Each of the superposed bands may have different line intensities, half-widths and spacing. As many different Elsasser bands as necessary may be superimposed in this model. For N randomly superposed Elsasser bands, the mean spectral emissivity is obtained by the relation

$$\varepsilon = 1-\prod_{i=1}^{N} [1-\tilde{A}_E(x_i, \beta_i)/\delta_i] \qquad (3.18)$$

where $\tilde{A}_E\ (x_i, \beta_i)$ is the absorptance of the ith Elsasser band and is given by

$$\tilde{A}_{E,i}/\delta_i = \int_0^\infty \bar{A}_{E,i}(x_i,\beta_i)P_E(S_i,S_{oi})dS_i \qquad (3.19)$$

where $P_E(S_i,S_{oi})$ is the line intensity distribution function.

If an exponential distribution of intensity for narrow Elsasser bands is assumed, then

$$P_E(S_i,S_{oi}) = (1/S_{oi})\ \exp(-S_i/S_{oi}) \qquad (3.20)$$

and Eq. (3.19) becomes

$$\tilde{A}_{E,i}/\delta_i = (\beta_i x_{oi}\sinh\beta_i)/[(\beta_i x_{oi}\sinh\beta_i + \cosh\beta_i)^2-1]^{1/2} \qquad (3.21)$$

A combination of Eqs. (3.18) and (3.21) yields the expression for mean spectral emissivity by a modified random Elsasser band model as

$$\epsilon = (\beta x_o\sinh\beta)/[(\beta x_o\sinh\beta + \cosh\beta)^2-1]^{1/2} \qquad (3.22)$$

The weak-line and strong-line approximations of the random Elsasser model can be expressed, respectively, as

$$\varepsilon = 1 - \prod_{i=1}^{N} [\exp(-\beta_i x_i)] \qquad \beta \to \infty, \quad x \ll 1 \qquad (3.23)$$

and

$$\varepsilon = 1 - \prod_{i=1}^{N} \{1 - \mathrm{erf}[(\frac{1}{2}\beta_i^2 x_i)^{1/2}]\} \qquad x \gg 1 \qquad (3.24)$$

The approximate forms of the modified random Elsasser model are given by the same relations as the general statistical model except the nonoverlapping-line approximation which depends on the line intensity distribution assumed.

3.2.4 Quasi-random Band Model

Quasi-random band model assumes neither a regular nor a random spacing of the spectral lines. The entire spectrum is divided into a number of narrow frequency intervals with equal spectral width. The lines within each narrow interval are assumed to be distributed randomly and grouped into five intensity decades. Average transmittance for the interval is computed for lines in each decade separately and final transmittance is obtained by multiplying them for the five decades. Then, using Eq. (2.1), the mean spectral emissivity is obtained.

The average transmittance over interval, δ, due to a single line may be expressed as

$$\tau_n(\omega) = \frac{1}{\delta} \int_{\delta} \exp[-S_n X f(\omega, \omega_n)] d\omega_n \qquad (3.25)$$

where $f(\omega, \omega_n)$ is the shape factor for the line with center at ω_o. The average transmittance, τ_d, due to all the lines in that decade is given by

$$\tau_d(\omega) = \left\{ \frac{1}{\delta} \int_{\delta} \exp[-\bar{S}_n X f(\omega,\omega_n)]d\omega_n \right\}^N \tag{3.26}$$

where N is the number of lines and $\bar{S}_n$ is the average intensity of all the lines within the decade. At last, the average transmittance due to all lines in the five intensity decades of the interval is expressed as

$$\tau_k(\omega) = \prod_{d=1}^{5} \tau_d(\omega) = \prod_{d=1}^{5} \left\{ \frac{1}{\delta_k} \int_{\delta_k} \exp[-\bar{S}_n X f(\omega,\omega_n)]d\omega_n \right\}^N \tag{3.27}$$

where k represents the kth interval of entire spectrum. The wings of the lines in the adjacent intervals also make a significant contribution to the absorption in δ_k. Therefore, the resultant transmittance over the interval δ_k is given by

$$\tau_k(\omega) = \tau_{k-k}(\omega) \prod_{\substack{j=1 \\ j\neq k}}^{k} \tau_{k-j}(\omega) \tag{3.28}$$

where $\tau_{k-j}(\omega)$ represents the transmittance in δ_k due to lines in

δ_j. For a complete discussion on the quasi-random band model, one should refer to [37, 39, 41].

The model formulations discussed above represent the emissions of gases under homogeneous conditions. They can be extended to nonisothermal nonhomogeneous optical paths by employing various scaling approximations available in the literatures [1, 19, 33-36, 39, 46, 47].

The assumption of either regular or random spacing for spectral lines may be a serious defect of the Elsasser and statistical models because the spacing between the spectral line is in general neither uniform nor random. Furthermore, the wing contribution cannot accurately be taken into account by these models. Therefore, the quasi-random band model is probably the best model to represent the emission of a vibration-rotation band. In this study, only the quasi-random band model is used to make comparison with other formulations.

3.3 Wide Band Models.

Wide band models can be used to predict band emissivity without a lot of calculations but with reasonable accuracy. They are very simple and convenient for engineering applications. Detailed discussions on the wide band models are given in [11, 15, 18, 20, 24].

3.3.1 The Box Model

This model, first introduced by Penner [12], assumes that the absorption coefficient, K_ω, is constant over an effective band width $\Delta\omega$. The expression for the total absorptance by this model is given by

$$A = \int_{\Delta\omega} [1-\exp(-K_\omega X)]d\omega = (\Delta\omega)_e[1-\exp(-\bar{K}X)] \qquad (3.29)$$

where $(\Delta\omega)_e$ is the effective band width and $\bar{K}$ is the mean absorption coefficient for the interval $(\Delta\omega)_e$.

3.3.2 The Exponential Wide Band Model

Edwards et al. [18, 19] have considered various wide band models for the absorption of vibrational-rotational bands and have concluded that three parameters, which are the mean line intensity to spacing ratio, S/d, the mean line width to spacing ratio, $\pi\gamma/d$, and the effective broadening pressure, P_e, are necessary for a complete description of band absorption. The final forms of the total band absorptance relation presented by Edwards and Menard [19] and Edwards and Balakrishnan [21] are based on the formulation of the narrow statistical band model; and these are summarized in Table 3.1 and 3.2.

The other formulations of total band absorption with different narrow band models are discussed in detail in [24].

3.4 Band Model Correlations

In order to reduce the mathematical complexities and save the computational time, it is often desirable to express the integral form of the total band absorptance or the band emissivity by fairly accurate continuous correlations. Several continuous correlations for the total absorptance of a wide band are available in the literature. These are briefly discussed here in the sequence that they became available in the

Pressure Broadening Parameter $\beta = \frac{C_2^2 P_e}{4 C_1 C_3}$	Limits of A (cm^{-1})	Band Absorption A (cm^{-1})
$\beta \leq 1$	$0 \leq A \leq \beta C_3$	$A = C_1 X$
	$\beta C_3 \leq A \leq C_3(2-\beta)$	$A = C_2 (X P_e)^{1/2} - \beta C_3$
	$C_3(2-\beta) \leq A \leq \infty$	$A = C_3 \left[\ln \frac{C_2^2 X P_e}{4 C_3} + 2 - \beta \right]$
$\beta > 1$	$0 \leq A \leq C_3$	$A = C_1 X$
	$C_3 \leq A \leq \infty$	$A = C_3 \left[\ln \frac{C_1 X}{C_3} + 1 \right]$

C_1, C_2, C_3, b and n are correlation parameters [11,19], X is mass path length, g/m^2, $P_e = [(P_k + bP_a)/P_o]^n$, P_o= 1 atm, P_a is the absorbing-gas partial pressure, P_k is the broadening-gas partial pressure.

Table 3.2 Band absorption correlation by Edwards and Balakrishnan for isothermal gas

Pressure Broadening Parameter $\beta = \gamma P_e$	Limits of u	Band Absorption A (cm^{-1})
$\beta < 1$	$0 \le u \le \beta$	$A = \omega u$
	$\beta \le u \le 1/\beta$	$A = (2\beta u - \beta)$
	$1/\beta \le u \le \infty$	$A = \omega(\ln \beta u + 2 - \beta)$
$\beta \ge 1$	$0 \le u \le 1$	$A = \omega u$
	$1 \le u \le \infty$	$A = \omega(\ln u + 1)$

β is π times the ratio of mean line width to spacing, P_e is effective broadening pressure, $u = X\alpha/\omega$, X is mass path length, g/m^2, α is integrated band intensity, γ is line width parameter, ω is band width parameter.

literature.

3.4.1 Tien and Lowder Correlation

In 1966, a continuous correlation was proposed by Tien and Lowder [22], and this is of the form

$$\bar{A}(u,\beta) = A(u,\beta)/\omega$$

$$= \ln(uf(t)\{(u+2)/[u+2f(t)]\}+1) \qquad (3.30)$$

where

$$f(t) = 2.94[1-\exp(-2.6t)], \qquad t=\beta/2 \qquad (3.31)$$

$\bar{A}(u,\beta)$ is dimensionless total band absorptance, $u=SX/\omega$ is the non-dimensional path length and $\beta = 2\pi\gamma/d$ is the line structure parameter. This correlation does not reduce to the correct limiting form in the square-root limit [20], and its use should be made for $\beta \gtrsim 0.1$.

3.4.2 Goody and Belton Correlation

In 1967, another continuous correlation was proposed by Goody and Belton as [48]

$$\bar{A}(u,\beta)=2\ln\{1+u/[4+\pi u/4t)]^{1/2}\} \qquad (3.32)$$

Although this correlation satisfies the linear, square-root, and logarithmic limits, its use is restricted to relatively small β values.

3.4.3 Tien and Ling Correlation

In 1969, a simple two-parameter correlation was developed by Tien and Ling as [49]

$$\bar{A}(u) = \sinh^{-1}(u) \tag{3.33}$$

This is valid only for the limit of large β.

3.4.4 Cess and Tiwari Correlations

A relatively simple correlation has been proposed by Cess and Tiwari as [20]

$$\bar{A}(u,\beta) = 2\ln(1+u/\{2+[u(1+1/\bar{\beta})]^{1/2}\}) \tag{3.34}$$

where $\bar{\beta} = 4t/\pi$. The use of this correlation is justified at relatively high pressure for gases whose spectral behavior can be described by the general statistical model. By slightly modifying Eq. (3.34), another form of the wide band absorptance was obtained as [24]

$$\bar{A}(u,\beta)=2\ln(1+u/\{2+[u(C+\Pi/2\beta)]^{1/2}\}) \tag{3.35}$$

where

$$C = \begin{cases} 0.1, & \beta < \text{ and all u values} \\ 0.1, & \beta > 1 \text{ and } u \leq 1 \\ 0.25, & \beta > 1 \text{ and } u > 1 \end{cases}$$

Both Eq. (3.34) and Eq. (3.35) reduce to all the limiting forms [20, 24].

3.4.5 Edwards and Balakrishnan Correlation

In 1972, a continuous correlation was proposed by Edwards and Balakrishnan as [50]

$$\bar{A}(u) = \ln(u) + E_1(u) + \gamma + \frac{1}{2} - E_3(u) \qquad (3.36)$$

This is valid for large pressure and at large path lengths.

3.4.6 Felske and Tien Correlation

In 1974, Felske and Tien proposed a correlation for $\bar{A}(u,\beta)$ as [23]

$$\bar{A}(u,\beta) = 2E_1(t\rho_u) + E_1(\rho_u/2) - E_1[(\rho_u/2)(1+2t)] + \ln[(t\rho_u)^2/(1+2t)] + 2\gamma \qquad (3.37)$$

where

$$\rho_u = \{(t/u)\ [1+(t/u)]\}^{-1/2} \qquad (3.38)$$

$E_1(x)$ is exponential integral of the first order, and γ=0.5772156, is the Euler's constant. This correlation is based on the general statistical model and its validity is claimed for the entire range of the governing parameters.

3.4.7 Tiwari and Batki Correlation

In 1975, Tiwari and Batki proposed the following correlation [24, 51]

$$\bar{A}(u) = \gamma + \ln(u) + E_1(u) \qquad (3.39)$$

This correlation is valid for all path lengths but for $t=(\beta/2)>1$.

3.4.8 Wang-Correlation

A continuous correlation has been proposed recently by Wang as [25]

$$\bar{A}(z) = \exp(4\beta_1)\{E_1[2\beta_1(1+z)] - E_1(4\beta_1)\} + \ln(1+z) -$$

$$\ln 2 + E_1[2\beta_1(z-1)] + \ln[2\beta_1(z-1)] + \gamma \qquad (3.40)$$

where $\beta_1 = \beta/4$, $z=(1+u/\beta_1)^{1/2}$. This total band absorptance correlation is obtained by employing the Malkmus narrow band model [45] and the

Edwards and Menard wide band approximation [16]. The predicted total band absorptance of this correlation is always smaller than the Felske and Tien.

Band absorptance results of various correlations are compared and discussed in some detail in [24, 51]. The Felske and Tien correlation agrees well with the general statistical model while the Tien and Lowder correlation is in general agreement with the Elsasser model. In this study, only these two correlations are employed to calculate the total emissivity.

Chapter 4

PHYSICAL CONDITIONS AND DATA SOURCES

The primary atmospheric absorbers and the primary radiating species of the hot gases of combustion are the carbon dioxide and water vapor due to their comparatively high absorptivities and emissivities in the near infrared region. The total emissivities of these two gases were calculated by using the quasi-random band model (only at room temperature), Edwards and Balakrishnan wide band model relation, Tien and Lowder correlation and Felske and Tien correlation under conditions of temperatures at 300, 600, 1000, 2000 K, pressures at 0.1, 0.5, 1.0, 5.0, 10.0 atm, and path lengths from 0.1 to 1000 atm-cm. Moreover, results of transmittance and total band absorptance were obtained for several bands of these two gases under conditions for which experimental measurements were available.

The line parameters (position, strength, line width etc.) needed for this study were obtained from McClatchey et al. [52]; the "McClatchey Tape" is available at the NASA Langley Research Center. Rotational and vibrational partition functions required to account for the temperature dependence of the line strengths were taken from McClatchey et al. [52]. Table 4.1 lists the significant bands of CO_2 and H_2O which provide the essential contributions to the gas emissivity.

The band absorptance parameters (the integrated band intensity, α, the line-width parameter, β, and the band width parameter, ω) for the

Table 4.1 Significant band regions

Gas	n	Band	Spectral Location (cm^{-1})	Line Number
Carbon Dioxide	1	1 5μm	500 --- 800	17,883
	2	1 0μm	875 --- 1125	1,509
	3	4.3μm	2150 --- 2450	12,436
	4	2.7μm	3400 --- 3800	10,104
	5	2μm	4500 --- 5400	5,406
Water Vapor	1	Rotational	0 --- 900	3,473
	2	6.3 μm	1200 --- 2100	5,576
	3	2.7 μm	2525 --- 4500	12,917
	4	1.87μm	4525 --- 6000	5,198
	5	1.38μm	6025 --- 7700	4,638

wide band models and correlations are obtained from Edwards et al. [21, 15]. Table 4.2 lists these parameters for CO_2 and H_2O. The temperature and pressure dependence of these parameters are given by the following relations:

$$\alpha(T) = \alpha_0 \frac{[1-\exp(-\Sigma_{k=1}^{m} \pm u_k \delta_k)]\Psi(T)}{[1-\exp(-\Sigma_{k=1}^{m} u_{o,k} \delta_k)]\Psi(T_o)} \tag{4.1}$$

$$\beta(T) = \beta 0 (T/T_o)^{1/2} \Phi(T)/\Phi(T_o) \tag{4.2}$$

$$\omega(T) = \omega_o (T/T_o)^{1/2} \tag{4.3}$$

where

$$\Psi(T) = \frac{\prod_{k=1}^{m} \sum_{v_k=v_{o,k}}^{\infty} \frac{(v_k + g_k + \delta_k - 1)!}{(g_k-1)!\, v_k!} e^{-u_k v_k}}{\prod_{k=1}^{m} \sum_{v_k=0}^{\infty} \frac{(v_k + g_k - 1)!}{(g_k-1)!\, v_k!} e^{-u_k v_k}} \tag{4.4}$$

$$\Phi(T) = \frac{\left\{ \prod_{k=1}^{m} \sum_{v_k=v_{o,k}}^{\infty} \left[\frac{(v_k + g_k + \delta_k - 1)!}{(g_k-1)!\, v_k!} e^{-u_k v_k} \right]^{1/2} \right\}^2}{\prod_{k=1}^{m} \sum_{v_k=v_{o,k}}^{\infty} \frac{(v_k + g_k + \delta_k - 1)!}{(g_k-1)!\, v_k!} e^{-u_k v_k}} \tag{4.5}$$

$$u_k = hc\, \nu_k/kT, \quad U_{o,k} = hc\nu_k/kT_o \tag{4.6}$$

in which $T_o = 100$ K, and $hc/k \cong 1.4388$ cm-K

Table 4.2 Exponential wide-band parameters

Gas	Vibrations ν_k (cm^{-1})	Bands $\delta_1, \delta_2, \ldots$	Pressure parameters n	Pressure parameters ζ ($T_0 = 100$ K)	Spectral location ν_1 (cm^{-1})	Spectral location ν_2 (cm^{-1})	Spectral location ν_3 (cm^{-1})	Band absorption parameters α_0 (cm^{-1}/gm m^{-2})	Band absorption parameters β_0	Band absorption parameters ω_0 (cm^{-1})
(1) H_2O	$m = 3$	(1) Rotational								
	$\nu_1 = 3652$		1	$8.6(T_0/T)^{1/2}+0.5$	0[b]			5200.0[b]	0.14311[b]	28.4[b]
	$\nu_2 = 1595$	0,0,0								
	$\nu_3 = 3756$	(2) 6.3 μm		$8.6(T_0/T)^{1/2}+0.5$		1600		41.2	0.09427	56.4
	$g_1 = 1$	0,1,0	1							
	$g_2 = 1$	(3) 2.7 μm								
	$g_3 = 1$	0,2,0						0.19		
		1,0,0	1	$8.6(T_0/T)^{1/2}+0.5$		3760		2.30	0.13219	60.0
		0,0,1						22.40		
		(4) 1.87 μm	1	$8.6(T_0/T)^{1/2}+0.5$		5350		3.0	0.08169	43.1
		0,1,1								
		(5) 1.38 μm	1	$8.6(T_0/T)^{1/2}+0.5$		7250		2.5	0.11628	32.0
		1,0,1								
(2) CO_2[d]	$m = 3$	(1) 15 μm								
	$\nu_1 = 1351$	0,1,0	0.7	1.3		667		19.0	0.06157	12.7
	$\nu_2 = 667$	(2) 10.4 μm								
	$\nu_3 = 2396$	−1,0,1	0.8	1.3		960		2.47×10^{-9}	0.04017	13.4
	$g_1 = 1$	(3) 9.4 μm								
	$g_2 = 2$	0,−2,1[e]	0.8	1.3		1060		2.48×10^{-9}[e]	0.11888[e]	10.1
	$g_3 = 1$	(4) 4.3 μm								
		0,0,1	0.8	1.3			2410	110.0	0.24723	11.2
		(5) 2.7 μm								
		1,0,1	0.65	1.3		3660		4.0	0.13341	23.5
		(6) 2.0 μm								
		2,0,1	0.65	1.3		5200		0.066	0.39305	34.5

Chapter 5

RESULTS AND DISCUSSIONS

Spectral transmittance of important bands of carbon dioxide and water vapor are evaluated by employing the line-by-line (LBL) and quasi-random band (QRB) models; and these are compared with available experimental results. The total band absorptance and the total emissivity of these two gases are calculated by the QRB model, Edwards and Balakrishnan wide-band absorptance relations, Tien and Lowder correlation, and Felske and Tien correlation. The nonisothermal band absorptance and emission, however, are calculated only by using the wide-band model correlations. All these results are compared with experimental results available in the literature.

5.1 Homogeneous Results for Carbon Dioxide

The spectral transmittance and total band absorptance results of selected bands (15μ CO_2, 10μ CO_2, 4.3μ CO_2 and 2.7μ CO_2), as well as the results of total emissivity, of carbon dioxide are presented in this section.

5.1.1 15μ CO_2 Band

The spectral transmittance results for this band, as calculated by the QRB model, are shown in Fig. 5.1 along with experimental results. The agreement between these results is quite good over the entire band pass.

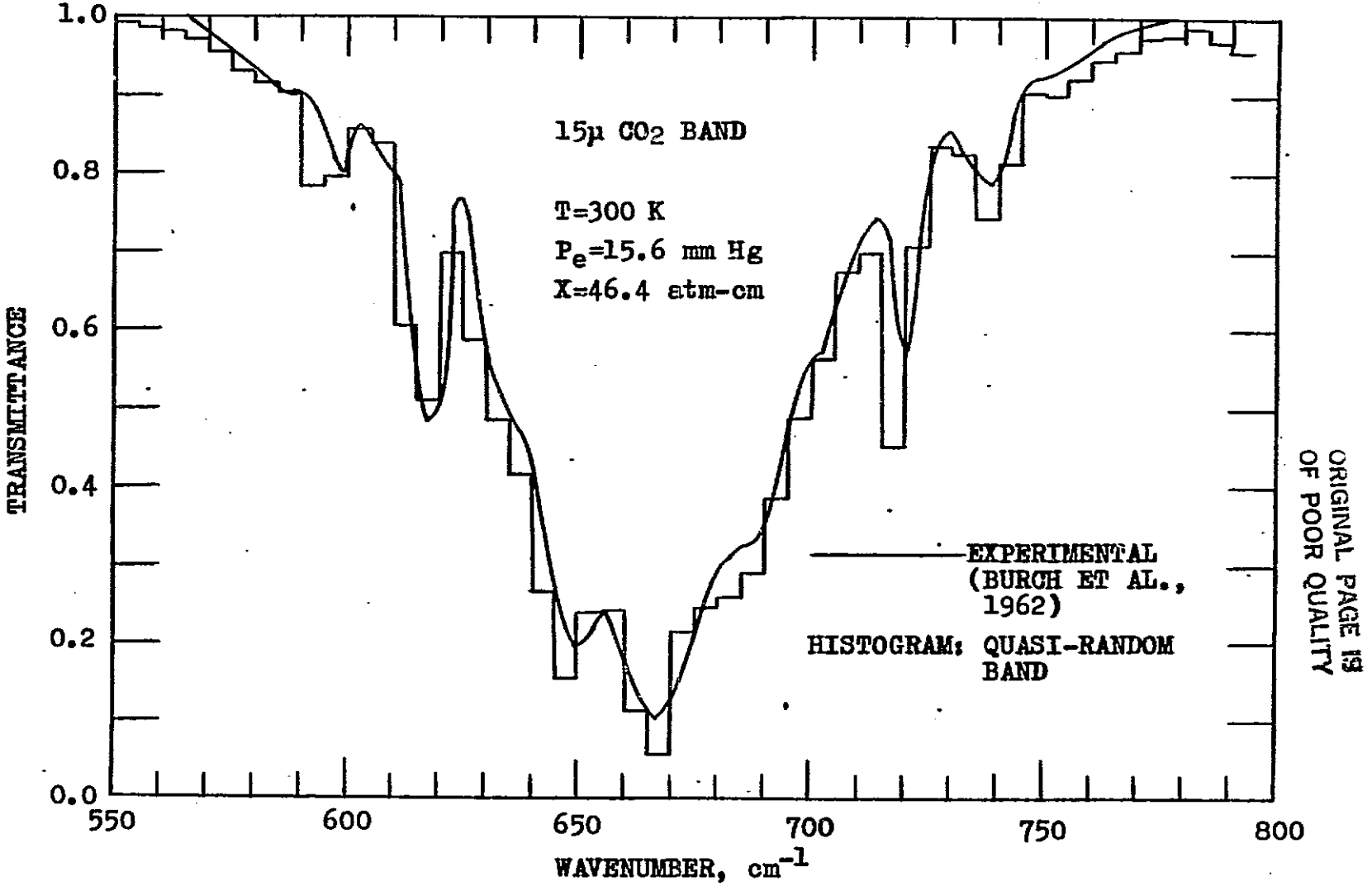

Fig. 5.1 Comparison of transmittances of the 15μ CO_2 band.

The total band absorptance results were calculated by the QRB model (only at 300 K) and wide-band model correlations at four different temperatures and are presented in Tables 5.1-5.4. At 300 K, the QRB model results agree very well with experimental results at large path lengths but give lower values than the experimental values for very small path lengths. Among the results of the correlations, Edwards and Balakrishnan, and Tien and Lowder correlations generally show better agreement for medium and high pressures as well as for large path lengths, while Felske and Tien's correlation yields much lower values than experimental values. For low pressures and small path lengths, however, Felske and Tien's correlation provides better agreement; Edwards and Balakrishnan, and Tien and Lowder correlations give higher values than experimental values.

5.1.2 10μ CO_2 (Hot) Band

The spectral transmittance results, as calculated by the QRB and/or line-by-line models, are presented in Figs. 5.2 and 5.3 for two different pressures and path lengths. The QRB model results show very good agreement with the experimental results in Fig. 5.2; however, the QRB model results exhibit a slightly lower absorption in Fig. 5.3 for higher pressure and longer path length. This may be because the QRB formulation neglects the contributions of weaker lines under these conditions. The agreement between experimental and line-by-line results is seen to be excellent.

Table 5.1 Comparison of total band absorptance for the 15μ CO_2 band at T=300 K

Effective Pressure	Mass Path Length	Total Band Absorptance Results, A (cm^{-1})								
		Exp. (26)	Quasi-random Band		Edwards & Balakrishnan		Tien & Lowder		Felske & Tien	
P_e (atm)	W (g/m^2)	A_E	A	PD	A	PD	A	PD	A	PD
2.24	0.098	2.02	1.3	-35	1.86	- 8	1.77	-12	1.59	-21
1.095	7.04	30.9	31.13	+ 1	28.57	- 8	34.5	-12	22.48	-27
2.21	7.04	35.6	35.51	0	35.9	+ 1	40.36	+13	26.48	-26
0.4	846.0	128.0	136.0	+ 6	116.58	- 9	117.23	- 8	97.21	-24
1.005	846.0	141.0	147.86	+ 5	130.0	- 8	130.36	- 8	109.96	-22

PD=$((A-A_E)/A_E)X100$

Table 5.2 Comparison of total band absorptance for the 15μ CO_2 band at T=555 K

Effective Pressure	Mass Path Length	Total Band Absorptance Results, A (cm^{-1})						
		Exp. (28)	Edwards & Balakrishnan		Tien & Lowder		Felske & Tien	
P_e (atm)	W (g/m^2)	A_E	A	PD	A	PD	A	PD
0.49	0.177	4.0	3.33	-17	3.1	-22	2.61	-35
1.0	3.58	22.3	30.71	+38	35.08	+57	22.81	+ 2
0.59	86.5	122.1	109.26	-11	110.53	- 9	83.05	-32
1.0	20.0	64.0	75.14	+17	77.46	+21	53.22	-17
10.3	202.0	174.0	174.33	0	172.7	- 1	144.08	-17
12.9	3626.0	272.0	261.44	- 4	261.0	- 4	232.4	-15

$PD=((A-A_E)/A_E)X100$

Table 5.3 Comparison of total band absorptance for the 15μ CO_2 band at T=833 K

Effective Pressure	Mass Path Length	Total Band Absorptance Results, A (cm^{-1})						
		Exp. (28)	Edwards & Balakrishnan		Tien & Lowder		Felske & Tien	
P_e (atm)	W (g/m^2)	A_E	A	PD	A	PD	A	PD
0.294	0.71	4.4	11.25	+158	11.25	+156	8.51	+ 93
0.25	5.51	36.8	38.44	+ 4	45.49	+ 24	29.34	- 20
0.55	54.6	136.0	130.57	- 4	130.49	- 4	96.27	- 29
1.02	13.7	91.0	91.63	+ 1	88.85	- 2	61.26	- 33
10.5	277.0	227.0	218.7	- 4	220.19	- 3	188.84	- 17
13.0	2440.0	307.0	298.5	- 3	300.94	- 2	270.1	- 12

$PD=((A-A_E)/A_E)X100$

Table 5.4 Comparison of total band absorptance for the 15μ CO_2 band at T=1110 K

Effective Pressure	Mass Path Length	Total Band Absorptance Results, A (cm^{-1})						
		Exp. (28)	Edwards & Balakrishnan		Tien & Lowder		Felske & Tien	
P_e (atm)	W (g/m^2)	A_E	A	PD	A	PD	A	PD
0.26	0.45	8.0	8.55	+ 7	7.94	- 1	6.85	-14
1.05	1.91	23.1	35.26	+53	30.04	+30	24.28	+ 5
0.26	4.69	33.0	48.56	+47	51.6	+56	34.45	+ 5
1.07	18.9	105.0	128.2	+22	119.3	+14	87.29	-17
1.06	20.0	98.0	130.57	+33	121.84	+24	89.28	- 9
1.30	187.0	235.0	227.27	- 3	224.28	- 5	183.67	-22
1.31	1872.0	331.0	327.37	- 1	330.51	0	298.71	-10

PD=((A-A_E)/A_E)X100

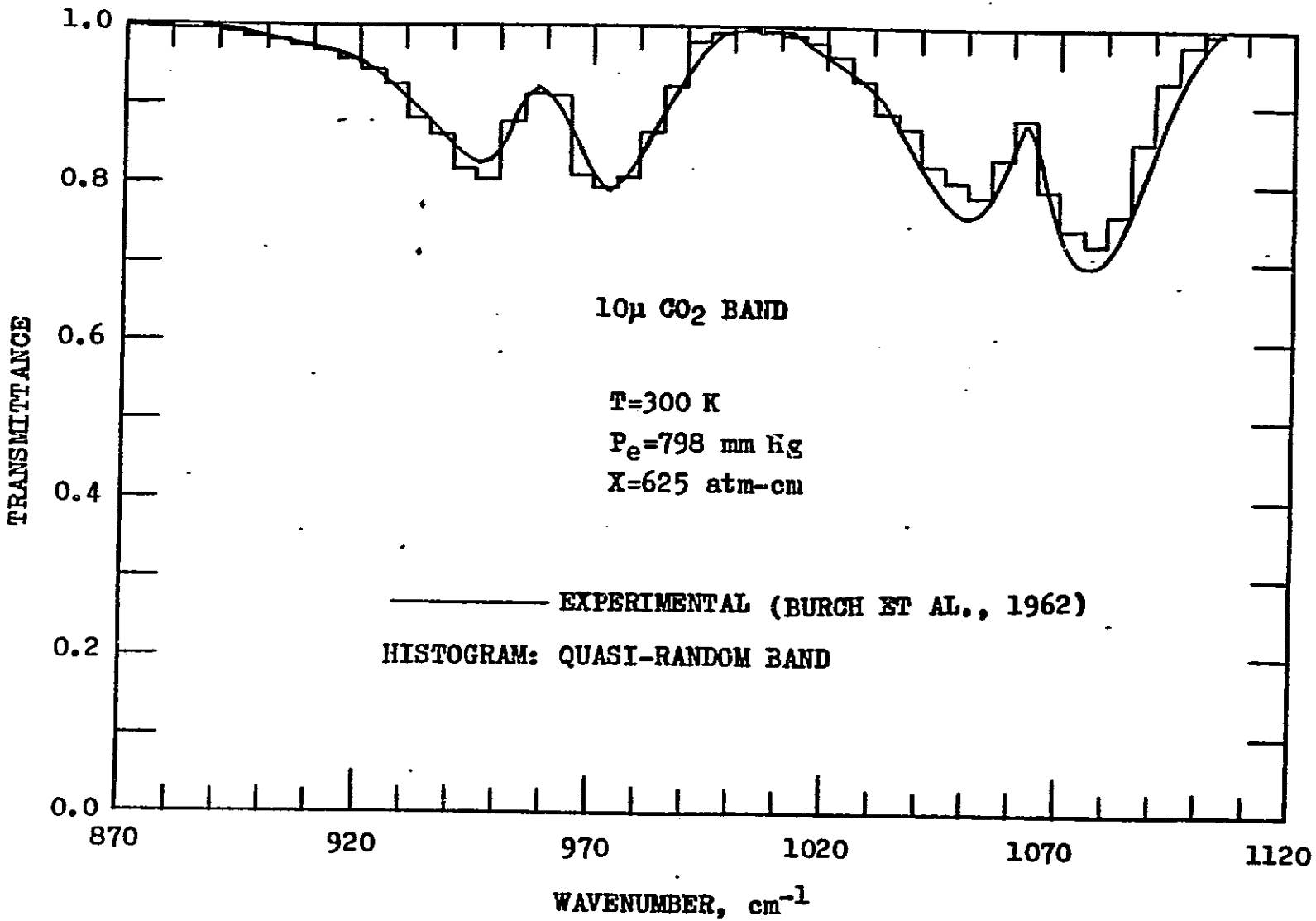

Fig. 5.2 Comparison of transmittances of the 10μ CO_2 band.

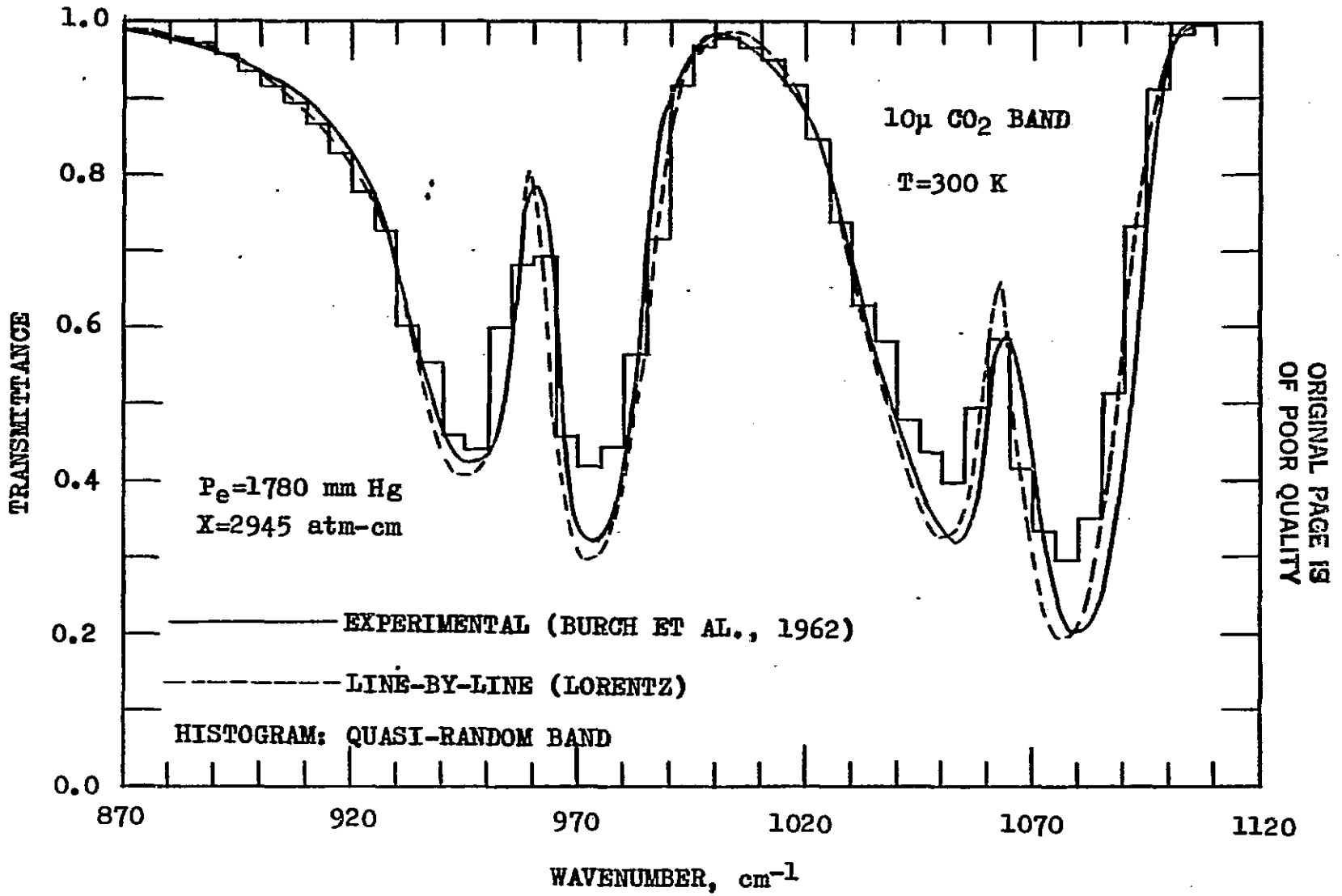

Fig. 5.3 Comparison of transmittances of the 10μ CO_2 band.

5.1.3 4.3μ CO_2 Band

The spectral transmittance results of the QRB model are compared with the experimental results in Fig. 5.4 for P_e = 137 mm Hg and X = 0.195 atm-cm. The agreement between the results is seen to be good except in the central portion of the band where the QRB model results exhibit a slightly lower absorption.

The total band absorptance results for this band, as calculated by the QRB model (only at 300 K) and different correlations are compared with the experimental results in Tables 5.5-5.8 for four different temperatures. The QRB model results are seen to compare very well with the experimental results except for low pressures and small path lengths. Among the results of correlations, the Edwards and Balakrishnan, and Tien and Lowder results show, in general, reasonable agreement with the experimental results; but the comparisons are not very good for low pressures and small path lengths. The Felske and Tien's results are lower for almost all cases considered.

5.1.4 2.7μ CO_2 Band

The transmittance results of the QRB model are compared with the experimental results in Figs. 5.5 and 5.6 for different pressures and path lengths. In general, the agreement between these results is seen to be good, except that the QRB results show a consistently lower absorption (higher transmittance) in Fig. 5.5.

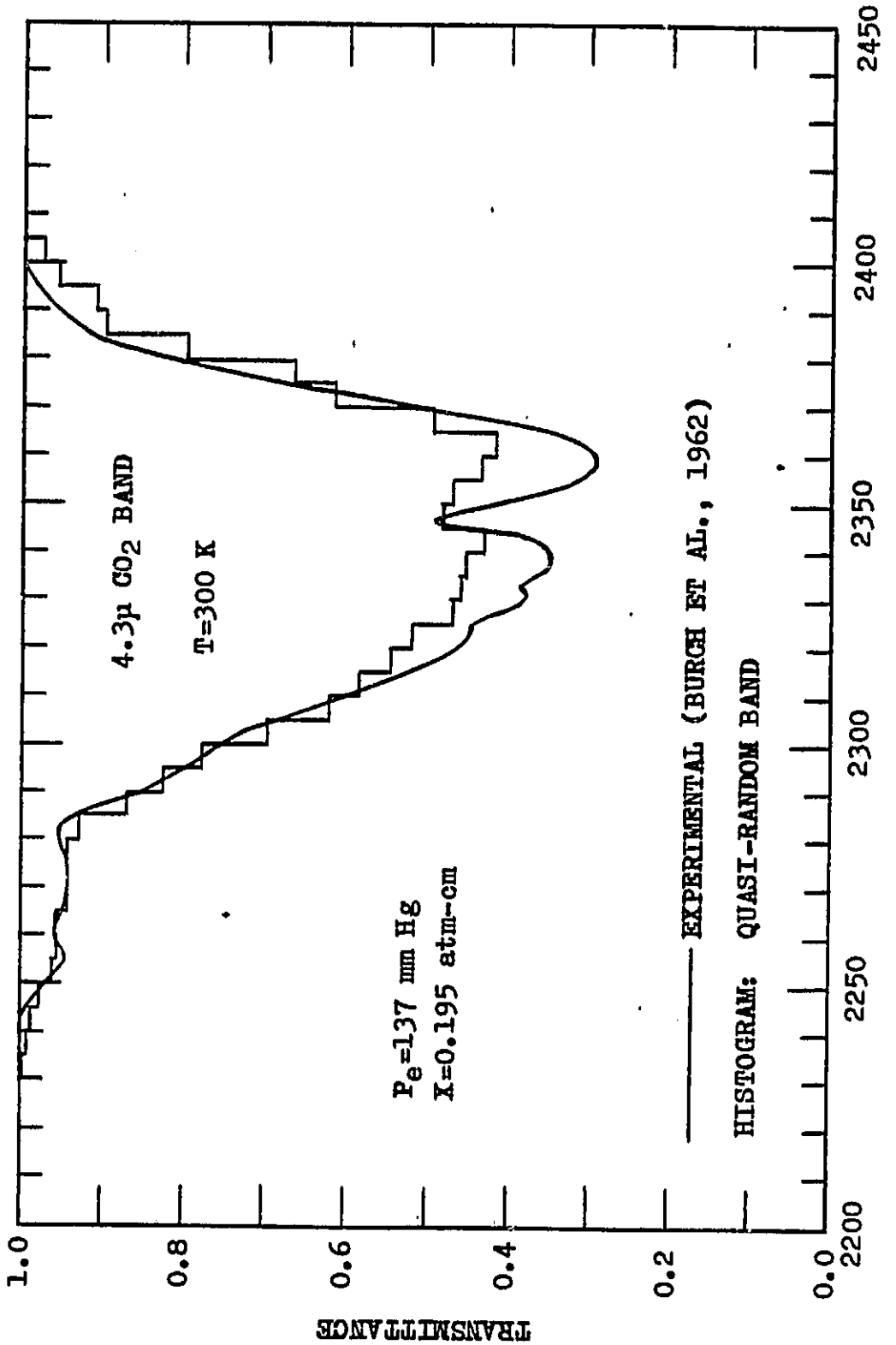

Fig. 5.4 Comparison of transmittances of the 4.3μ CO_2 band.

Table 5.5 Comparison of total band absorptance for the 4.3μ CO_2 band at T=300 K

Effective Pressure	Mass Path Length	Total Band Absorptance Results, A (cm^{-1})							
		Exp. (26)	Quasi-random Band		Edwards & Balakrishnan		Tien & Lowder		Felske & Tien	
P_e (atm)	W (g/m^2)	A_E	A	PD	A	PD	A	PD	A	PD
0.529	0.0948	2.4	9.04	+277	3.4	+42	3.88	+62	2.98	+24
0.61	6.27	81.4	78.17	- 4	71.23	-12	71.4	-12	53.2	-35
2.15	6.27	92.9	94.43	+ 2	84.73	- 9	83.0	-11	64.5	-31
2.13	91.0	138.0	147.91	+ 7	136.55	- 1	135.6	- 2	116.38	-16
2.59	416.0	165.0	177.68	+ 7	167.48	+ 2	166.54	+ 1	147.36	-11

PD=((A-A_E)/A_E)X100

Table 5.6 Comparison of total band absorptance for the 4.3μ CO_2 band at T=555 K

Effective Pressure	Mass Path Length	Total Band Absorptance Results, A (cm^{-1})						
		Exp. (28)	Edwards & Balakrishnan		Tien & Lowder		Felske & Tien	
P_e (atm)	W (g/m^2)	A_E	A	PD	A	PD	A	PD
0.27	0.0977	13.2	9.63	-27	9.17	-31	7.11	-46
0.29	1.06	43.4	44.08	+ 2	47.0	+ 8	30.91	-29
0.50	16.57	132.0	125.16	- 5	124.14	- 6	198.31	-26
1.22	199.0	185.0	201.23	+ 9	199.94	+ 8	173.95	- 6
1.04	41.1	146.0	158.2	+ 8	156.67	+ 7	130.72	-10
1.30	374.0	184.0	218.36	+19	217.15	+18	191.2	+ 4
12.9	3670.0	303.0	280.67	- 7	282.73	- 7	263.83	-13

$PD=((A-A_E)/A_E)X100$

Table 5.7 Comparison of total absorptance for the 4.3μ CO_2 band at T=830 K

Effective Pressure	Mass Path Length	Total Band Absorptance Results, A (cm^{-1})						
		Exp. (28)	Edwards & Balakrishnan		Tien & Lowder		Felske & Tien	
Pe (atm)	W (g/m^2)	A_E	A	PD	A	PD	A	PD
0.29	0.0679	9.7	6.58	-32	7.04	-27	6.31	-35
0.26	0.315	28.5	29.0	+ 2	26.6	- 7	19.9	-30
1.0	2.45	107.0	100.9	- 6	93.9	-12	72.9	-32
0.29	31.5	177.0	174.0	- 2	172.3	- 3	140.5	-21
1.16	133.0	215.0	230.0	+ 7	231.1	+ 7	201.8	- 6
1.0	27.4	181.0	179.0	- 1	178.8	- 1	149.6	-17
1.33	249.0	223.0	250.3	+12	251.9	+13	223.0	0
12.9	2480.0	326.0	324.6	0	327.1	0	305.0	- 6

$PD=((A-A_E)/A_E)X100$

Table 5.8 Comparison of total band absorptance for the 4.3μ CO_2 band at T=1110 K

Effective Pressure	Mass Path Length	Total Band Absorptance Results, A (cm^{-1})						
		Exp. (28)	Edwards & Balakrishnan		Tien & Lowder		Felske & Tien	
P_e (atm)	W (g/m^2)	A_E	A	PD	A	PD	A	PD
0.26	0.477	43.4	48.4	+11	39.33	- 9	31.0	-29
0.25	4.24	135.0	129.6	- 4	122.6	- 9	92.3	-32
0.31	42.8	227.0	217.4	- 4	215.6	- 5	180.15	-21
1.04	20.0	197.0	189.5	- 4	190.3	- 3	161.31	-18
1.3	187.0	260.0	273.0	+ 5	275.6	+ 6	246.2	- 5
1.31	1891.0	362.0	359.3	- 1	362.2	0	338.0	- 7

PD=((A-A_E)/A_E)X100

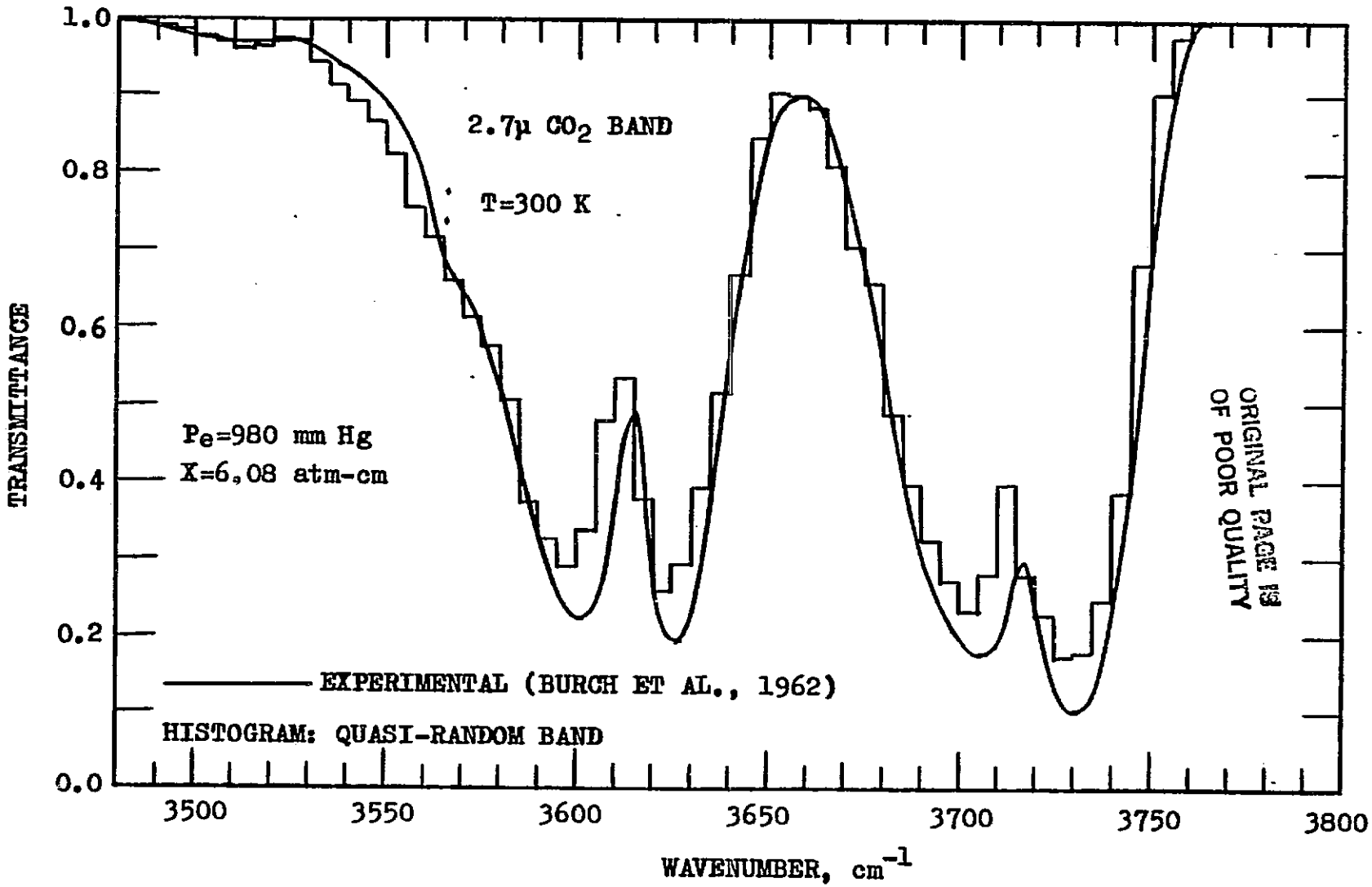

Fig. 5.5 Comparison of transmittances of the 2.7μ CO_2 band.

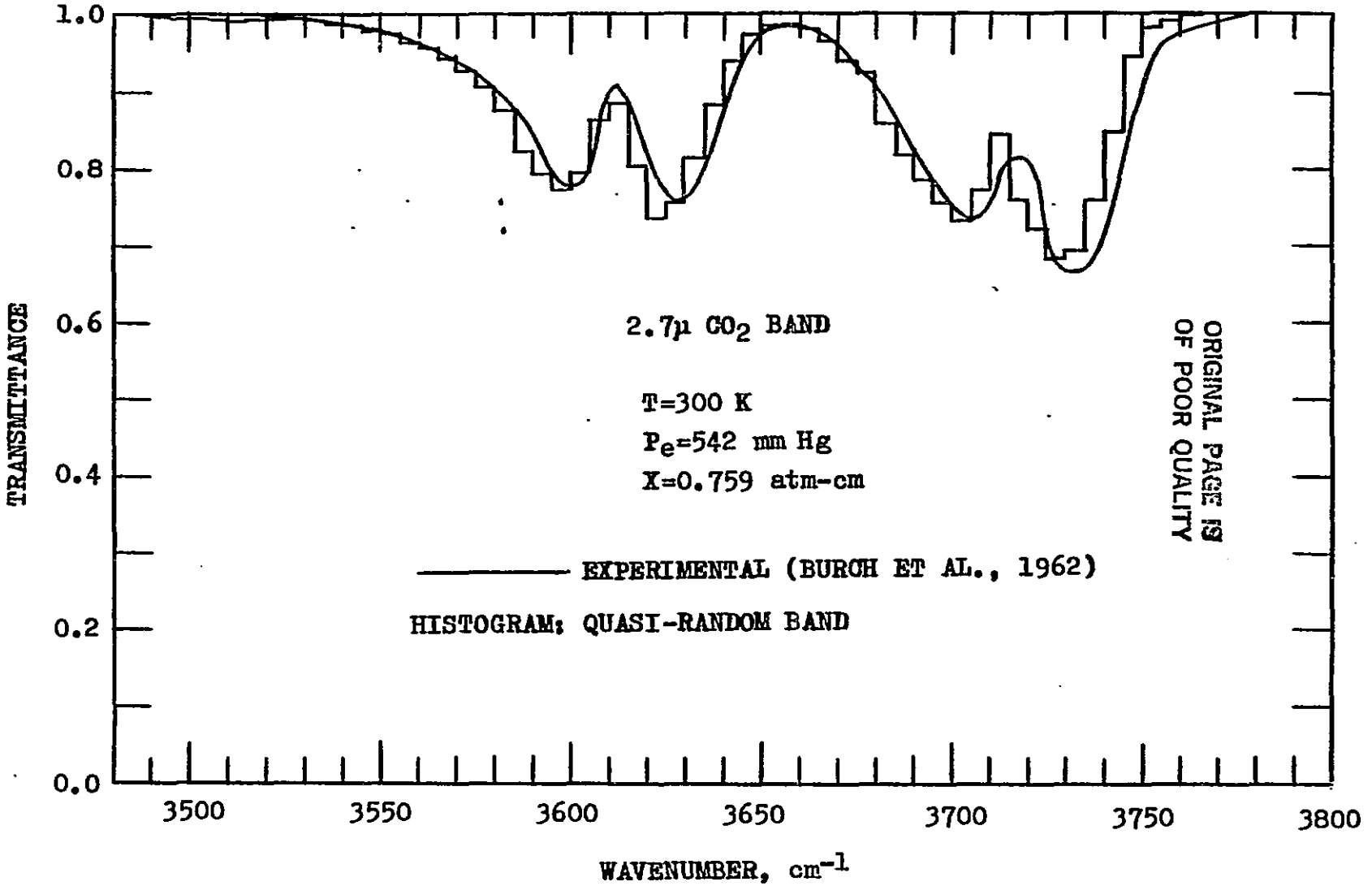

Fig. 5.6 Comparison of transmittances of the 2.7μ CO_2 band.

The total band absorptance results, as calculated by the QRB model (only at 300 K) and wide-band correlations, are presented in Tables 5.9-5.12 for four different temperatures. It should be noted that the QRB model results are not in good agreement with the experimental results for low pressures and small path lengths; however, they are in good agreement for large path lengths. Inspecting the results of wide-band correlations, it is noted that the Edwards and Balakrishnan, and Tien and Lowder results compare well with the experimental results except for a few cases considered. The Felske and Tien's correlation, however, always provides lower values.

5.1.5 Total Emissivity for CO_2

By using the QRB model (only at 300 K) and wide-band correlations, the total emissivity has been calculated according to Eq. (2.2) and Eq. (2.3) for the path lengths from 0.1 to 1000 atm-cm in order to make a comparison with the measured emissivities of Hottel et al. [9]. These results are presented in Figs. 5.7, 5.9, 5.11, and 5.13 for four different temperatures and P_e = 1 atm. The QRB model results are seen to be in quite good agreement for all the path lengths. Among the correlations, the Edwards and Balakrishnan, and Tien and Lowder results show good agreement with the experimental results for long path lengths. The Felske and Tien's correlation yields lower values for all path lengths in all cases considered.

The total emissivity results obtained by using the wide-band correlations are compared in Figs. 5.8, 5.10, 5.12 and 5.14 for four differ-

Table 5.9 Comparison of total band absorptance for the 2.7μ CO_2 band at T=300 K

Effective Pressure	Mass Path Length	Total Band Absorptance Results, A (cm^{-1})							
		Exp. (26)	Quasi-random Band		Edwards & Balakrishnan		Tien & Lowder		Felske & Tien	
P_e (atm)	W (g/m^2)	A_E	A	PD	A	PD	A	PD	A	PD
0.549	1.477	6.5	5.3	-18	5.74	-12	5.36	-18	4.43	-32
0.569	12.25	27.9	25.77	- 7	24.44	-12	28.81	+ 3	18.98	-32
0.676	110.9	98.2	89.53	- 9	86.51	-12	92.02	- 6	62.16	-37
2.33	110.9	127.4	118.38	- 7	125.71	- 1	111.9	-12	77.93	-39
2.72	445.0	179.0	182.0	+ 1	172.34	- 4	170.9	- 4	131.55	-27

PD=((A-A_E)/A_E)X100

Table 5.10 Comparison of total band absorptance for the 2.7μ CO_2 band at T=555 K

Effective Pressure	Mass Path Length	Total Band Absorptance Results, A (cm^{-1})						
		Exp. (28)	Edwards & Balakrishnan		Tien & Lowder		Felske & Tien	
P_e (atm)	W (g/m^2)	A_E	A	PD	A	PD	A	PD
0.26	4.76	15.0	16.8	+12	16.5	+10	12.6	-16
0.99	18.3	44.4	55.7	+25	53.6	+21	38.3	-14
1.04	41.0	89.0	93.5	+ 5	90.0	+ 1	61.6	-31
1.04	411.0	253.0	244.9	- 3	242.7	- 4	198.5	-22
12.9	3670.0	343.0	366.0	+ 7	369.1	+ 8	321.8	- 6

PD=((A-A_E)/A_E)X100

Table 5.11 Comparison of total band absorptance for the 2.7μ CO_2 band at T=830 K

Effective Pressure	Mass Path Length	Total Band Absorptance Results, A (cm^{-1})						
		Exp. (28)	Edwards & Balakrishnan		Tien & Lowder		Felske & Tien	
P_e (atm)	W (g/m^2)	A_E	A	PD	A	PD	A	PD
1.04	27.4	83.0	106.2	+28	86.0	+ 4	66.8	-20
1.33	249.0	269.0	257.7	- 4	247.2	- 8	191.7	-29
12.9	2480.0	387.0	413.9	+ 7	417.8	+ 8	368.4	- 5

$PD=((A-A_E)/A_E)X100$

Table 5.12 Comparison of total band absorptance for the 2.7μ CO_2 band at T=1110 K

Effective Pressure	Mass Path Length	Total Band Absorptance Results, A (cm^{-1})						
		Exp. (28)	Edwards & Balakrishnan		Tien & Lowder		Felske & Tien	
P_e (atm)	W (g/m^2)	A_E	A	PD	A	PD	A	PD
1.05	1.92	9.5	9.7	+ 2	9.4	- 1	9.2	- 3
1.07	21.0	65.5	101.7	+55	81.5	+24	70.1	+ 7
0.31	63.8	114.0	184.7	+62	161.2	+41	119.1	+ 4
1.04	20.0	105.0	97.9	- 7	78.5	-25	67.6	-36
1.3	187.0	280.0	273.0	- 3	262.3	- 6	213.3	-24
1.31	1891.0	415.0	454.2	+ 9	458.2	+10	406.9	- 2

PD=((A-A_E)/A_E)X100

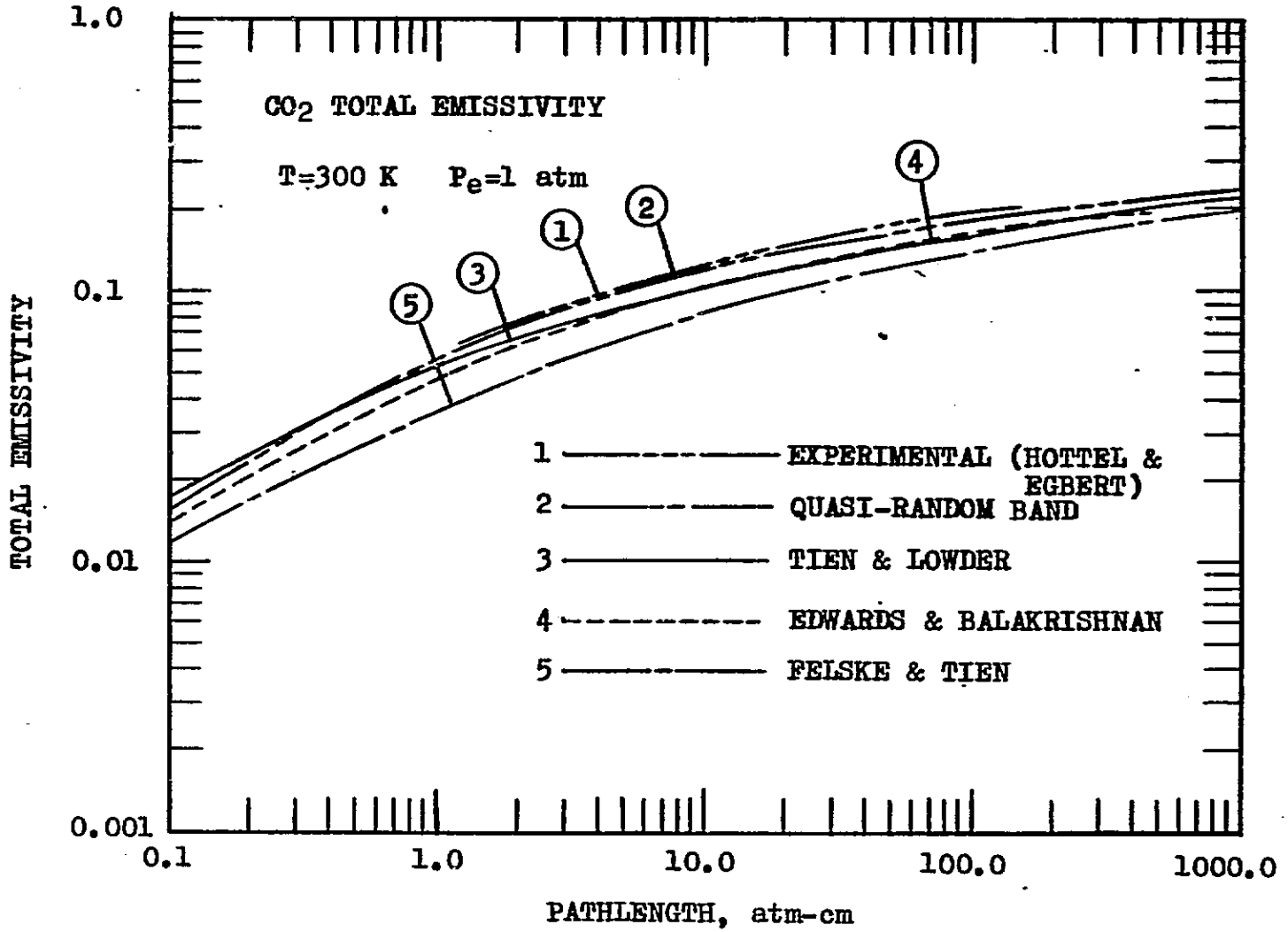

Fig. 5.7 Comparison of total emissivity of carbon dioxide at T=300 K.

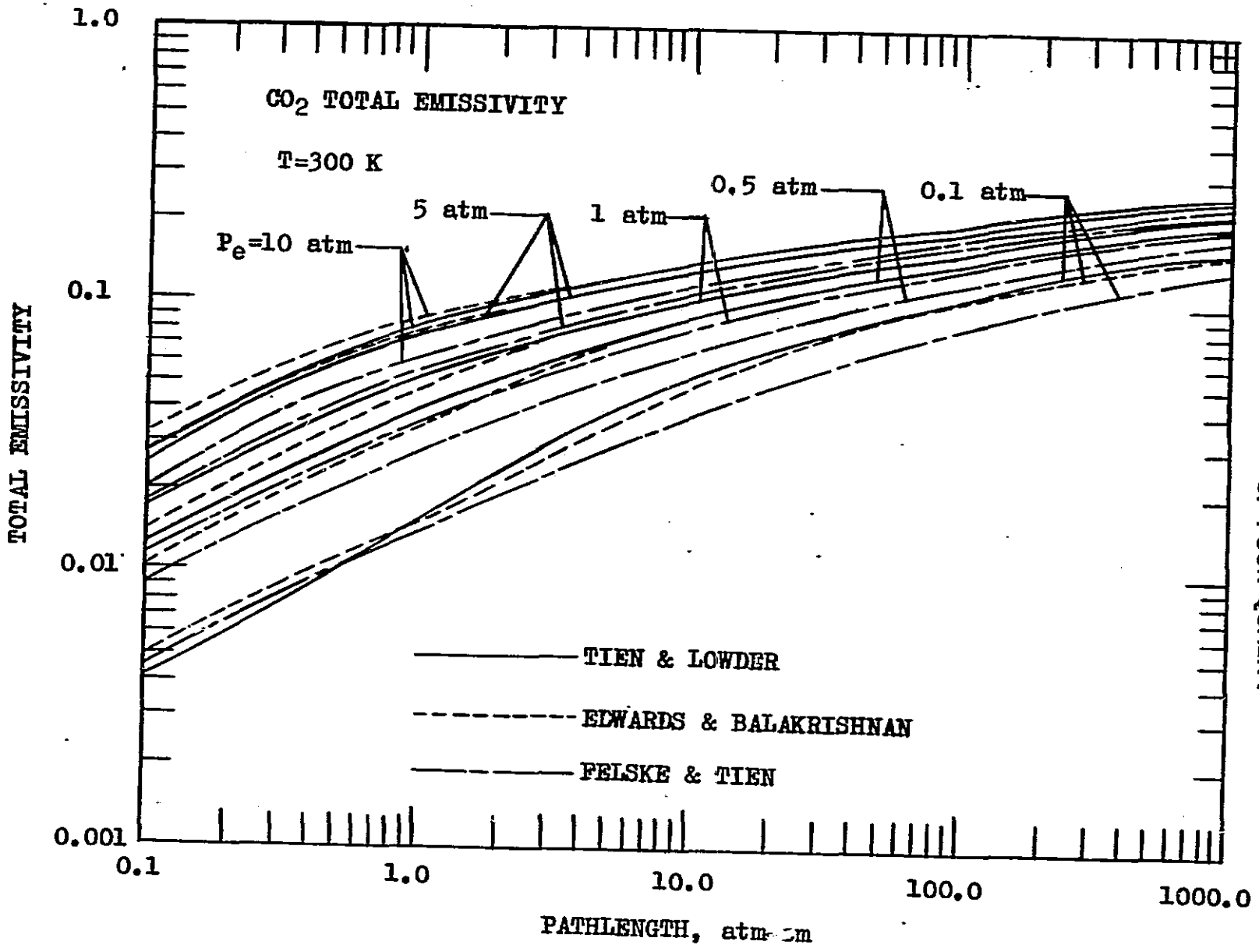

Fig. 5.8 Comparison of results of total emissivity by using wide band correlations.

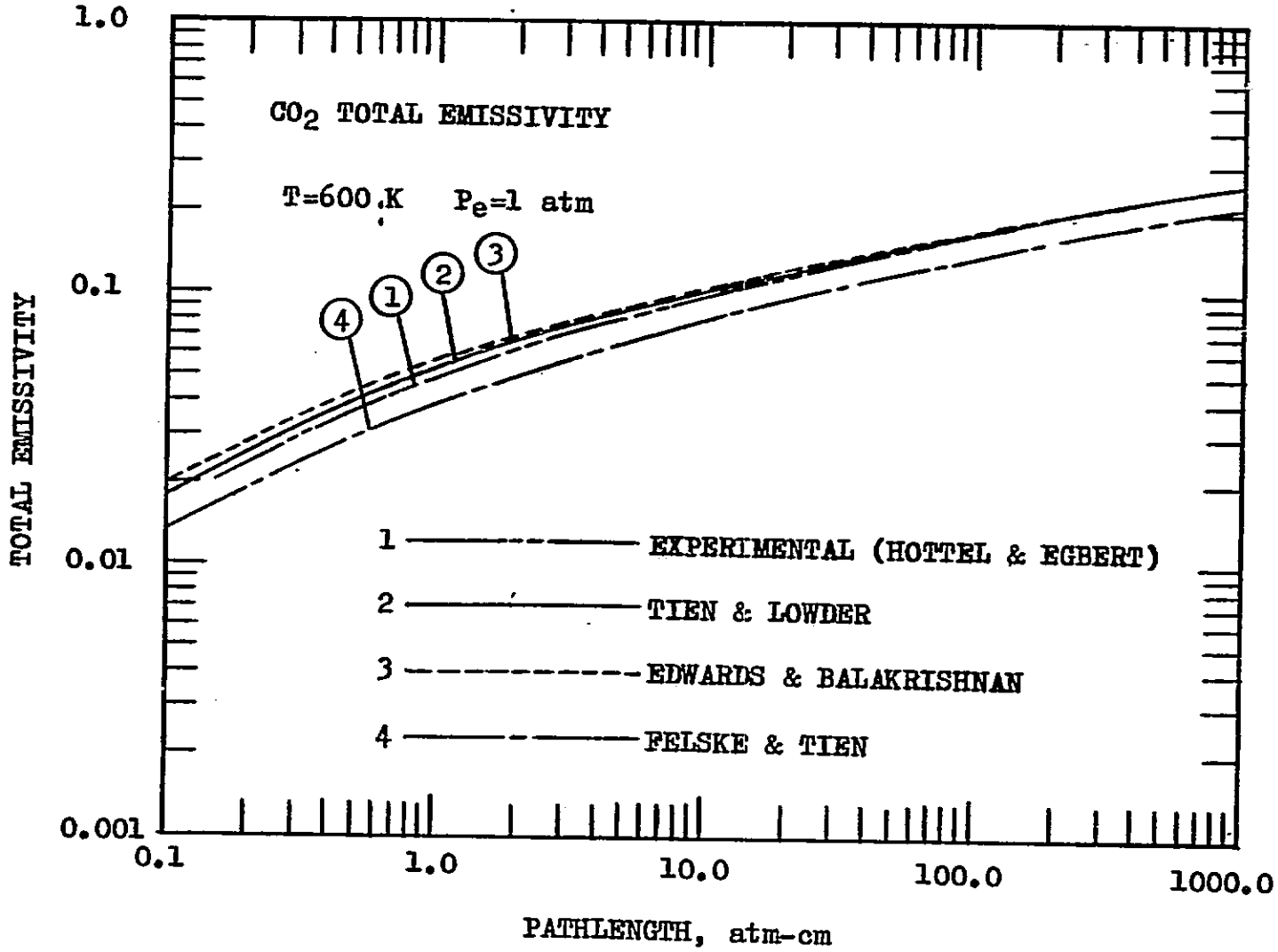

Fig. 5.9 Comparison of total emissivity of carbon dioxide at T=600 K.

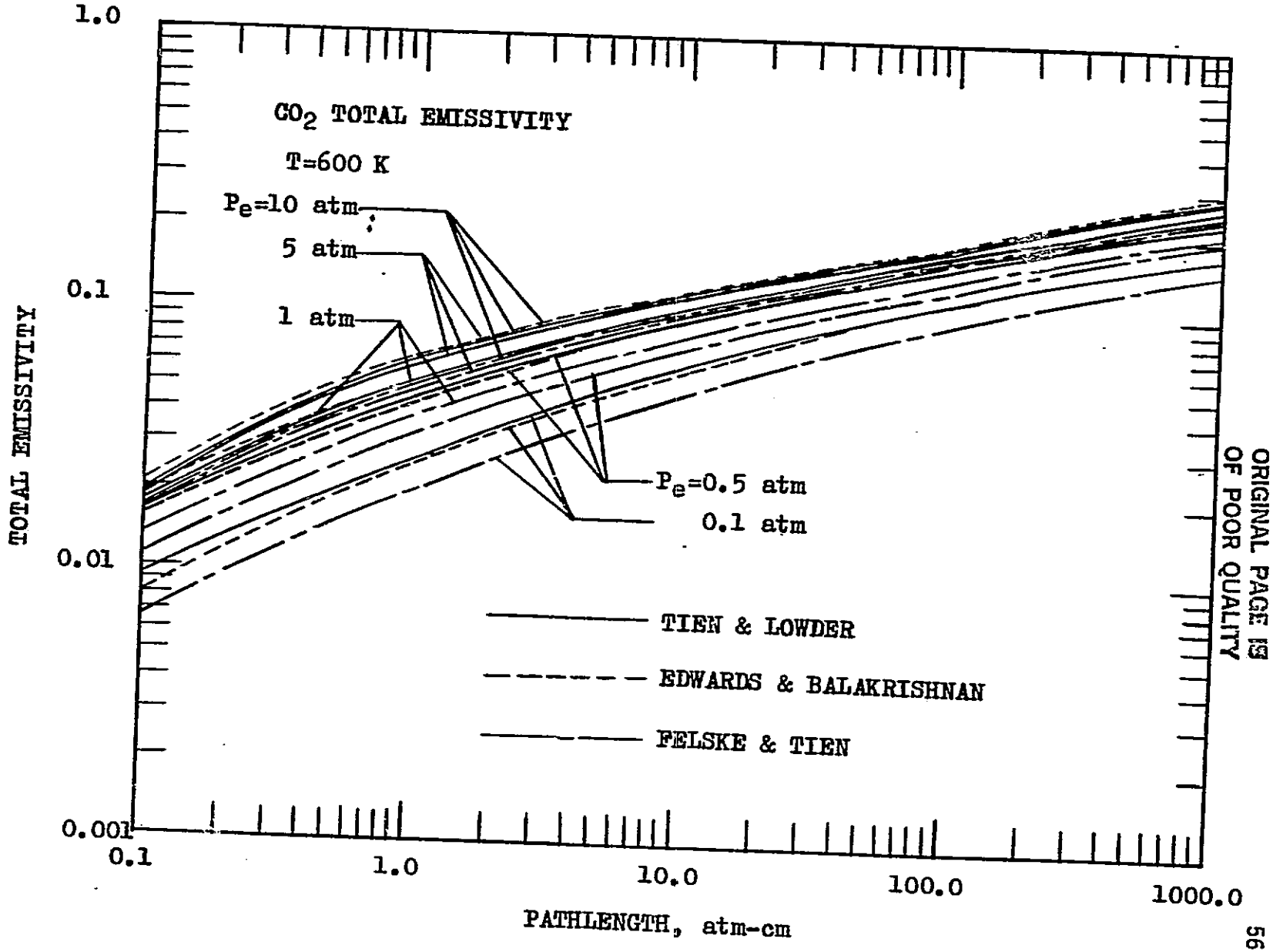

Fig. 5.10 Comparison of results of total emissivity by using wide band correlations.

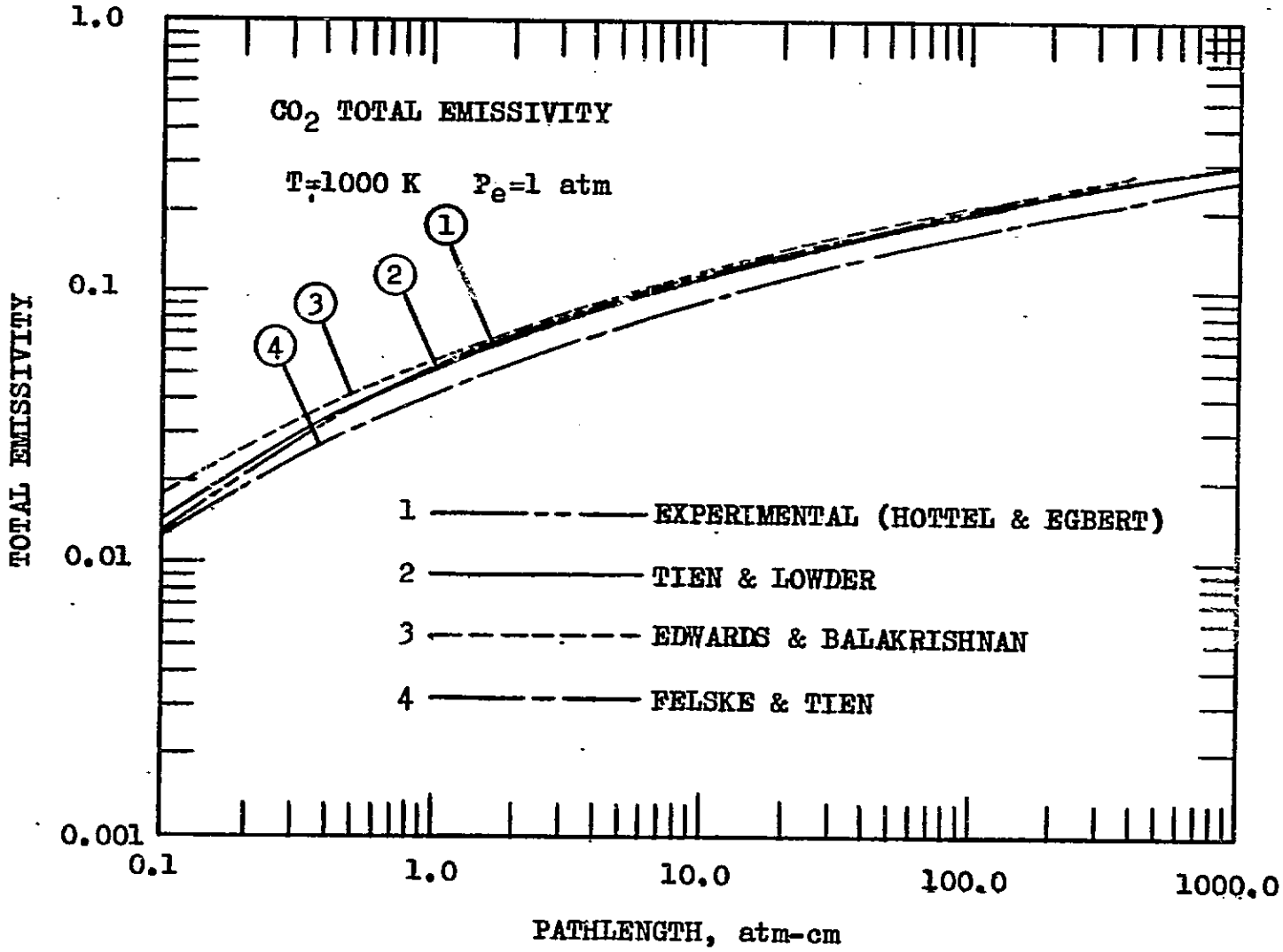

Fig. 5.11 Comparison of total emissivity of carbon dioxide at T=1000 K.

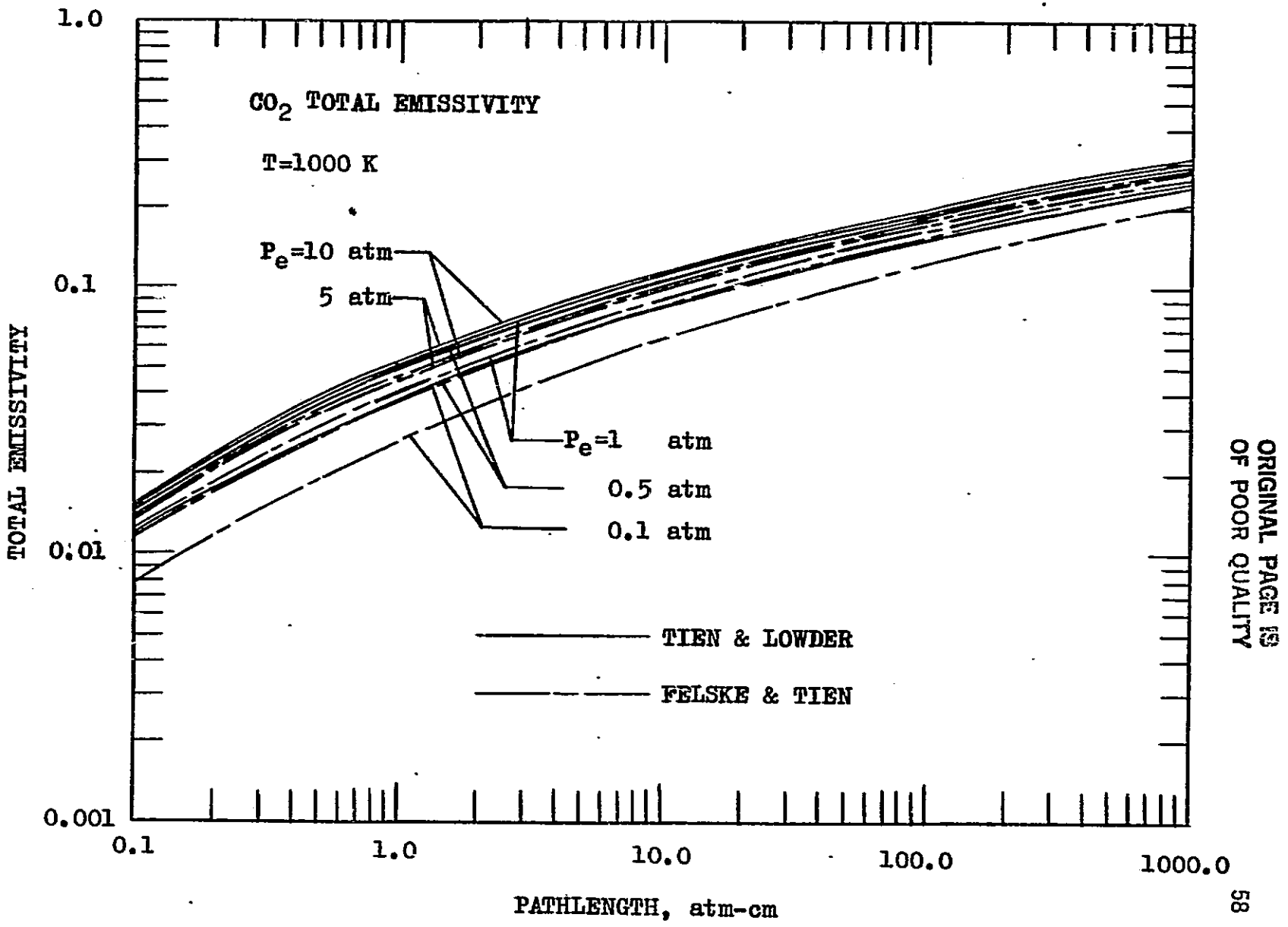

Fig. 5.12 Comparison of results of total emissivity by using wide band correlations.

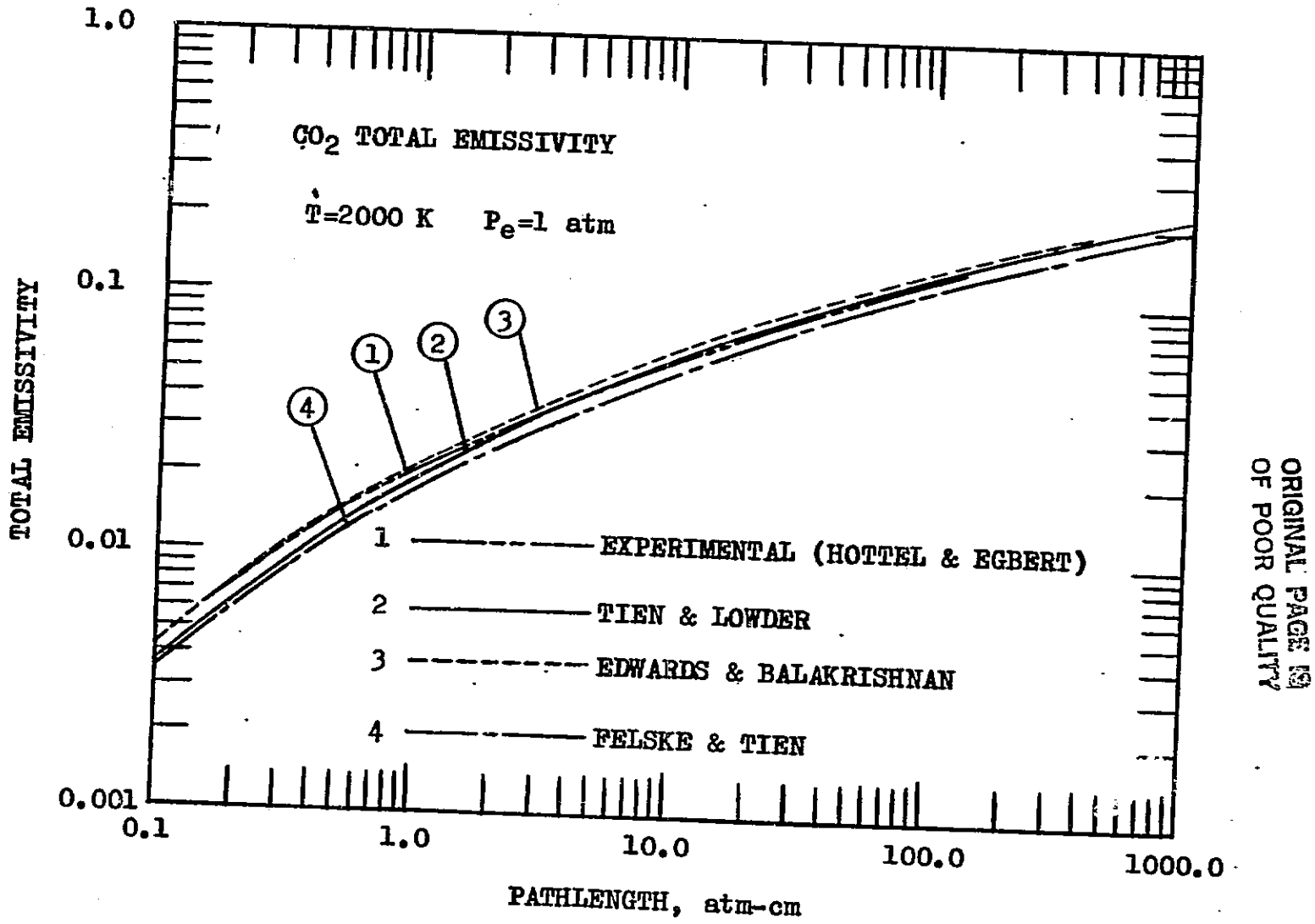

Fig. 5.13 Comparison of total emissivity of carbon dioxide at T=2000 K.

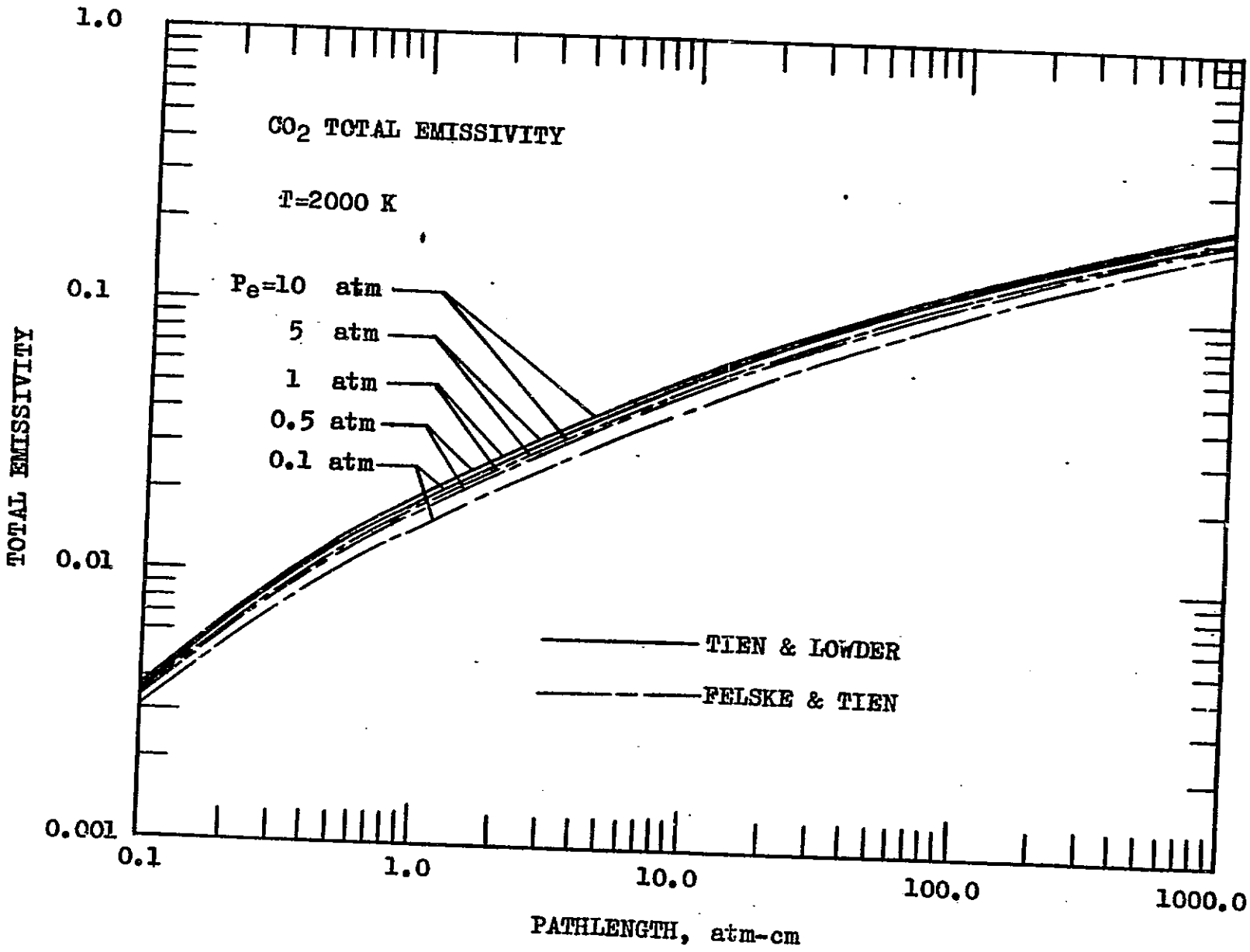

Fig. 5.14 Comparison of total emissivity of carbon dioxide at T=2000 K.

ent temperatures and five different effective broadening pressures. It is noted that the Felske and Tien's results are always lower than the results of other two correlations. This can be expected because the general statistical model always predicts lower absorption than the Elsasser model due to more overlapping of the spectral lines in the statistical models. At low pressures, the Tien and Lowder's results do not follow the trend of other results. This would be expected because the low-pressure situation corresponds to the case of the square-root limit which is not satisfied by the Tien and Lowder's correlation. Therefore, use of the Tien and Lowder's correlation is not recommended for low pressures. For large path lengths, the Edwards and Balakrishnan, and Tien and Lowder correlations will give close results. For small path lengths, the Edwards and Balakrishnan's correlation provides lower results at low pressures while it yields higher results at high pressures than the Tien and Lowder's correlation.

5.2 Homogeneous Results for Water Vapor

The spectral transmittance and total band absorptance results of selected bands (rotational, 6.3μ H_2O, 2.7μ H_2O and 1.87μ H_2O), as well as the results of total emissivity, of water vapor are presented in this section.

5.2.1 Rotational Band

The results for spectral emissivities obtained by the QRB model are

compared with the experimental results of Ludwig et al. [17] in Figs. 5.15-5.20 for six different temperatures and path lengths. The QRB model results, in general, are seen to be higher than the experimental data. The results for T = 590 K (Fig. 5.15) appear to be relatively in good agreement indicating that at low temperatures the QRB model will provide accurate results. The agreements, however, are not good for the temperature range of 800-1,800 K. For T = 2,000 K, the QRB results are lower at shorter wavelengths and relatively higher at longer wavelengths. The behavior exhibited in these figures could be due to a combination of several factors; but, overlapping of the spectral lines at higher temperatures will play the major role. At higher temperatures, the spectral lines overlap considerably and the QRB model does not account for this effect accurately. However, one can expect the QRB model to yield accurate results at temperatures closer to the room temperature since the line parameters are compiled at this temperature.

5.2.2 6.3μ H_2O Band

The comparison of spectral transmittance of this band is shown in Figs. 5.21a-5.21c. In order to present these results clearly, it is necessary to show them in three figures. The QRB model results show a quite good agreement with the experimental results.

The total band absorptance results of this band are shown in Tables 5.13-5.16 for four different temperatures. The QRB model results presented in Table 5.13 for T = 300 K provide higher values at low pressures; however, the results agree very well with the experimental

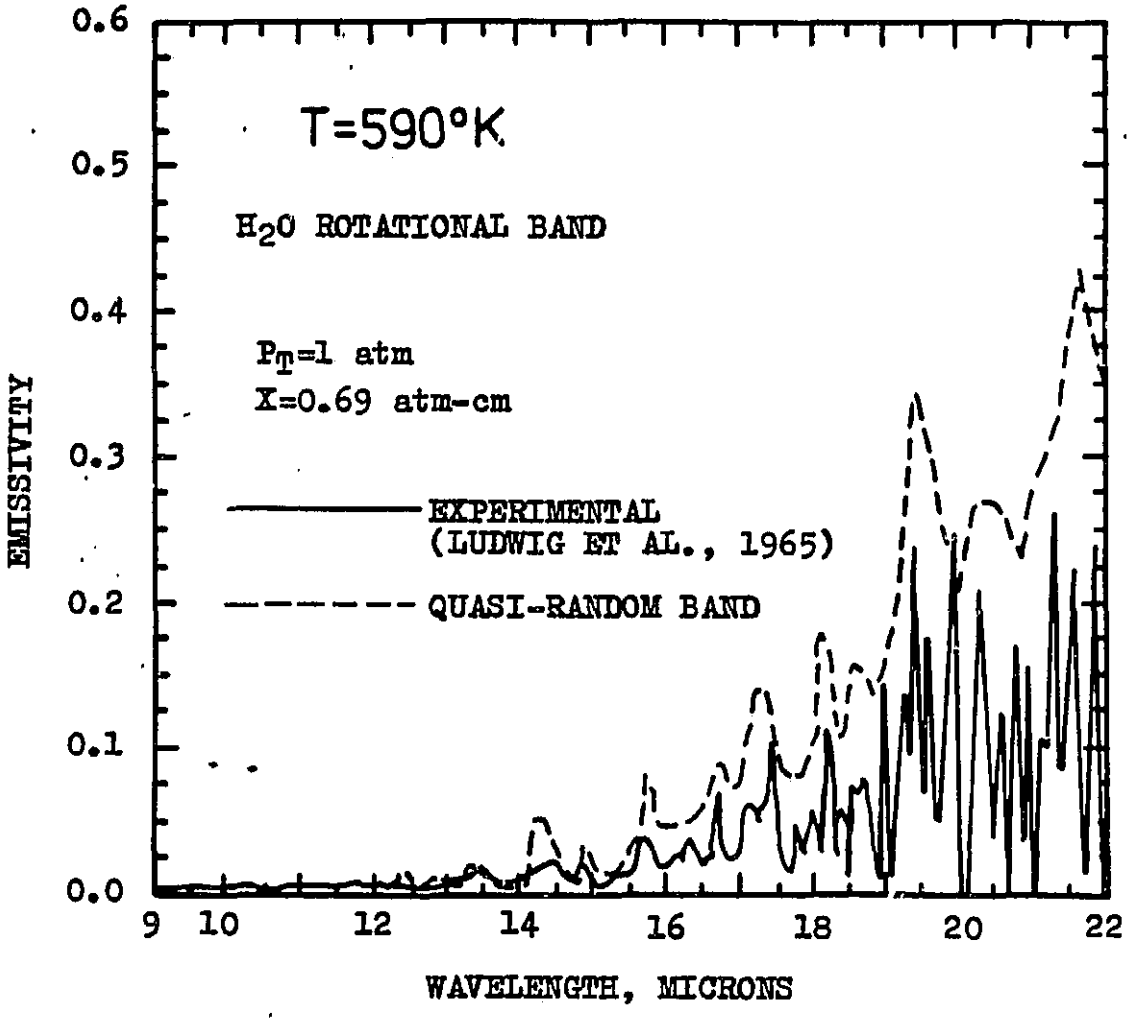

Fig. 5.15 Comparison of spectral emissivities of the rotational band of H_2O at T=590 K.

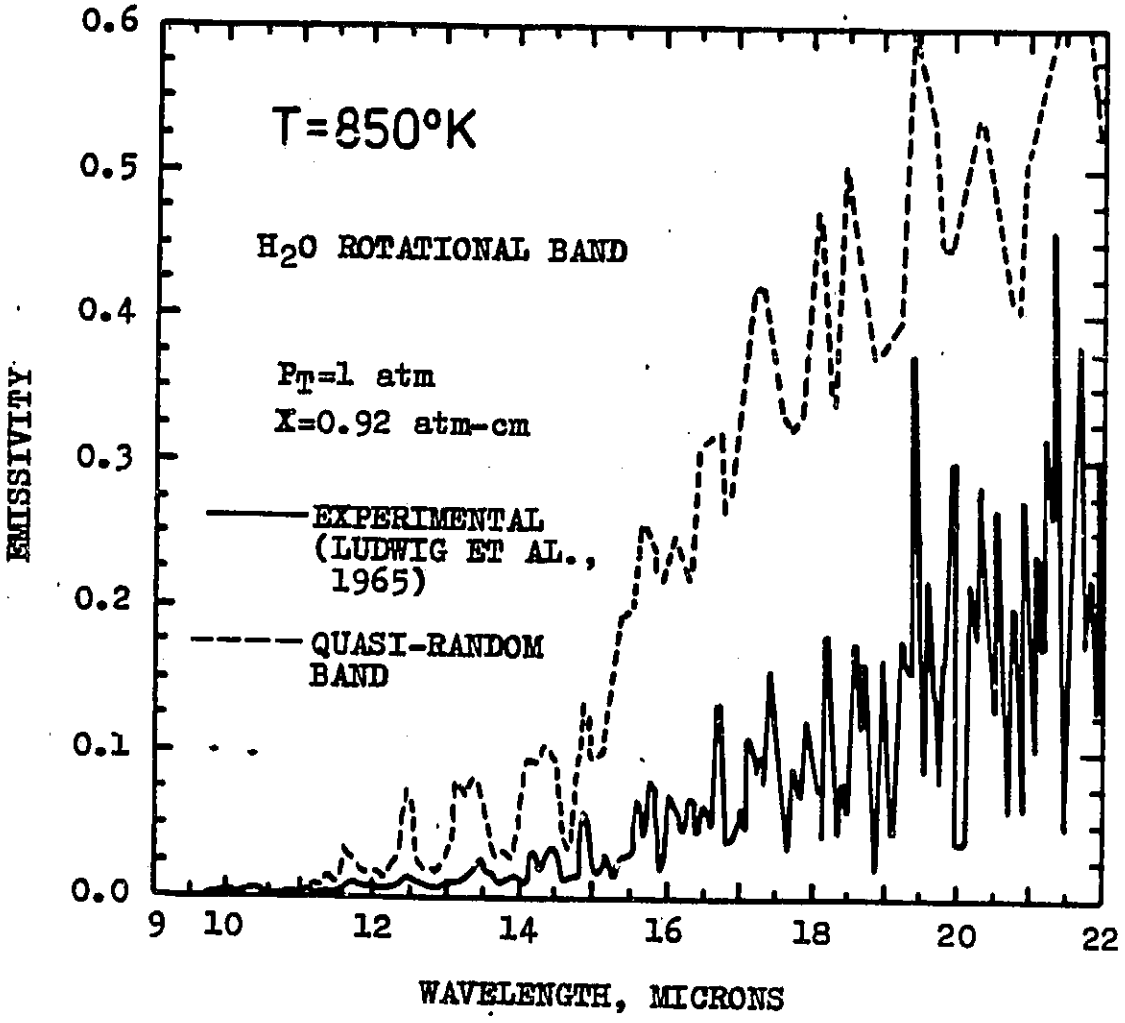

Fig. 5.16 Comparison of spectral emissivities of the rotational band of H_2O at T=850 K.

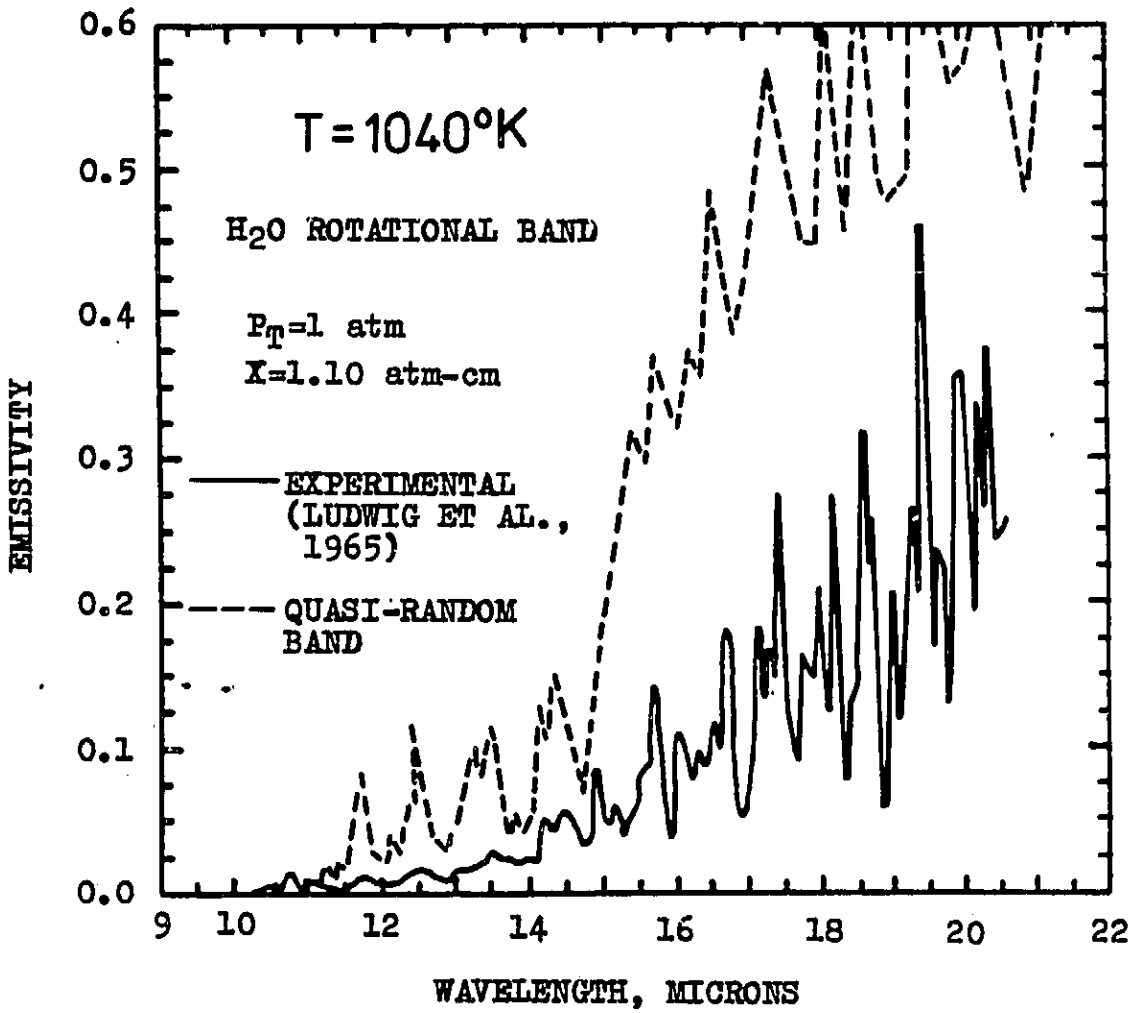

Fig. 5.17 Comparison of spectral emissivities of the rotational band of H_2O at T=1040 K.

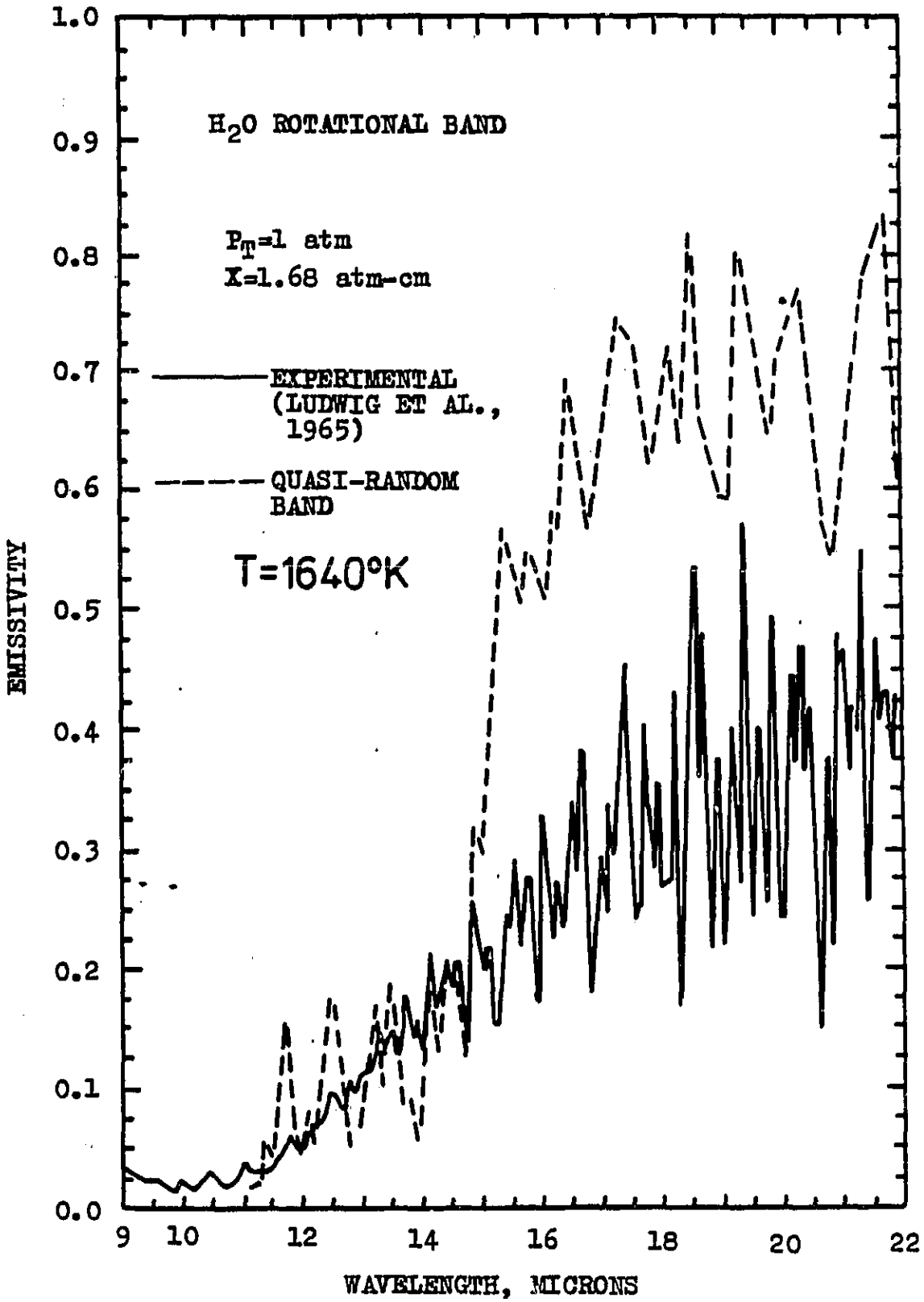

Fig. 5.18 Comparison of spectral emissivities of the rotational band of H_2O at T=1640 K.

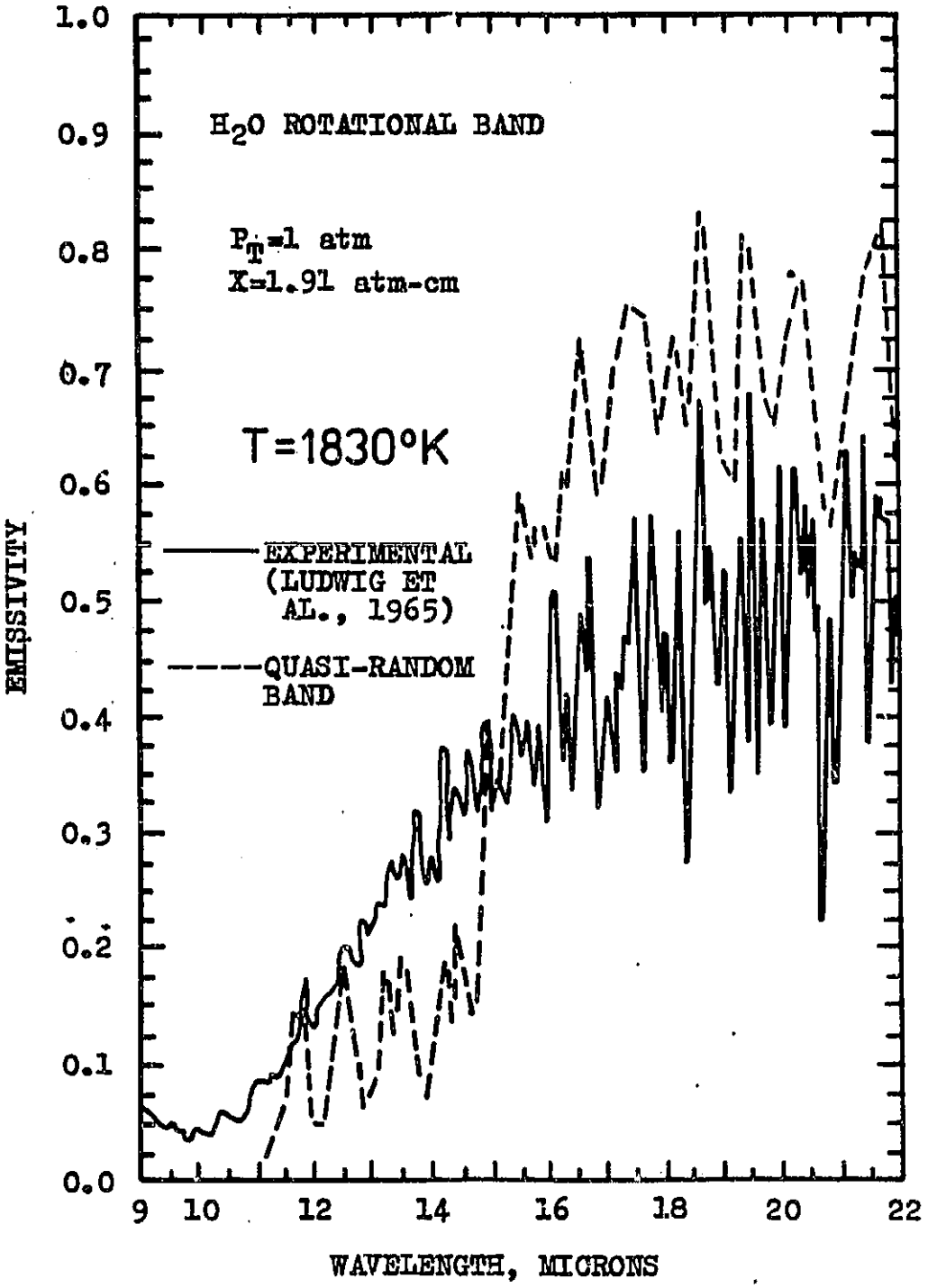

Fig. 5.19 Comparison of spectral emissivities of the rotational band of H_2O at T=1640 K.

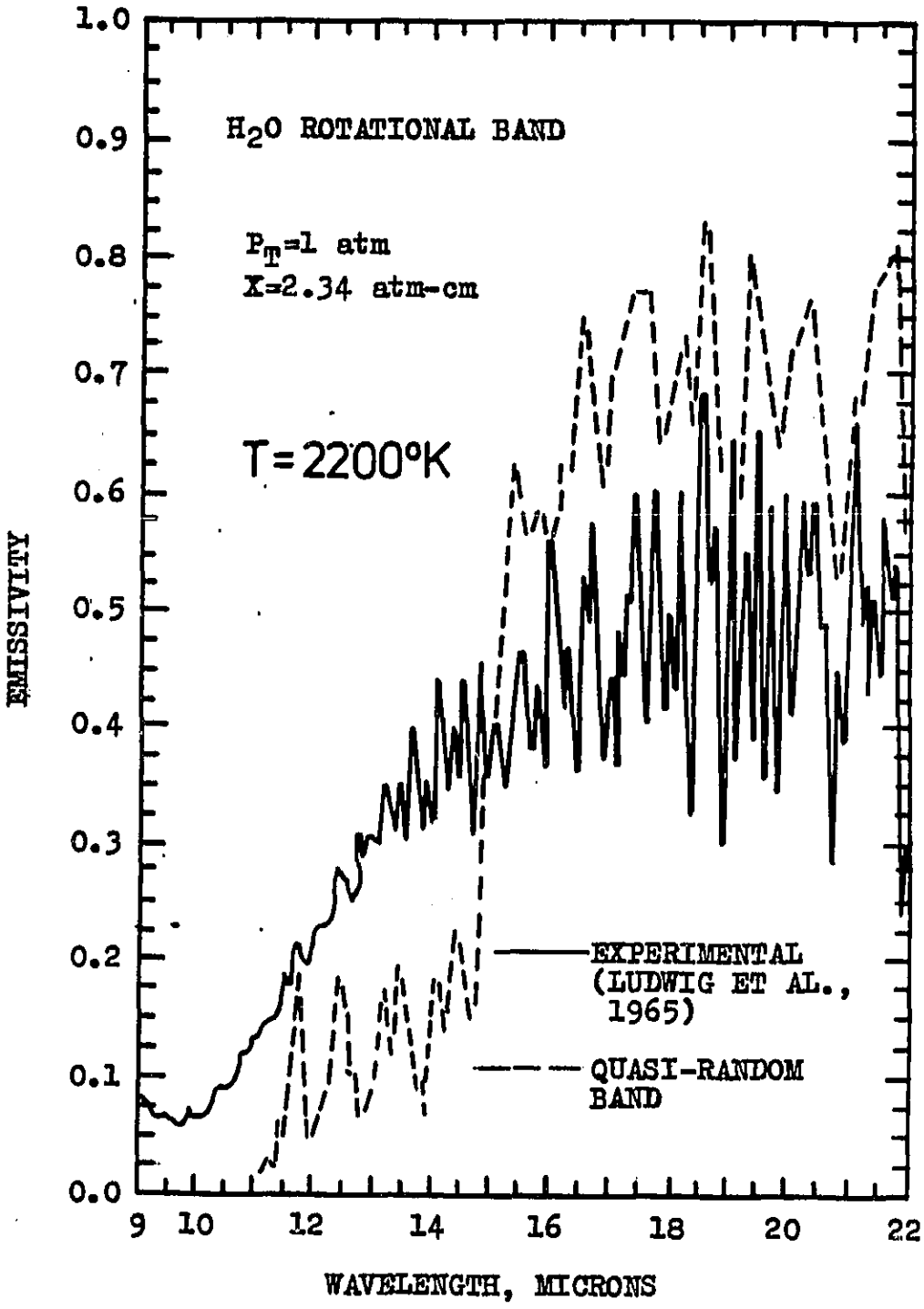

Fig. 5.20 Comparison of spectral emissivities of the rotational band of H_2O at T=2200 K.

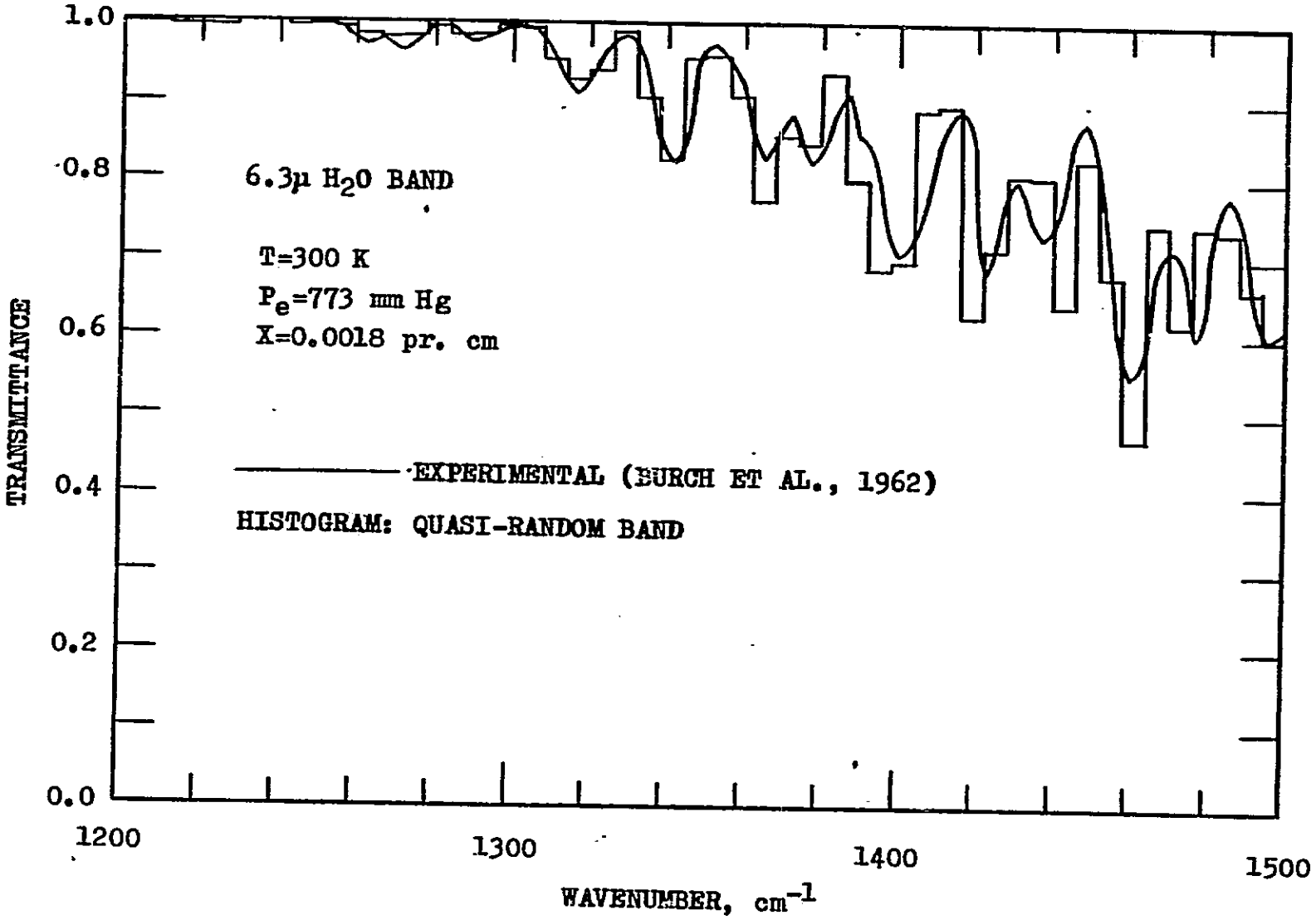

Fig. 5.21a Comparison of transmittances of the 6.3μ H_2O band.

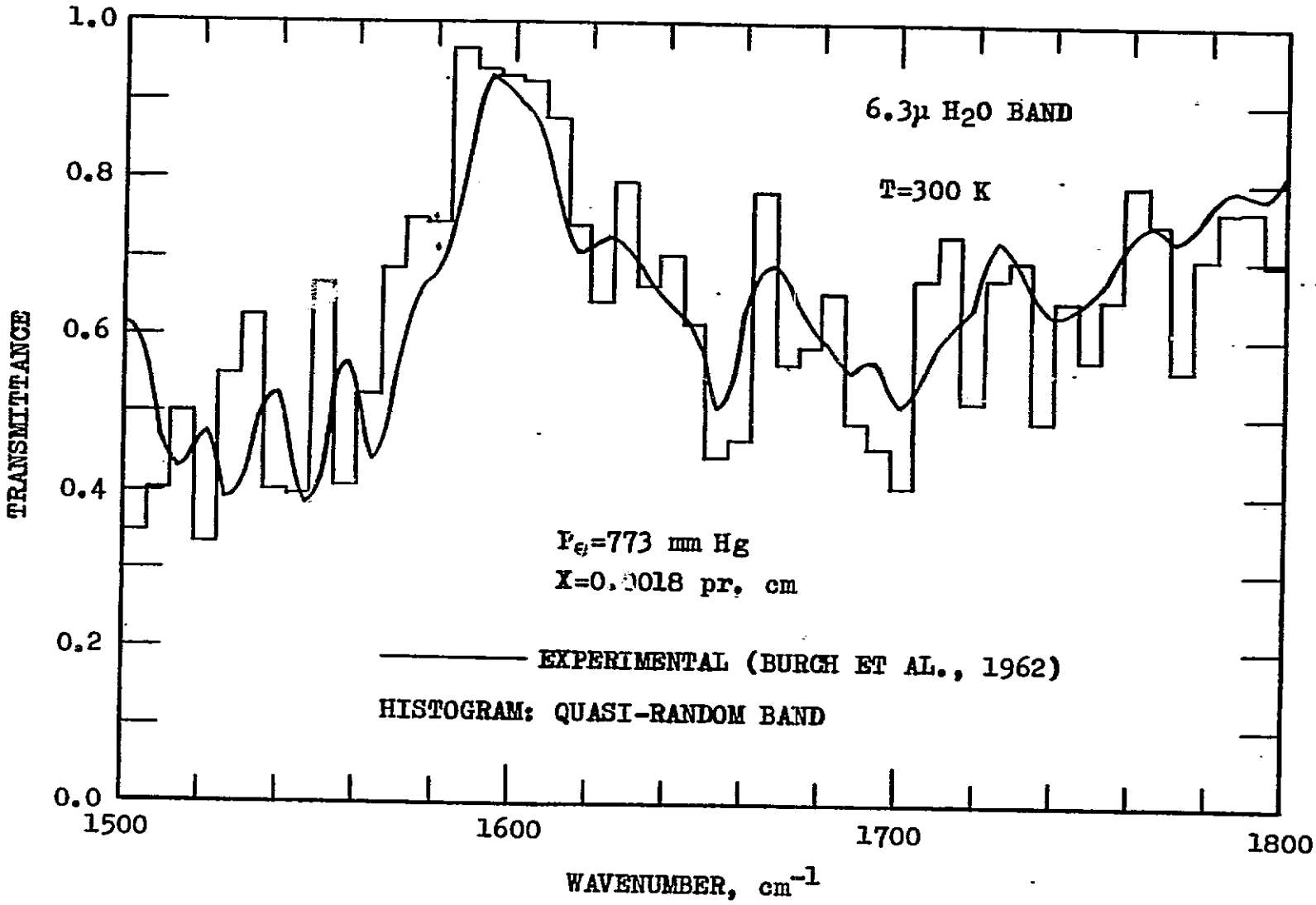

Fig. 5.21b Comparison of transmittances of the 6.3μ H_2O band.

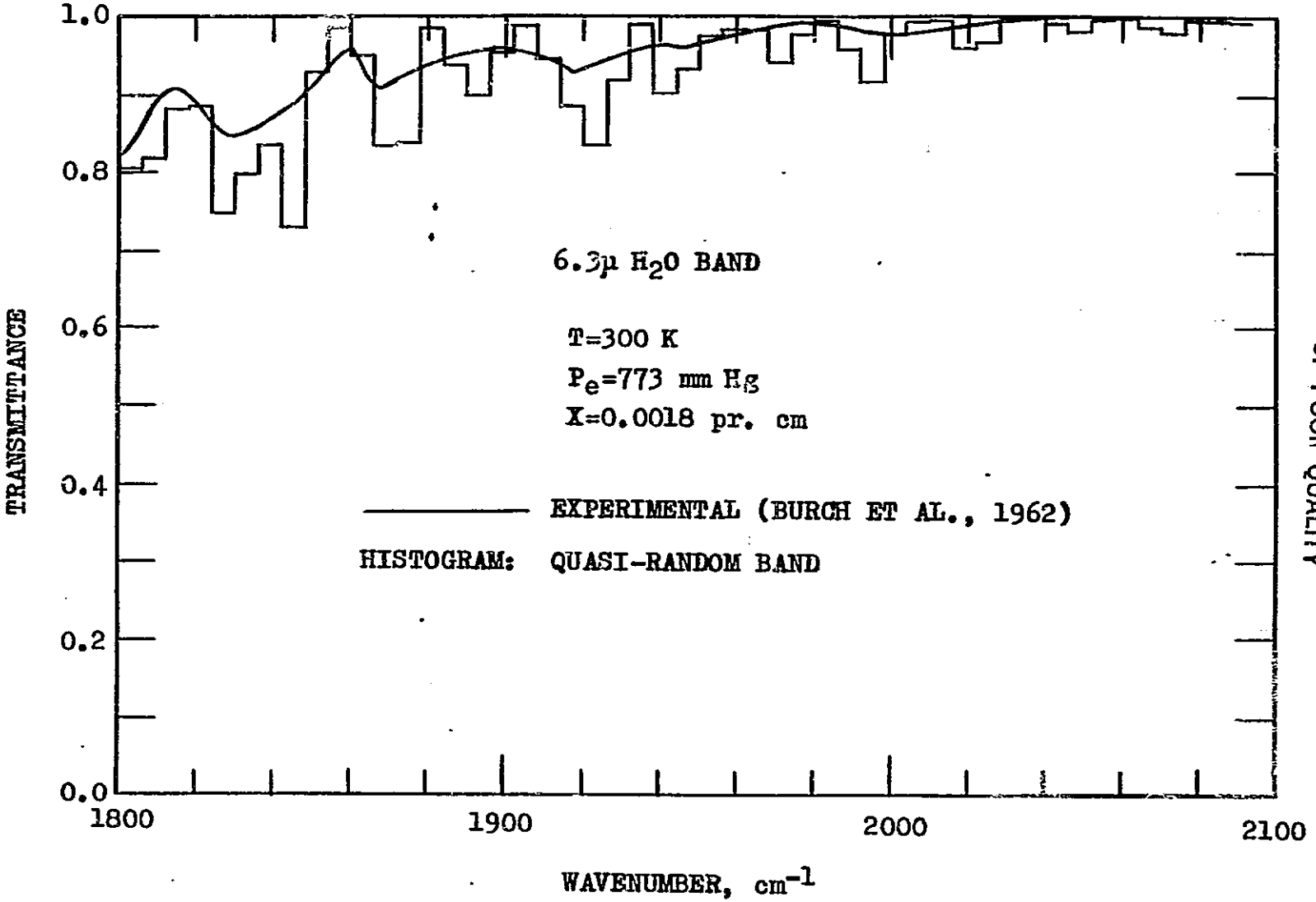

Fig. 5.21c Comparison of transmittances of the 6.3μ H_2O band.

Table 5.13 Comparison of total band absorptance for the 6.3μ H_2O band at T=300 K

Effective Pressure	Mass Path Length	Total Band Absorptance Results, A (cm^{-1})							
		Exp. (26)	Quasi-random Band		Edwards & Balakrishnan		Tien & Lowder		Felske & Tien	
P_e (atm)	W (g/m^2)	A_E	A	PD	A	PD	A	PD	A	PD
0.02	17.0	25.0	32.7	+30	18.0	-28	7.6	-70	17.18	-31
0.02	34.0	31.8	46.4	+46	25.51	-20	13.16	-59	24.16	-24
1.016	36.0	216.0	230.9	+ 7	178.87	-17	200.6	- 7	137.69	-36
1.038	95.0	335.0	337.86	+ 1	275.22	-18	285.15	-15	205.53	-39
0.658	95.0	287.0	297.4	+ 3	232.75	-19	246.78	-14	176.12	-39

PD=$((A-A_E)/A_E)X100$

Table 5.14 Comparison of total band absorptance for the 6.3μ H_2O band at T=555 K

Effective Pressure	Mass Path Length	Total Band Absorptance Results, A (cm^{-1})						
		Exp. (27)	Edwards & Balakrishnan		Tien & Lowder		Felske & Tien	
P_e (atm)	W (g/m^2)	A_E	A	PD	A	PD	A	PD
10.0	307.0	764.0	722.4	- 5	713.2	- 7	584.0	-24
5.0	153.0	621.0	576.8	- 7	571.6	- 8	442.6	-29
3.02	89.0	503.0	453.3	-10	455.5	- 9	333.1	-34
3.185	16.3	235.0	233.6	- 1	249.1	+ 6	164.0	-30
1.527	16.3	178.7	167.3	- 6	199.1	+11	130.1	-27
0.712	16.3	147.2	116.6	-21	142.0	- 4	98.4	-33
1.532	15.3	182.0	161.7	-11	193.4	+ 6	126.2	-31
1.342	6.92	108.9	98.8	- 9	121.7	+12	79.2	-27
1.237	1.79	53.0	43.7	-18	50.1	- 5	34.4	-35

$PD=((A-A_E)/A_E)X100$

Table 5.15 Comparison of total band absorptance for the 6.3μ H_2O band at T=833 K

Effective Pressure	Mass Path Length	Total Band Absorptance Results, A (cm^{-1})						
		Exp. (27)	Edwards & Balakrishnan		Tien & Lowder		Felske & Tien	
P_e (atm)	W (g/m^2)	A_E	A	PD	A	PD	A	PD
10.0	204.0	766.0	799.7	+ 4	786.2	+ 3	633.9	-17
5.45	108.0	542.0	654.8	+21	640.4	+18	486.7	-10
5.0	102.0	594.0	636.8	+ 7	624.0	+ 5	470.6	-21
3.03	60.8	479.0	495.7	+ 3	494.1	+ 3	350.6	-27
3.19	10.9	194.7	228.0	+17	237.1	+22	158.1	-19
1.526	10.9	174.5	166.2	- 5	197.3	+13	127.2	-27
0.718	10.9	112.9	118.2	+ 5	146.4	+30	98.1	-13
1.346	4.56	106.3	95.7	-10	112.4	+ 6	74.2	-30
1.248	1.19	26.8	39.7	+48	40.4	+51	30.2	+13

$PD=((A-A_E)/A_E)X100$

Table 5.16 Comparison of total band absorptance for the 6.3μ H_2O band at T=1111 K

Effective Pressure	Mass Path Length	Total Band Absorptance Results, A (cm^{-1})						
		Exp. (27)	Edwards & Balakrishnan		Tien & Lowder		Felske & Tien	
P_e (atm)	W (g/m^2)	A_E	A	PD	A	PD	A	PD
10.0	153.0	779.0	848.3	+ 9	836.0	+ 7	673.5	-14
5.0	76.7	654.0	689.8	+ 5	663.5	+ 1	497.1	-24
3.0	45.3	467.0	535.7	+15	521.0	+12	366.0	-22
3.0	45.0	479.0	534.4	+12	519.8	+ 9	365.0	-24
3.19	8.23	193.2	232.2	+20	222.3	+15	156.6	-19
1.54	8.21	153.2	175.2	+14	195.7	+28	128.9	-16
0.71	8.18	98.5	125.4	+27	154.2	+57	100.6	+ 2
1.346	3.49	95.2	98.3	+ 3	105.2	+10	73.4	-33
1.238	0.887	34.6	35.5	+ 3	33.0	- 5	27.1	-22

$PD=((A-A_E)/A_E)X100$

results at high pressures and long path lengths. Among the results of the correlations, it is noted that all the correlations underestimate the absorptance at low temperatures. At high temperatures, the Edwards and Balakrishnan, and Tien and Lowder correlations can predict the total band absorptance with reasonable accuracy. The Felske and Tien's results are always found to be lower than the experimental results by about 20 to 40 percent.

5.2.3 2.7μ H_2O Band

Figures 5.22 and 5.23 illustrate a comparison of the spectral transmittance results, as calculated by the QRB model, with the experimental results for two pressures and path lengths. These results disagree in the wing regions of the band, although they agree well in the central portion.

The total band absorptance results calculated by the QRB model and wide-band correlations are compared with the experimental results in Tables 5.17-5.20. The QRB model is found to estimate the absorptance of this band quite accurately. Among the results of correlations, the Edwards and Balakrishnan, and Tien and Lowder correlations yield good agreement with experimental results for high pressures and large path lengths; however, they overestimate the band absorption by about 20 percent for low pressures and small path lengths. Note again, that the Felske and Tien's correlation usually underestimates the total band absorptance by about 20 percent.

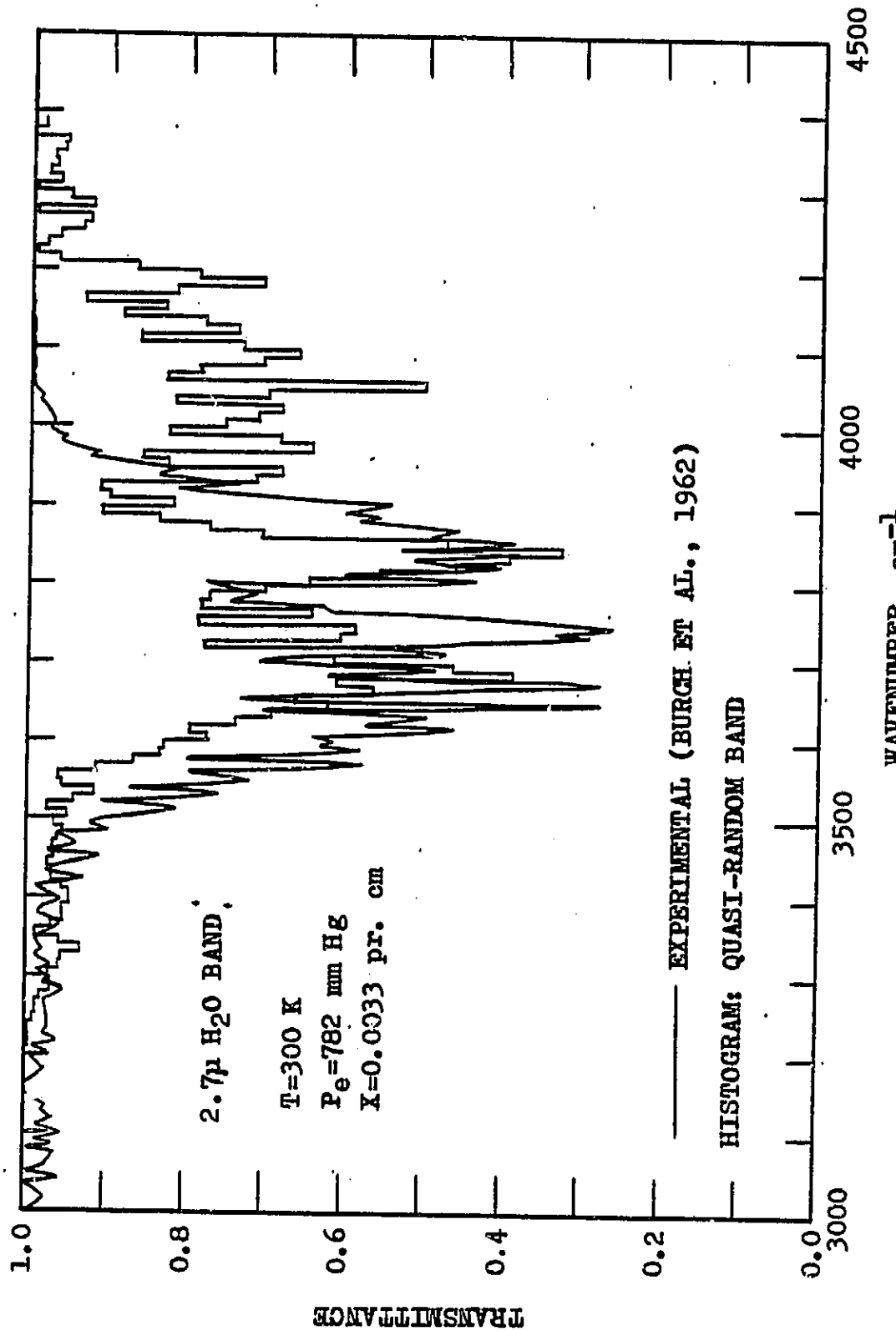

Fig. 5.22 Comparison of transmittances of the 2.7μ H_2O band.

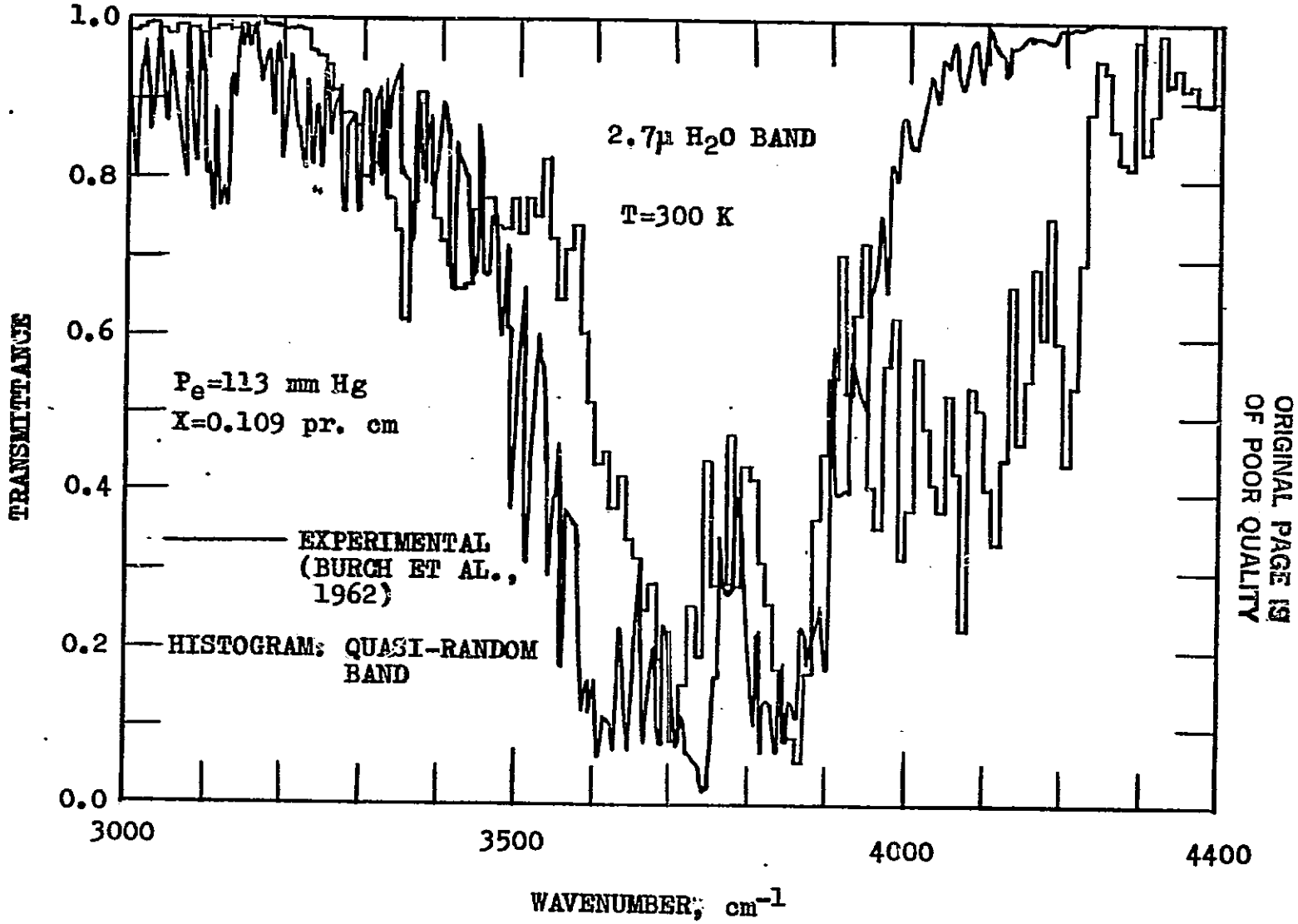

Fig. 5.23 Comparison of transmittances of the 2.7μ H_2O band.

Table 5.17 Comparison of total band absorptance for the 2.7μ H_2O band at T=300 K

Effective Pressure P_e (atm)	Mass Path Length W (g/m^2)	Total Band Absorptance Results, A (cm^{-1})								
		Exp. (27)	Quasi-random Band		Edwards & Balakrishnan		Tien & Lowder		Felske & Tien	
		A_E	A	PD	A	PD	A	PD	A	PD
1.032	23.8	155.0	170.3	+10	175.63	+13	193.6	+25	127.02	-18
0.557	23.8	125.0	139.3	+11	132.04	+ 6	157.7	+26	103.83	-17
0.044	172.0	141.8	140.9	- 1	105.23	-26	116.37	-18	92.6	-35
0.106	644.0	339.8	352.65	+ 4	294.8	-13	304.87	-10	225.34	-34

$PD=((A-A_E)/A_E)X100$

Table 5.18 Comparison of total band absorptance for the 2.7μ H_2O band at T=555 K

Effective Pressure	Mass Path Length	Total Band Absorptance Results, A (cm^{-1})						
		Exp. (27)	Edwards & Balakrishnan		Tien & Lowder		Felske & Tien	
P_e (atm)	W (g/m^2)	A_E	A	PD	A	PD	A	PD
10.0	307.0	740.0	705.4	- 5	704.4	- 5	583.3	-21
5.0	153.0	559.0	598.0	+ 7	580.9	+ 4	452.2	-19
3.02	89.0	470.7	488.5	+ 4	473.3	+ 1	347.1	-26
3.19	16.3	197.4	253.0	+28	229.4	+16	161.7	-18
1.526	16.3	156.0	189.4	+21	203.9	+31	134.2	-14
0.712	16.3	116.3	135.8	+17	164.4	+41	106.2	- 9
1.526	15.3	151.2	182.6	+21	196.7	+30	129.7	-14
1.346	6.92	96.4	107.9	+12	115.9	+20	78.9	-18
1.238	1.78	32.6	41.2	+26	38.8	+19	30.8	- 6

$PD=((A-A_E)/A_E)X100$

Table 5.19 Comparison of total band absorptance for the 2.7μ H_2O band at T=833 K

Effective Pressure	Mass Path Length	Total Band Absorptance Results, A (cm^{-1})						
		Exp. (27)	Edwards & Balakrishnan		Tien & Lowder		Felske & Tien	
P_e (atm)	W (g/m^2)	A_E	A	PD	A	PD	A	PD
10.0	204.0	741.0	758.4	+ 2	752.4	+ 2	619.5	-16
5.45	108.0	500.0	647.9	+30	620.5	+24	481.4	- 4
5.0	102.0	576.0	636.5	+11	606,9	+ 5	466.7	-19
3.03	60.8	425.0	518.9	+22	487,0	+15	352.4	-17
3.19	10.9	159.6	226.4	+42	194.3	+22	146.4	- 8
1.526	10.9	140.4	176.9	+26	179.4	+28	123.9	-12
0.718	10.9	99.4	130.7	+31	153.0	+54	100.0	+ 1
1.346	4.56	81.3	94.9	+17	91.3	+13	68.6	-16
1.248	1.19	24.5	29.7	+21	27.8	+13	24.3	- 1

$PD=((A-A_E)/A_E)X100$

Table 5.20 Comparison of total band absorptance for the 2.7μ H_2O band at T=1110 K

Effective Pressure	Mass Path Length	Total Band Absorptance Results, A (cm^{-1})						
		Exp. (27)	Edwards & Balakrishnan		Tien & Lowder		Felske & Tien	
P_e (atm)	W (g/m^2)	A_E	A	PD	A	PD	A	PD
10.0	153.0	785.0	790.0	+ 1	775.7	- 1	646.7	-18
5.0	76.7	560.0	651.8	+16	613.6	+10	480.5	-14
3.015	45.3	406.0	537.2	+32	482.1	+19	356.6	-12
3.015	45.0	416.0	536.0	+29	480.8	+16	355.6	-15
3.19	8.23	135.0	201.7	+49	166.0	+23	135.5	0
1.54	8.21	126.0	172.5	+37	158.5	+26	118.7	- 6
0.71	8.18	101.0	133.0	+32	142.6	+41	98.0	- 3
1.346	3.49	77.0	85.5	+11	77.0	0	63.0	-18
1.238	0.887	22.0	22.1	+ 1	21.4	- 3	19.84	-10

PD=((A-A_E)/A_E)X100

5.2.4 1.87μ H_2O Band

The spectral transmittance results, as calculated by the QRB model, are compared with experimental results in Figs. 5.24 and 5.25 for two different path lengths but for the same pressure of P_e = 765 mm Hg. The agreement between these results is quite good for the entire spectral range of the band except in the wing regions.

The total band absorptance results calculated by the QRB model (only at 300 K) and wide-band correlations are compared with the experimental results for four different temperatures in Tables 5.21-5.24. It is noted that the QRB model can be used to evaluate the band absorptance with reasonable accuracy. However, the agreement between the experimental results and results of three correlations is seen to be poor, especially at low temperatures.

5.2.5 Total Emissivity for H_2O

The total emissivity of water vapor, as calculated by the QRB model (only at 300 K) and wide-band correlations, are compared with the experimental results of Hottel et al. [9] in Figs. 5.26, 5.28, 5.30 and 5.32 for four different temperatures and P_e = 1 atm. The QRB model results do not agree very well with the experimental results at path lengths less than 2 atm-cm. However, there is a reasonable agreement between these results above 2 atm-cm. Since rotational band contributes about 80 percent of the total emissivity at room temperature, the discrepancy may be due to an error in the description of the line structure

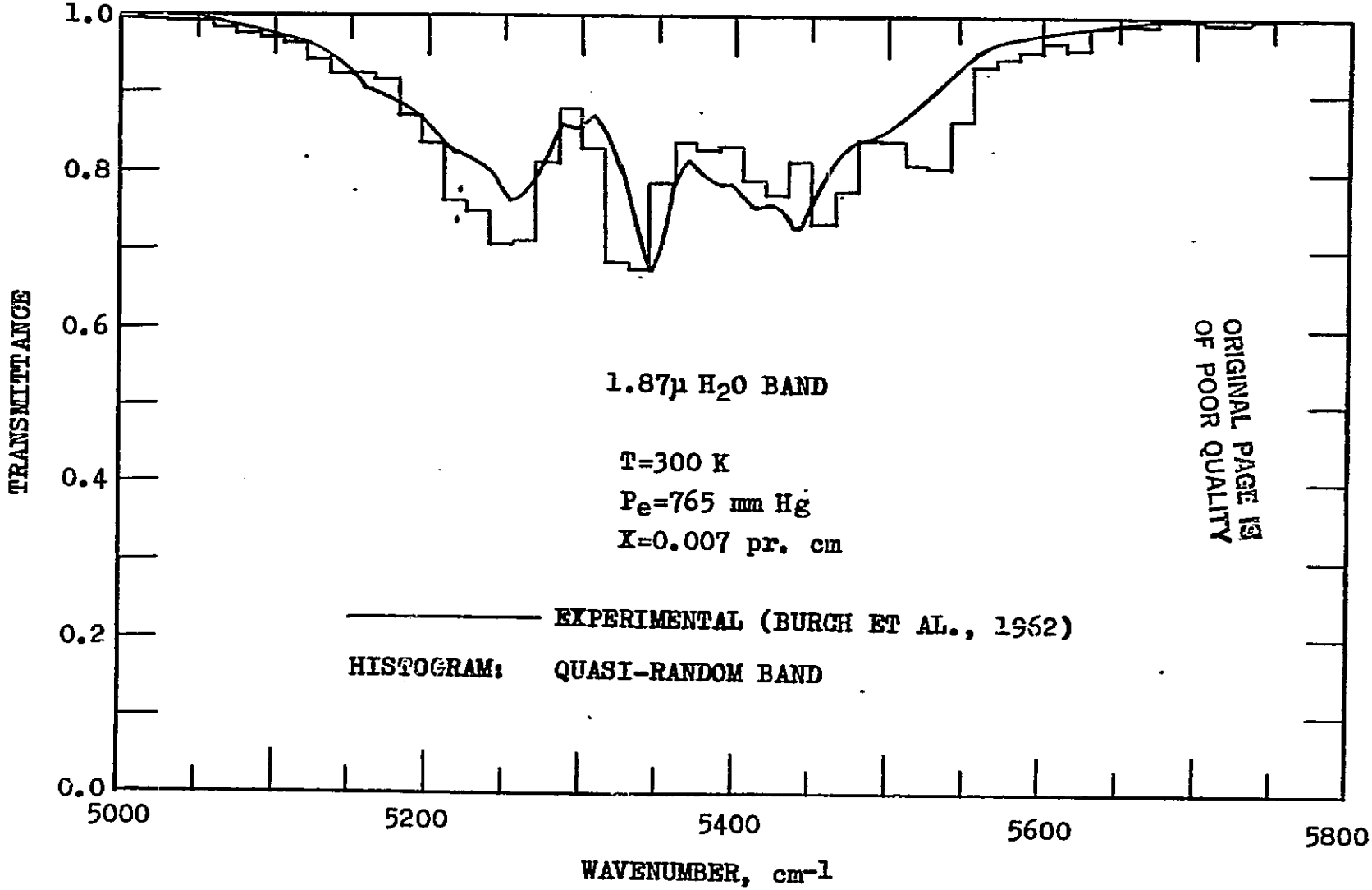

Fig. 5.24 Comparison of transmittances of the 1.87μ H_2O band.

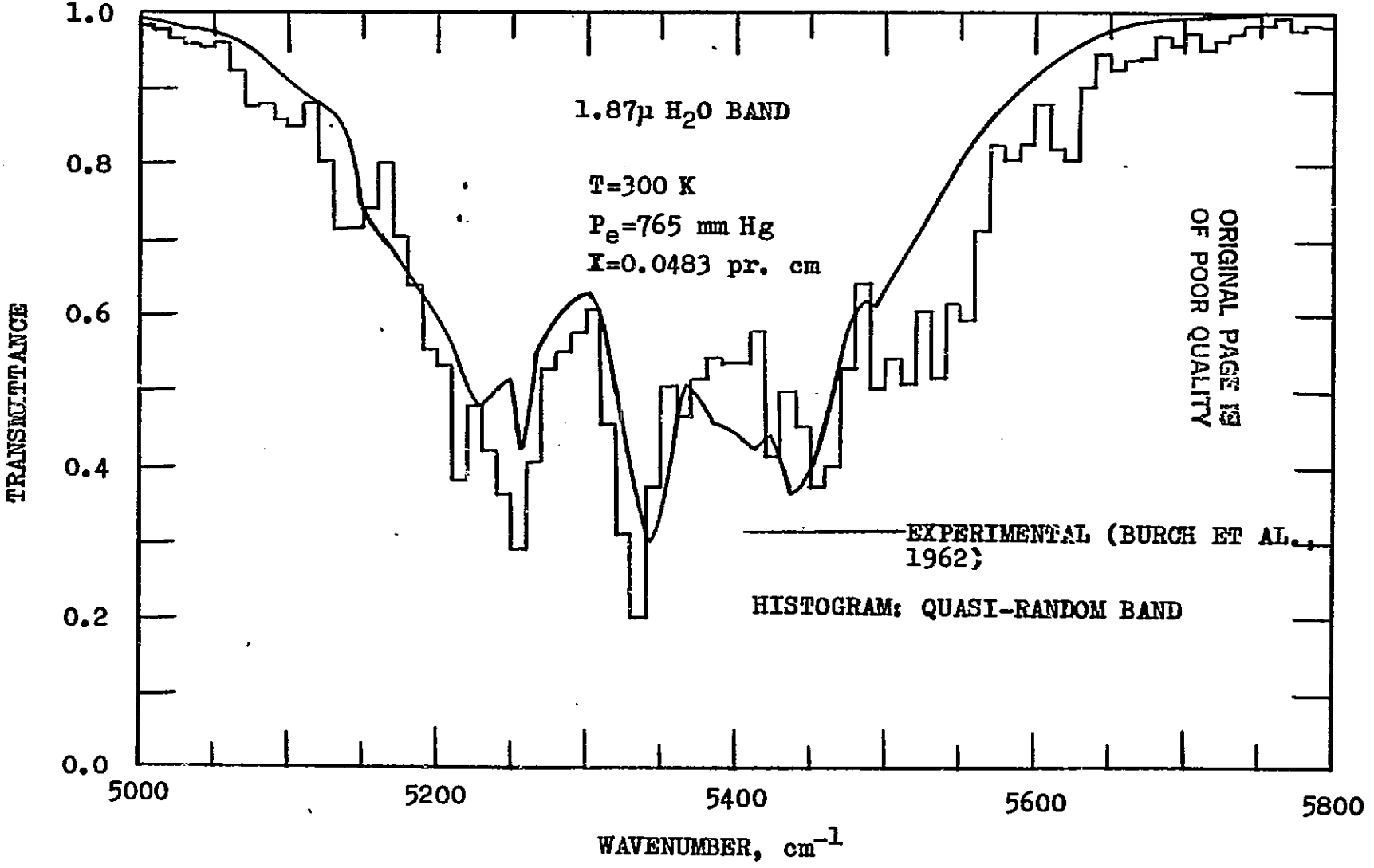

Fig. 5.25 Comparison of transmittances of the 1.87μ H_2O band.

Table 5.21 Comparison of total band absorptance for the 1.87μ H_2O band at T=300 K

Effective Pressure	Mass Path Length	Total Band Absorptance Results, A (cm^{-1})							
		Exp. (26)	Quasi-random Band		Edwards & Balakrishnan		Tien & Lowder		Felske & Tien	
P_e (atm)	W (g/m^2)	A_E	A	PD	A	PD	A	PD	A	PD
0.19	33.0	27.0	31.53	+16	16.0	-41	14.6	-46	14.9	-45
0.434	33.0	38.0	42.3	+11	23.8	-37	26.9	-29	21.0	-45
1.028	33.0	51.1	54.96	+ 7	35.2	-31	43.4	-15	29.2	-43
1.059	120.0	126.0	127.79	+ 1	71.7	-43	87.7	-30	59.2	-53
0.105	480.0	114.0	110.91	- 3	47.4	-58	45.9	-60	43.3	-62

$PD=((A-A_E)/A_E)X100$

Table 5.22 Comparison of total band absorptance for the 1.87μ H_2O band at T=555 K

Effective Pressure	Mass Path Length	Total Band Absorptance Results, A (cm^{-1})						
		Exp. (27)	Edwards & Balakrishnan		Tien & Lowder		Felske & Tien	
P_e (atm)	W (g/m^2)	A_E	A	PD	A	PD	A	PD
10.0	307.0	291.0	308.6	+ 6	290.6	0	210.4	-28
5.0	153.0	164.0	193.5	+18	194.7	+19	130.3	-21
3.02	89.0	124.0	114.8	- 7	130.9	+ 6	85.0	-31
3.19	16.3	41.0	40.8	0	40.5	- 1	30.2	-26
1.526	16.3	33.7	31.6	- 6	35.5	+ 5	24.8	-26
0.712	16.3	36.1	23.4	-35	28.0	-22	19.4	-46
1.526	15.3	30.0	30.6	+ 2	33.9	+13	23.8	-21
1.346	6.92	19.0	17.3	- 9	17.5	- 8	13.3	-30

PD=$((A-A_E)/A_E)X100$

Table 5.23 Comparison of total band absorptance for the 1.87μ H_2O band at T=833 K

Effective Pressure	Mass Path Length	Total Band Absorptance Results, A (cm^{-1})						
		Exp. (27)	Edwards & Balakrishnan		Tien & Lowder		Felske & Tien	
P_e (atm)	W (g/m^2)	A_E	A	PD	A	PD	A	PD
10.0	204.0	244.0	323.3	+33	289.0	+18	212.5	-13
5.45	108.0	132.0	207.7	+57	194.8	+48	135.2	+ 2
5.0	102.0	157.0	194.0	+24	186.3	+19	128.3	-18
3.03	60.8	121.0	116.4	- 4	124.0	+ 2	83.7	-31
3.19	10.9	28.1	34.5	+22	31.6	+12	26.2	- 7
1.526	10.9	27.6	29.7	+ 8	29.5	+ 7	22.5	-18
0.718	10.9	32.3	23.2	-28	25.7	-20	18.3	-43

$PD=((A-A_E)/A_E)X100$

Table 5.24 Comparison of total band absorptance for the 1.87μ H_2O band at T=1111 K

Effective Pressure	Mass Path Length	Total Band Absorptance Results, A (cm^{-1})						
		Exp. (27)	Edwards & Balakrishnan		Tien & Lowder		Felske & Tien	
P_e (atm)	W (g/m^2)	A_E	A	PD	A	PD	A	PD
10.0	153.0	260.0	331.1	+27	284.7	+10	220.0	-15
5.0	76.7	152.0	205.0	+35	179.5	+18	131.9	-13
3.015	45.3	106.0	121.8	+15	117.0	+10	85.0	-20
3.015	45.0	107.0	121.4	+13	116.5	+ 9	84.6	-21
3.19	8.23	27.0	28.5	+ 6	26.9	0	24.0	-11
1.54	8.21	28.3	28.0	- 1	26.0	- 8	21.6	-24
0.71	8.18	24.9	23.9	- 4	23.9	- 4	18.3	-27
1.346	3.49	22.6	12.1	-47	11.5	-49	10.4	-54

$PD=((A-A_E)/A_E)X100$

in the rotational band. It is noted that the Felske and Tien's results have a reasonable agreement with the experimental results for small path lengths; however, the Edwards and Balakrishnan, and Tien and Lowder results agree well with the experimental results for large path lengths except for the high temperature of 2000 K. It should be pointed out that although the agreement between the Felske and Tien's results and the experimental results is excellent at 2000 K, it does not mean that this correlation can estimate the total emissivity of water vapor accurately at high temperatures. This is because the data from the Hottel's charts, at high temperatures, are estimated from extrapolation and, therefore, are less accurate for the entire path lengths.

Figures 5.27, 5.29, 5.31 and 5.33 show the comparisons of the results of total emissivity, as obtained by wide-band correlations, for four different temperatures and five different pressures. It is again found that the Felske and Tien's results are lower than the results of the other two correlations for all cases; and the Tien and Lowder's results do not have the trend of other results at low pressure. The Edwards and Balakrishnan's correlation yields lower values at low pressures and higher values at high pressures than the Tien and Lowder's correlation.

5.3 Homogeneous Results for CO_2 + H_2O

Table 5.25 shows the comparison of numerical results of total emissivity, as calculated by the wide-band correlations for the mixtures of water vapor, carbon dioxide and nitrogen, with the experimental results

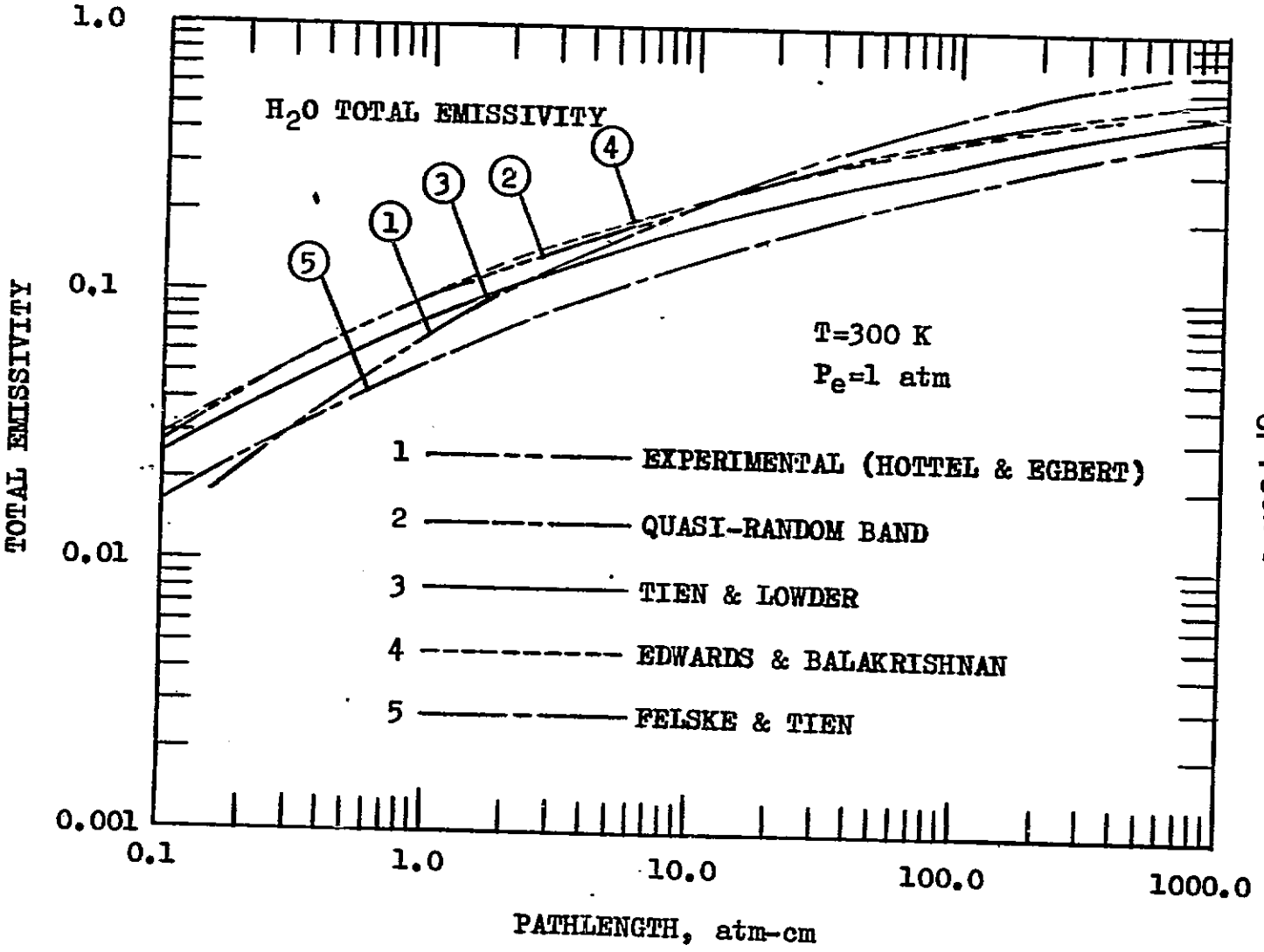

Fig. 5.26 Comparison of total emissivity of water vapor at T=300 K.

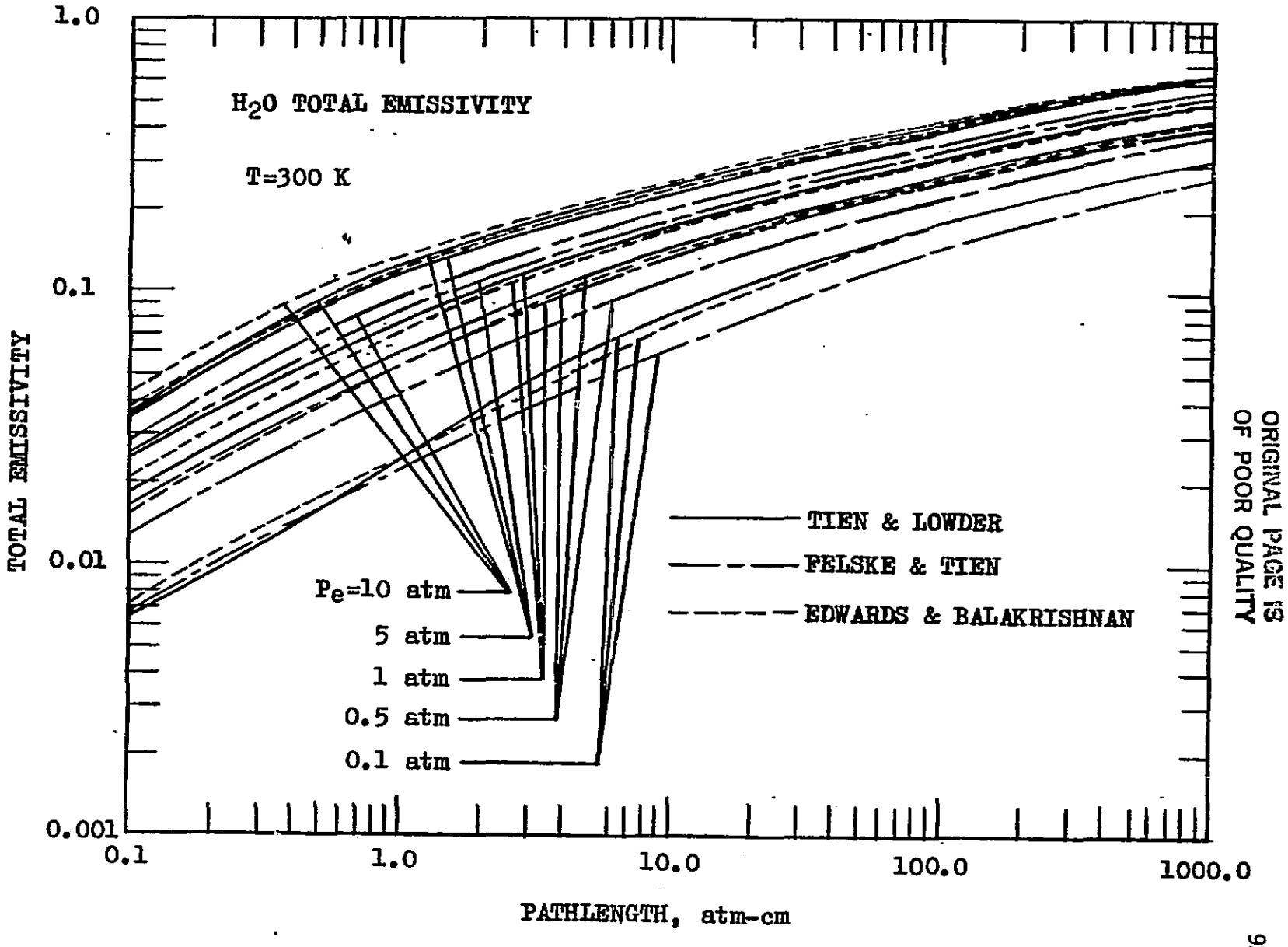

Fig. 5.27 Comparison of results of total emissivity by using wide band correlations.

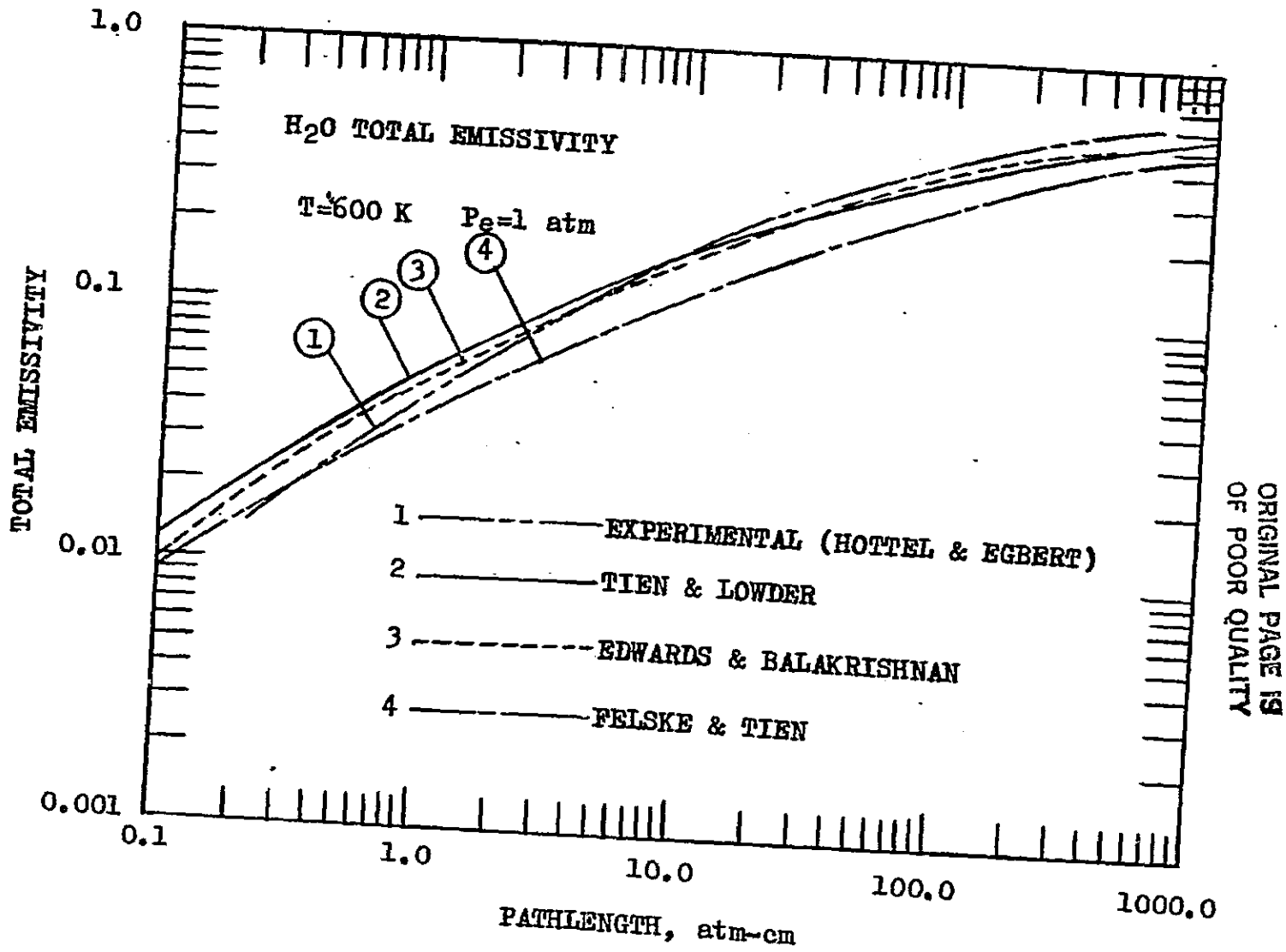

Fig. 5.28 Comparison of total emissivity of water vapor at T=600 K.

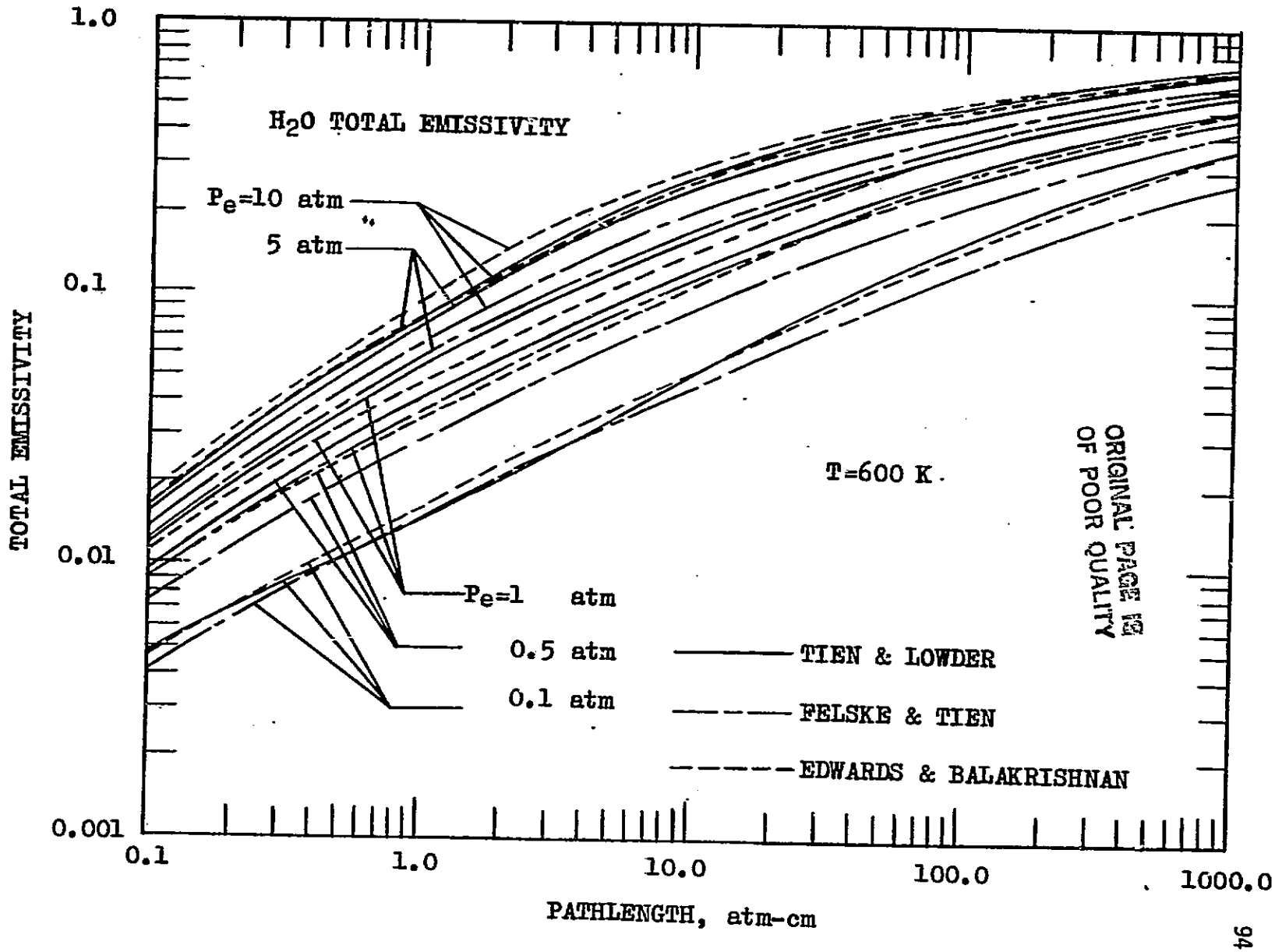

Fig. 5.29 Comparison of results of total emissivity by using wide band correlations.

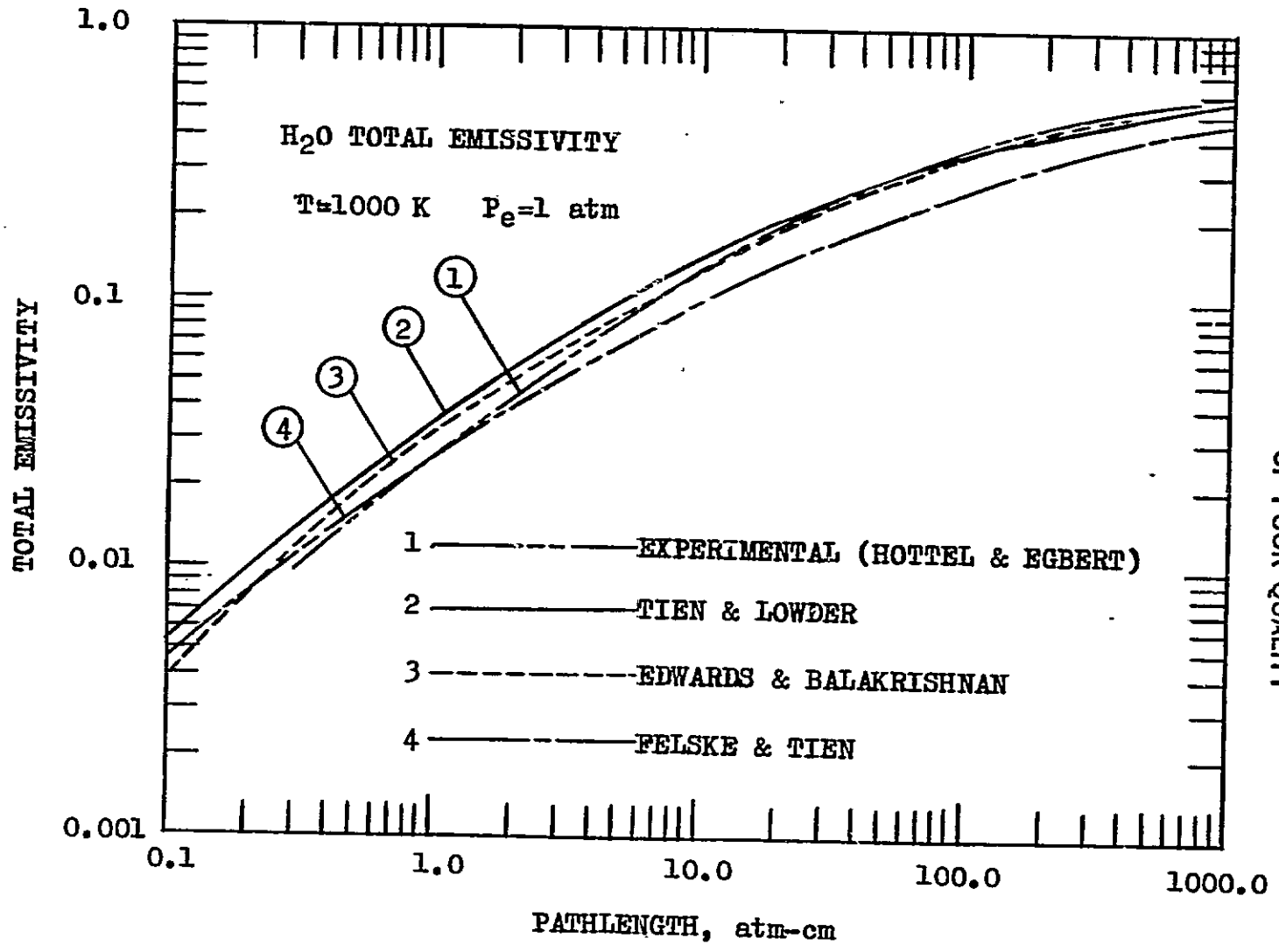

Fig. 5.30 Comparison of total emissivity of water vapor at T=1000 K.

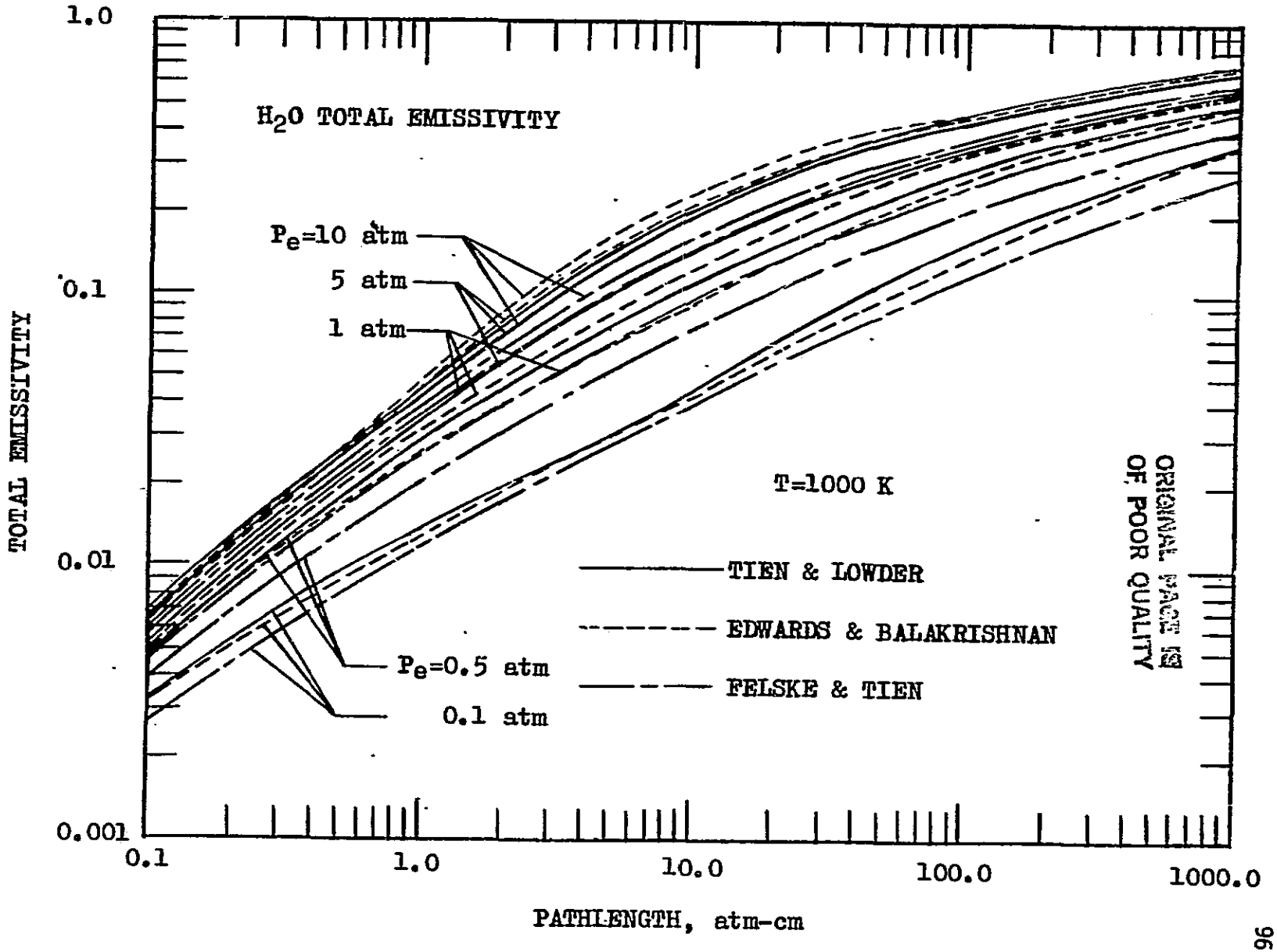

Fig. 5.31 Comparison of results of total emissivity by using wide band correlations.

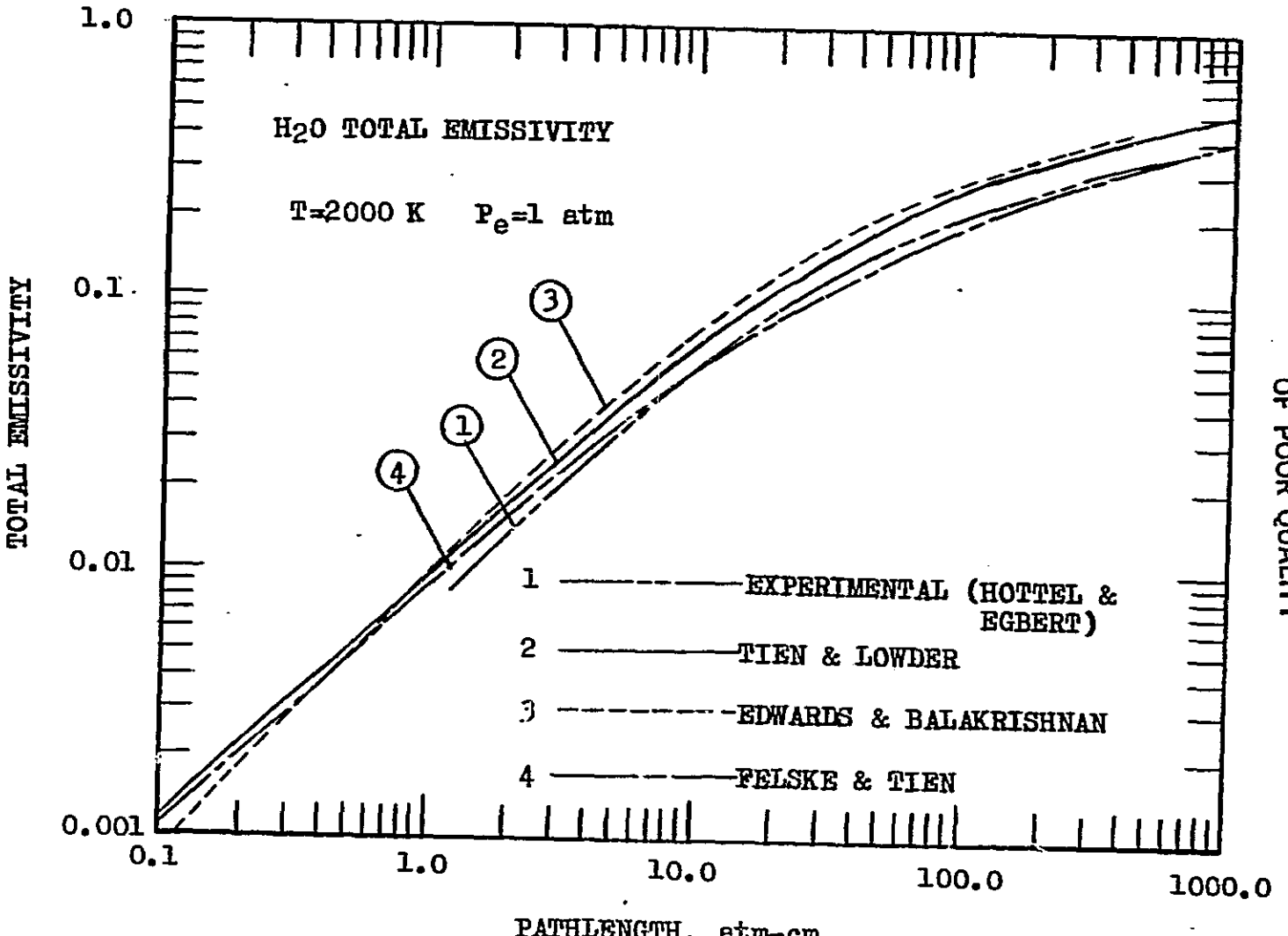

Fig. 5.32 Comparison of total emissivity of water vapor at T=2000 K.

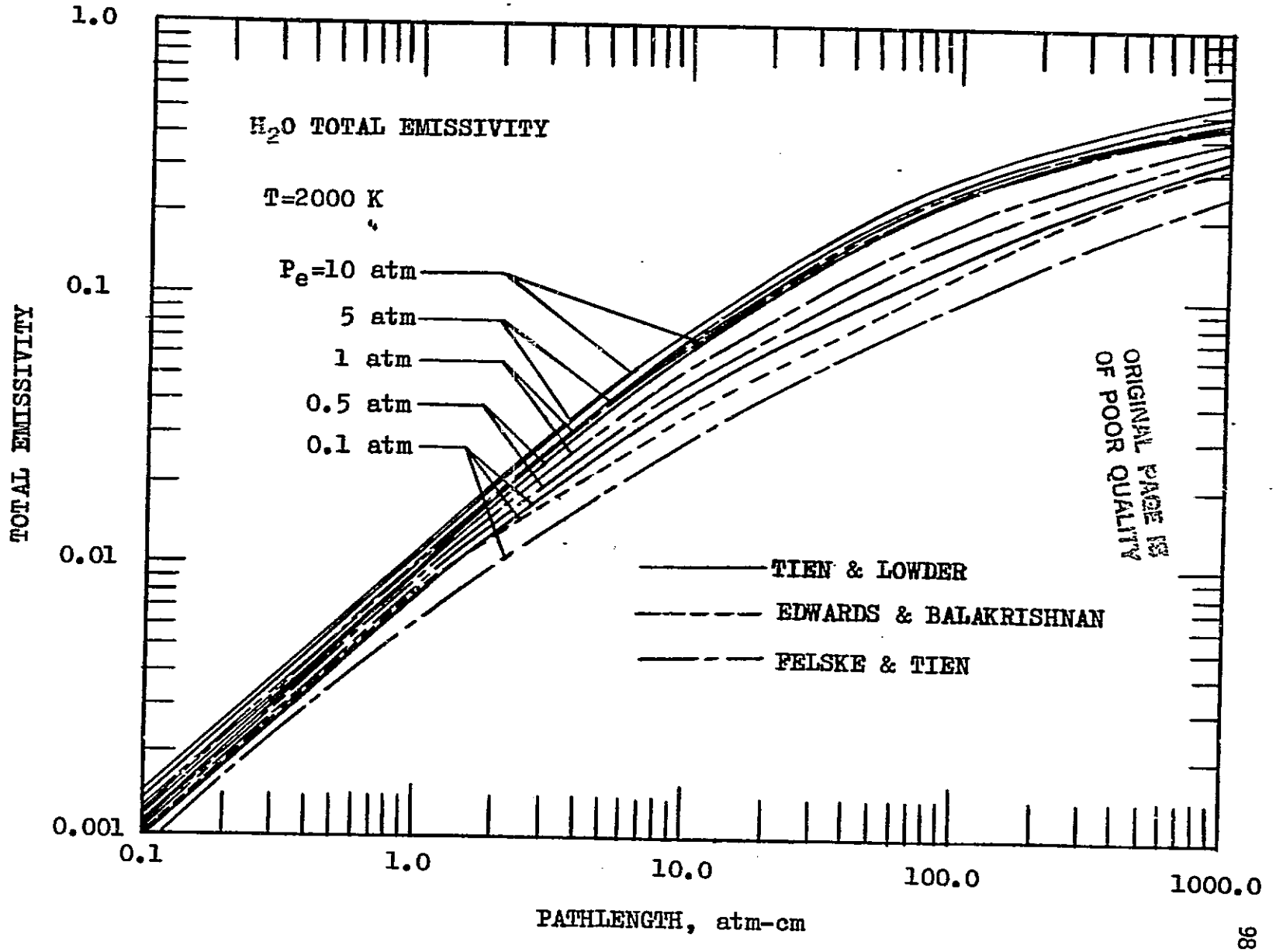

Fig. 5.33 Comparison of results of total emissivity by using wide band correlations.

Table 5.25 Comparison of total gas emissivities for mixtures of water vapor, carbon dioxide and nitrogen

Run	Total Pressure	Temperature	Mole Fraction		Total Gas Emissivity Results			
	P_T (atm)	T (K)	H_2O	CO_2	Exp. (53)	Edwards & Balakrishnan	Tien & Lowder	Felske & Tien
1	1.042	546	0.258	0.254	0.233	0.247	0.256	0.180
2	1.098	550	0.051	0.249	0.138	0.144	0.156	0.112
5	1.093	550	0.241	0.046	0.206	0.227	0.237	0.163
6	1.070	820	0.250	0.249	0.206	0.270	0.277	0.196
12	1.14	550	0.101	0.099	0.150	0.167	0.183	0.126
13	1.178	817	0.100	0.098	0.143	0.182	0.193	0.137
14	1.17	550	0.752	0.248	0.332	0.392	0.388	0.291

of Ref. 53. Values of emissivities are corrected for partial overlapping in accordance with Penner and Varanasi [32]. The Edwards and Balakrishnan, and Tien and Lowder correlations overestimate the values, while the Felske and Tien's correlation underestimates them. However, all these results agree with the experimental results reasonably well.

5.4 Nonhomogeneous Results

Since no experimental results of nonhomogeneous gas emissivity are available in the literature, comparisons of nonisothermal band absorptance and emission are made only in this section.

The results of nonisothermal band absorptance for three different bands of CO_2, as calculated from Eqs. (2.9) to (2.11) by employing the wide-band correlations, are compared with the experimental results of Edwards et al. [19] in Table 5.26. It is noted that the Edwards and Balakrishnan and Tien and Lowder results have a reasonable agreement with the measured values. The Felske and Tien's results are generally lower than the experimental data.

Table 5.27 shows the comparisons between the numerical results of nonisothermal band absorptance and experimental results of Edwards et al. [19, 54] for two H_2O bands (6.3μ and 2.7μ). The results of all three correlations show reasonable agreement with the experimental results.

Table 5.28 shows the comparisons between the nonisothermal band emission results of 2.7μ H_2O, as calculated with Eq. (2.12) by using the wide-band correlations, and the experimental results of Edwards et al. [54] and Simmons [55]. The results of correlations, in general, show a good agreement with the experimental results except the Felske

Table 5.26 Comparison of nonisothermal band absorptance for CO_2 gas

Band (μ)	Run	Ref.	Total Band Absorptance Results, A (cm^{-1})						
			Exp.	Edwards & Balakrishnan		Tien & Lowder		Felske & Tien	
			A_E	A	PD	A	PD	A	PD
1.5	T10	19	253.0	219.2	-13	217.9	-14	185.4	-27
	T11		143.0	140.1	- 2	138.4	- 3	106.4	-26
	T15		43.0	65.0	+50	63.1	+47	42.8	0
4.3	T 6	19	254.0	257.8	+ 1	259.1	+ 2	233.8	- 8
	T 5		189.0	193.0	+ 2	193.5	+ 2	167.4	-11
	T16		132.0	125.2	- 5	123.1	- 7	98.8	-25
2.7	T 6	19	348.0	308.9	-11	305.0	-12	249.2	-28
	T 5		191.0	169.2	-11	153.1	-20	113.9	-40

$PD=((A-A_E)/A_E)X100$

Table 5.27 Comparison of nonisothermal band absorptance for H_2O gas

Band (μ)	Run	Ref.	Total Band Absorptance Results, A (cm^{-1})						
			Exp.	Edwards & Balakrishnan		Tien & Lowder		Felske & Tien	
			A_E	A	PD	A	PD	A	PD
6.3	H 9	19	622.0	611.4	- 2	606.7	- 2	487.9	-22
	H11		591.0	694.2	+17	689.2	+17	558.9	- 5
	H12		602.0	639.6	+ 6	634.0	+ 5	500.3	-17
	H15		583.0	676.2	+16	671.7	+15	549.0	- 6
2.7	H 9	19	619.0	634.0	+ 2	623.2	+ 1	502.2	-19
	H11		566.0	720.0	+27	709.1	+25	575.2	+ 2
	H12		561.0	661.4	+18	646.4	+15	511.6	- 9
	H15		583.0	702.7	+21	693.2	+19	566.7	- 3
	12-10	54	598.9	579.6	- 3	558.6	- 7	421.0	-30
	9-13		450.8	499.4	+10	479.9	+ 6	347.4	-23
	12-1		372.1	492.8	+32	472.2	+27	339.5	- 9

$PD=((A-A_E)/A_E)X100$

Table 5.28 Comparison of nonisothermal band emission for 2.7μ H_2O band

Run	Partial Pressure P (atm)	Ref.	Band Emission Results, E (Btu ft^{-2} sec^{-1} $str.^{-1}$)						
			Exp.	Edwards & Balakrishnan		Tien & Lowder		Felske & Tien	
			E_E	E	PD	E	PD	E	PD
9-13	0.47	54	0.02975	0.02544	-14	0.02544	-14	0.01967	-34
12-1	0.45		0.0432	0.0583	+35	0.0537	+24	0.0376	-13
12-10	0.69		0.0665	0.0574	-14	0.0568	-15	0.0428	-36
112-4	0.528	55	0.211	0.218	+ 3	0.210	0	0.156	-26
122-8	0.517		0.225	0.233	+ 4	0.222	- 1	0.163	-28
1125-5	0.786		0.256	0.258	+ 1	0.254	- 1	0.196	-23

$PD=((E-E_E)/E_E)X100$

and Tien's results which are consistently lower than the measured data.

The discrepancies between numerical and experimental results are likely due to improperly approximating the temperature profiles. These may be also caused by the experimental error and the inaccuracy of the correlation parameters of the isothermal band absorptance.

Chapter 6

CONCLUSIONS

The results were obtained for spectral transmittance, spectral emissivity, band absorptance, and band emissivity for important infrared bands of carbon dioxide and water vapor by employing various absorption models in order to establish the validity and usefulness of a simplified model for atmospheric and engineering applications. For this purpose, selected results were obtained by using the line-by-line and quasi-random band models. Extensive results were obtained by using the wide-band model correlations of Edwards and Balakrishnan, Tien and Lowder, and Felske and Tien for a range of temperature, pressure, and path length conditions. The results are compared with available experimental results. The results were also obtained for total gas emissivities to further investigate the usefulness of a model under homogeneous and non-homogeneous conditions.

From a comparison of the spectral transmittance, band absorptance and total emissivity at room temperature, it is evident that the quasi-random band model results are in good agreement with the experimental results in most cases under homogeneous conditions. The quasi-random band model can also provide accurate results at higher temperatures if proper adjustments are made for overlapping of the lines in a band. The model provides accurate results also for nonhomogeneous conditions. Thus, use of the quasi-random band model is highly recommended for most

atmospheric and engineering applications. Unfortunately, the computational costs associated with this model can be prohibitive for many applications.

For engineering applications, use of the wide-band model correlations is highly recommended. These correlations require significantly less computational time and, if used properly, yield results with reasonable accuracy. The results of this study reveal that use of the Edwards and Balakrishnan and Tien and Lowder correlations is justified for carbon dioxide and water vapor at moderate and high pressures and relatively large path lengths. The Felske and Tien's correlation is useful for low pressures and small path lengths. For nonhomogeneous applications, use of the Curtis-Godson approximation, in conjunction with an appropriate wide-band correlation, is recommended. The Edwards and Balakrishnan and/or Tien and Lowder correlations are recommended for most engineering applications involving nonhomogeneous conditions.

For further study, it is suggested to investigate the feasibility of the wide-band model correlations for other important molecular species by comparing the band absorptance and total emissivity results with results of the quasi-random band formulation. The quasi-random band formulation can be easily extended to a mixture of molecular species. Thus, it would be desirable to investigate the applicability of a correlation for a gaseous mixture. This information could be very useful for applications involving combustion and flames.

REFERENCES

1. Goody, R.M., Atmospheric Radiation I: Theoretical Basis, Oxford University Press, London and New York, 1964.

2. Rogers, C.D., "The Use of Emissivity in Atmospheric Radiative Calculations," Quarterly Journal of the Royal Meteorological Society, Vol. 93, No. 395, Jan. 1967, pp. 45-54.

3. Cess, R.D., "Radiative Transfer Due to Atmospheric Water Vapor: Global Considerations of the Earth's Energy Balance," Journal of Quantitative Spectroscopy and Radiative Transfer, Vol. 14, No. 9, Sept. 1974, pp. 861-872.

4. Leckner, B., "The Spectral and Total Emissivity of Carbon Dioxide," Combustion and Flame, Vol. 17, No. 1, Aug. 1971, pp. 37-44.

5. Leckner, B., "Spectral and Total Emissivity of Water Vapor and Carbon Dioxide," Combustion and Flame, Vol. 19, No. 1, Aug. 1972, pp. 33-48.

6. Felske, J.D. and Tien, C.L., "Calculation of the Emissivity of Luminous Flames," Combustion Science and Technology, Vol. 7, No. 1, Mar. 1973, pp. 25-31.

7. Taylor, P.B. and Foster, P.J., "The Total Emissivities of Luminous and Non-Luminous Flames," International Journal of Heat and Mass Transfer, Vol. 17, No. 12, Dec. 1974, pp. 1591-1605.

8. Coppalle, A. and Vervisch, P., "The Total Emissivity of High-Temperature Flames," Combustion and Flame, Vol. 49, No. 1, Jan. 1983, pp. 101-108.

9. Hottel, H.C. and Sarofim, A.F., Radiative Transfer, McGraw-Hill, New York, 1967.

10. Penner, S.S. and Varanasi, P., "Approximation Band Absorption and Total Emissivity Calculations for H_2O," Journal of Quantitative Spectroscopy and Radiative Transfer, Vol. 5, No. 2, Mar. 1965, pp. 391-401.

11. Tien, C.L., "Thermal Radiation Properties of Gases," Advances in Heat Transfer, Vol. 5, Academic Press, New York, 1968.

12. Penner, S.S., Quantitative Molecular Spectroscopy and Gas Emissivities, Addison-Wesley, Reading, Massachusetts, 1959.

13. Penner, S.S., Radiation and Reentry, Academic Press, New York, 1968.

14. Modak, A.T., "Exponential Wide Band Parameters for the Pure Rotational Band of Water Vapor," Journal of Quantitative Spectroscopy and Radiative Transfer, Vol. 21, No. 2, Feb. 1979, pp.131-142.

15. Edwards, D.K., "Molecular Gas Band Radiation," Advances in Heat Transfer, Vol. 12, Academic Press, New York, 1976.

16. Ludwig, C.B., Ferriso, C.C., and Abeyta, C.N., "Spectral Emissivities and Integrated Intensities of the 6.3-μ Fundamental Band of H_2O," Journal of Quantitative Spectroscopy and Radiative Transfer, Vol. 5, No. 2, Mar. 1965, pp. 281-290.

17. Ludwig, C.B., Ferriso, C.C., Malkmus, W., and Boynton, F.P., "High-Temperature Spectra of the Pure Rotational Band of H_2O," Journal of Quantitative Spectroscopy and Radiative Transfer, Vol. 5, No. 5, Sept. 1965, pp. 697-714.

18. Edwards, D.K. and Menard, W.A., "Comparison of Methods for Correlation of Total Band Absorption," Applied Optics, Vol. 3, No. 5, May 1964, pp. 621-625.

19. Edwards, D.K., Glassen, L.K., Hauser, W.C., and Tuchscher, J.S., "Radiation Heat Transfer in Nonisothermal Nongray Gases," ASME Journal of Heat Transfer, Vol. 89, No. 3, Aug. 1967, pp. 219-229.

20. Cess, R.D. and Tiwari, S.N., "Infrared Radiative Energy Transfer in Gases," Advances in Heat Transfer, Vol. 8, Academic Press, New York, 1972.

21. Edwards, D.K. and Balakrishnan, A., "Thermal Radiation by Combustion Gases," International Journal of Heat and Mass Transfer, Vol. 16, No. 1, Jan. 1973, pp. 25-40.

22. Tien, C.L. and Lowder, J.E., "A Correlation for Total Band Absorptance of Radiating Gases," International Journal of Heat and Mass Transfer, Vol. 9, No. 7, July 1966, pp. 698-701.

23. Felske, J.D. and Tien, C.L., "A Theoretical Closed Form Expression for the Total Band Absorptance of Infrared-Radiating Gases," International Journal of Heat and Mass Transfer, Vol. 17, No. 1, Jan. 1974, pp. 155-158.

24. Tiwari, S.N., "Models for Infrared Atmospheric Radiation," School of Engineering, Old Dominion University, Norfolk, Va., IR-76-T10, June 1976. Also, in Advances in Geophysics, Vol. 20, Academic Press, 1978.

25. Wang, W.C., "An Analytical Expression for the Total Band Absorptance of Infrared-Radiating Gases," Journal of Quantitative Spectroscopy and Radiative Transfer, Vol. 29, No. 3, Mar. 1983, pp. 279-281.

26. Burch, E.E., Gryvnak, D.A., Singleton, E.B., France, W.L., and Williams, D., "Infrared Absorption by Carbon Dioxide, Water Vapor, and Minor Atmospheric Constituents," AFCRL-62-698, July 1962, Air Force Cambridge Research Laboratories, Bedford, Mass.

27. Edwards, D.K., Flornes, B.J., Glassen, L.K., and Sun, W., "Correlation of Absorption by Water Vapor at Temperatures from 300 K to 1100 K," Applied Optics, Vol. 4, No. 6, June 1965, pp. 715-721.

28. Edwards, D.K. and Menard, W.A., "Correlations for Absorption by Methane and Carbon Dioxide Gases," Applied Optics, Vol. 3, No. 7, July 1964, pp. 847-852.

29. Gray, L.D., "Spectral Emissivity Calculations for the Parallel Bands of the Carbon Dioxide at 4.3 Microns," Journal of Quantitative Spectroscopy and Radiative Transfer, Vol. 5, No. 4, July 1965, pp. 569-583.

30. Weiner, M.M. and Edwards, D.K., "Theoretical Expression of Water Vapor Spectral Emissivity with Allowance for Line Structure," International Journal of Heat and Mass Transfer, Vol. 11, No. 1, Jan. 1968, pp. 55-65.

31. Ben-Aryeh, Y., "Spectral Emissivity Calculations by the Statistical Model Applied to the 4.3μ Bands of CO_2 at High Temperatures," Applied Optics, Vol. 6, No. 6, June 1967, pp. 1049-1055.

32. Penner, S.S. and Varanasi, P., "Effect of (Partial) Overlapping of Spectral Lines on the Total Emissivity of H_2O-CO_2 Mixtures (T> 800 K)," Journal of Quantitative Spectroscopy and Radiative Transfer, Vol. 6, No. 2, Mar. 1966, pp. 181-192.

33. Chan, S.H. and Tien, C.L., "Total Band Absorptance of Nonisothermal Infrared-Radiating Gases," Journal of Quantitative Spectroscopy and Radiative Transfer, Vol. 9, No. 9, Sept. 1969, pp. 1261-1271.

34. Cess, R.D. and Wang, L.S., "A Band Absorptance Formulation for Nonisothermal Gaseous Radiation," International Journal of Heat and Mass Transfer, Vol. 13, No. 3, Mar. 1970, pp. 547-555.

35. Edwards, D.K. and Morizumi, S.J., "Scaling of Vibration-Rotation Band Parameters for Nonhomogeneous Gas Radiation," Journal of Quantitative Spectroscopy and Radiative Transfer, Vol. 10, No. 3, Mar. 1970, pp. 175-188.

36. Felske, J.D. and Tien, C.L., "Infrared Radiation from Nonhomogeneous Gas Mixtures Having Overlapping Bands," Journal of Quantitative Spectroscopy and Radiative Transfer, Vol. 14, No. 1, Jan. 1974, pp. 35-48.

37. Wyatt, P.J., Stull, V.R., and Plass, G.N., "Quasi-Random Model of Band Absorption," Journal of the Optical Society of America, Vol. 52, No. 11, Nov. 1962, pp. 1209-1217.

38. Kunde, V.G. and Maguire, W.C., "Direct Integration Transmittance Model," Journal of Quantitative Spectroscopy and Radiative Transfer, Vol. 14, No. 8, Aug. 1974, pp. 803-817.

39. Gupta, S.K. and Tiwari, S.N., "Evaluation of Upwelling Infrared Radiance from Earth's Atmosphere," School of Engineering, Old Dominion University, Norfolk, VA., TR-75-714, Nov. 1975.

40. Drayson, S.R., "Atmospheric Transmission in the CO_2 Bands Between 12μ and 18μ," Applied Optics, Vol. 5, No. 3, Mar. 1966, pp. 385-392.

41. Kunde, V.G., "Theoretical Computations of the Outgoing Infrared Radiance from a Planetary Atmosphere," NASA, TR D-4045, Aug. 1967.

42. Gupta, S.K. and Tiwari, S.N., "Evaluation of Transmittance of Selected Infrared Bands," School of Engineering, Old Dominion University, Norfolk, VA., TR-76-T7, April 1976.

43. Tiwari, S.N. and Gupta, S.K., "Accurate Spectral Modeling for Infrared Radiation," ASME Journal of Heat Transfer, Vol. 100, May 1978, pp. 240-246.

44. Elsasser, W.M., Heat Transfer by Infrared Radiation in the Atmosphere, Harvard Meteorological Studies, No. 6, Harvard University Press, Cambridge, Massachusetts, 1942.

45. Ludwig, C.B., Malkmus, W., Reardon, J.E., and Thomson, J.A.L., Handbook of Infrared Radiation from Combustion Gases, NASA SP-3080, 1973.

46. Young, S.J., "Band Model Formulation for Inhomogeneous Optical Paths," Journal of Quantitative Spectroscopy and Radiative Transfer, Vol. 15, No. 6, June 1975, pp. 483-501.

47. Young, S.J., "Addendum to: Band Model Formulation for Inhomogeneous Optical Paths," Journal of Quantitative Spectroscopy and Radiative Transfer, Vol. 15, No. 12, Dec. 1975, pp. 1137-1140.

48. Goody, R.M. and Belton, M.J.S., "Radiative Relaxation Times for Mars (A Discussion of Martian Atmospheric Dynamics)," Planetary and Space Sciences, Vol. 15, No. 2, Feb. 1967, pp. 247-256.

49. Tien, C.L. and Ling, G.R., "On a Simple Correlation for Total Band Absorptance of Radiating Gases," International Journal of Heat and Mass Transfer, Vol. 12, No. 9, Sept. 1969, pp. 1179-1181.

50. Edwards, D.K. and Balakrishnan, A., "Slab Band Absorptance for Molecular Gas Radiation," Journal of Quantitative Spectroscopy Radiative Transfer, Vol. 12, No. 10, Oct. 1972, pp. 1379-1337.

51. Tiwari, S.N. and Batki, R.R., "Infrared Band Models for Atmospheric Radiation," School of Engineering, Old Dominion University, Norfolk, VA., TR-75-T17, Nov. 1975.

52. McClatchey, R.A., Benedict, W.S., Clough, S.A., Burch, D.E., Calfee, R.F., Fox, K., Rothman, L.S., and Garing, J.S., AFCRL Atmospheric Line Parameters Compilation," AFCRL-TR-73-0096, Air Force Cambridge Research Laboratories, Bedford, Mass., Jan. 1973.

53. Hines, W.S. and Edwards, D.K., "Infrared Absorptives of Mixtures of Carbon Dioxide and Water Vapor," Chemical Engineering Progress Symposium Series, Vol. 64, No. 82, 1968, pp. 173-180.

54. Weiner, M.M. and Edwards, D.K., "Nonisothermal Gas Radiation in Superposed Vibration-Rotation Bands," Journal of Quantitative Spectroscopy and Radiative Transfer, Vol. 8, No. 5, May 1968, pp. 1171-1183.

55. Simmons, F.S., "Band Models for Nonisothermal Radiating Gas," Applied Optical, Vol. 5, No. 11, Nov. 1966, pp. 1801-1811.

APPENDIX A

EXPLANATION OF SYMBOLS USED IN COMPUTER PROGRAMS

APPENDIX A

EXPLANATION OF SYMBOLS USED IN COMPUTER PROGRAMS

A-1 Symbols used in program QRB.FOR

AL	average half-width of the lines of the molecule
AVSI	average of the intensities of the lines within one intensity decade
BEMI	band emissivity
BIG	upper intensity limit for individual intensity decades
BIGI	intensity of the strongest line within one interval
DEL	width of an interval
EL	energy of the lower states for the individual line
EM	emissivity from lines within one interval
FR	frequencies of the individual lines
FRB	frequencies at the interval boundaries
FRC	frequencies at the interval centers
FRL	lower frequency boundary of the band
FRU	upper frequency boundary of the band
IR	index which lets the transmittance be computed for the unshifted and shifted meshes
JD	number of adjacent intervals on both sides of an interval from which the contribution is taken into account
KR	number of interval in the band
LE	total number of lines in the spectrum
LIB	serial number of the first line in an interval
LIE	serial number of the last line in an interval

NSI	number of lines within one decade of an interval
PCK	Planck's function
PL,PL1	pressure path length of the absorber
PNTP	pressure referring to NTP (760 mm Hg)
PREC	effective pressure of the absorber
RP	exponent to account for the temperature-dependence of the rotational partition function
SI	intensities of the individual lines
SSI	sum of the intensities of all the lines within one decade of an interval
T1,T2	weighting factors used in the numerical integration of direct and wing contribution, respectively
TEMC	temperature of the absorber
TEMR	reference temperature for the molecular spectral parameters
TRA	array of transmittance values containing results from unshifted- and shifted-mesh computations
TRD	contribution to the total transmittance from lines within an interval
VP	factor accounting for the temperature-dependence of the vibrational partition function
X1,X2	abscissa values for the numerical integration of the direct and wing contribution, respectively

A-2 Symbols used in program NONHOM.FOR

A,B	length
ABSO	band absorptance
BC	band centers
BIN	integrated band intensity at TEMC
BLP	line structure parameter at PREC
BRO	self-broadening parameter

BWP	band width parameter at TEMC
DENS	density of the absorber
HBIN	scaled integrated intensity
HBLP	scaled line width to spacing ratio
HBWP	scaled band width parameter
PLCK	Planck's function
PML	mass path length
PRE	partial pressure of the absorber
PREC	effective broadening pressure
PTOT	total pressure
TEMC	temperature of the absorber
SUM	band emission

A-3 Symbols used in subroutine WATER.FOR

BETA	line structure parameter at P_e = 1 atm
F(I)	line-width-to-spacing temperature-variation parameter
G(I)	band-intensity temperature-variation parameter
OMG	band width parameter at T = 100 K
RTH	integrated band intensity at T_1 = 100 K
U(I)	the quantity hcν/kT

APPENDIX B

QUASI-RANDOM BAND MODEL COMPUTER PROGRAM

APPENDIX B

QUASI-RANDOM BAND MODEL COMPUTER PROGRAM

```
C   PROGRAM TO CALCULATE BAND EMISSIVITY WITH QUASI-RANDOM BAND MODEL
      INTEGER X,W
      DIMENSION FR(10150),SI(10150),EL(10150),FRB(85),FRC(85),LIB(85)
     *,LIE(85),MP(85),BIGI(85),BIG(6,85),SSI(5,85),NSI(5,85),
     *AVSI(5,85),TRG(85),X1(26),T1(26),X2(21),T2(21),PCK(85),
     *PL1(9),TRA(9,170)
      DATA PL1/0.1,0.4,1.0,4.0,10.0,40.0,100.0,400.0,1000.0/
      DATA FRL,FRU,DEL/3400.0,3800.0,5.0/
      DATA PNTP,PREC,TNTP,TEMR/1.0,0.1,273.0,296.0/
      DATA LE,JD/10104,10/
      DATA RP,AL/1.0,0.07/
      DATA X1/0.0,0.001,0.0015,0.002,0.003,0.004,0.005,0.006,0.008,
     1        0.01,0.015,0.02,0.03,0.04,0.05,0.06,0.08,0.10,0.15,
     2        0.2,0.3,0.4,0.5,0.6,0.8,1.0/
      DATA T1/0.0006,0.0006,0.0006,0.0007,0.001,0.001,0.001,0.0015,
     1        0.002,0.003,0.005,0.008,0.01,0.01,0.01,0.015,0.02,0.03,
     2        0.05,0.08,0.1,0.1,0.1,0.15,0.2,0.1/
      DATA X2/-1.0,-0.9,-0.8,-0.7,-0.6,-0.5,-0.4,-0.3,-0.2,-0.1,
     1        0.0,0.10,0.20,0.30,0.40,0.50,0.60,0.70,0.80,0.90,1.0/
      DATA T2/0.1,0.4,0.2,0.4,0.2,0.4,0.2,0.4,0.2,0.4,
     1        0.2,0.4,0.2,0.4,0.2,0.4,0.2,0.4,0.2,0.4,0.1/
         ACCEPT *, TEMC
         ACCEPT *, VP
      READ(23,13) (FR(X),SI(X),EL(X),X=1,LE)
   13 FORMAT(F10.4,E15.8,F12.4)
C    CONVERTS THE LINE INTENSITIES AND THE AVERAGED LINE-WIDTHS FROM
C     REFERENCE TO AMBIENT CONDITIONS OF TEMPERATURE AND PRESSURE
      CST=(SQRT(TEMR/TEMC))*PREC/PNTP
      PART=VP*((TEMR/TEMC)**RP)*2.69E+19
      FACT=1.439*(TEMC-TEMR)/(TEMC*TEMR)
      DO 101 X=1,LE
  101 SI(X)=SI(X)*PART*EXP(EL(X)*FACT)
      ALA=AL*CST
C    INITIALIZES THE FREQUENCY INTERVAL BOUNDARIES FOR THE UNSHIFTED MESH
      DELA=0.5*DEL
      RK=(FRU-FRL)/DEL+0.1
      KR=RK
      FRB(1)=FRL
      DO 201 K=1,KR
      FRB(K+1)=FRB(K)+DEL
      FRC(K)=FRB(K)+DELA
C    CALCULATES PLANCK FUNCTION FOR EACH FREQUENCY INTERVAL
      RNUM=1.1925*DEL*FRC(K)*FRC(K)*FRC(K)*1.E-05
      EEX=1.4388*FRC(K)
  201 PCK(K)=RNUM/(EXP(EEX/TEMC)-1.)
      WRITE(3,222) PREC,TEMC
  222 FORMAT(////10X,16HTHE PRESSURE IS ,F10.4,4H ATM,
```

```
     *10X,19HTHE TEMPERATURE IS ,F10.2,2H K)
      IR=0
C   STARTS THE COMPUTATION FOR THE UNSHIFTED MESH
      GO TO 121
  122 KR=KR-1
      FRB(1)=FRL+DELA
C   DEFINES THE FREQUENCIES AT THE INTERVAL BOUNDARIES AND CENTERS
  121 DO 100 K=1,KR
      FRB(K+1)=FRB(K)+DEL
  100 FRC(K)=FRB(K)+DELA
C   DETERMINES THE NUMBER OF LINES IN EACH FREQUENCY INTERVAL
      X=0
      DO 102 K=1,KR
      M=0
  104 IF(X.GE.LE) GO TO 103
      X=X+1
      IF(FR(X).LT.FRB(K)) GO TO 104
      IF(FR(X).GE.FRB(K+1)) GO TO 105
      M=M+1
      GO TO 104
  105 IF(K.GE.KR) GO TO 103
      X=X-1
  103 MP(K)=M
  102 CONTINUE
C   ASSIGNS NUMBERS TO THE FIRST AND LAST LINE OF EACH INTERVAL
      X=0
      DO 106 K=1,KR
      IF(MP(K).EQ.0) GO TO 106
      LIB(K)=X+1
      LIE(K)=LIB(K)+MP(K)-1
      X=LIE(K)
  106 CONTINUE
C   FIND OUT THE HIGHEST INTENSITY IN THE INTERVAL,GENERATES THE
C    INTENSITY DECADES,DISTRIBUTES LINES INTO INTENSITY DECADES,
C     DETERMINES THE NUMBER OF LINES IN EACH DECADE AND THEN COMPUTES
C      AVERAGE INTENSITY FOR EACH DECADE
      DO 107 K=1,KR
      IF(MP(K).EQ.0) GO TO 440
      JB=LIB(K)
      JE=LIE(K)
      BIGI(K)=SI(JB)
      JC=JB+1
      DO 108 J=JC,JE
      IF(BIGI(K).GE.SI(J)) GO TO 108
      BIGI(K)=SI(J)
  108 CONTINUE
      DO 109 I=1,6
      IX=-I+1
  109 BIG(I,K)=BIGI(K)*10.**IX
      DO 110 I=1,5
      N=0
      SSI(I,K)=0.
      DO 111 J=JB,JE
      IF(SI(J).GT.BIG(I,K)) GO TO 111
      IF(SI(J).LE.BIG(I+1,K)) GO TO 111
```

```
      N=N+1
      SSI(I,K)=SSI(I,K)+SI(J)
  111 CONTINUE
      NSI(I,K)=N
      IF(NSI(I,K).GE.1) GO TO 110
      NSI(I,K)=1
  110 AVSI(I,K)=SSI(I,K)/FLOAT(NSI(I,K))
      GO TO 107
  440 DO 441 I=1,5
      NSI(I,K)=1
  441 AVSI(I,K)=0.
  107 CONTINUE
      PI=3.14159
      RHO=ALA/DELA
C   STARTS THE COMPUTATION OF TRANSMITTANCES FOR EACH INTERVAL
      DO 301 IPL=1,9
      PL=PL1(IPL)
      DO 112 K=1,KR
      TRG(K)=1.
      DO 113 J=1,KR
      TRD=1.
      JA=IABS(J-K)
      IF(JA.GT.JD) GO TO 113
      ZI=FRC(K)-FRC(J)
      EPSI=ZI/DELA
      DO 115 I=1,5
      NSJ=NSI(I,J)
      PNUM=RHO*RHO*AVSI(I,J)*PL/(PI*ALA)
      RES=0.
      IF(J.NE.K) GO TO 116
C   EVALUATES THE INTEGRAL FOR DIRECT CONTRIBUTION
      DO 117 W=1,26
      YY=PNUM/(X1(W)*X1(W)+RHO*RHO)
      IF(YY.GT.90.) GO TO 119
      Y=EXP(-YY)
      GO TO 117
  119 Y=0.
  117 RES=RES+Y*T1(W)
      GO TO 244
C   EVALUATES THE INTEGRAL FOR WING CONTRIBUTION
  116 DO 118 W=1,21
      YY=PNUM/((EPSI-X2(W))*(EPSI-X2(W)))
      IF(YY.GT.90.) GO TO 120
      Y=EXP(-YY)
      GO TO 118
  120 Y=0.
  118 RES=RES+Y*T2(W)
      RES=RES/6.
  244 IF(RES.EQ.0.) GO TO 234
  255 TRD=TRD*RES**NSJ
      GO TO 115
  234 TRD=0.
  115 CONTINUE
  113 TRG(K)=TRG(K)*TRD
  112 CONTINUE
```

```
      IF(IR.GE.1) GO TO 123
      DO 114 K=1,KR
  114 TRA(IPL,2*K-1)=TRG(K)
      GO TO 301
  123 DO 124 K=1,KR
  124 TRA(IPL,2*K)=TRG(K)
  301 CONTINUE
      IR=IR+1
C     GOES TO 122 AND STARTS COMPUTATION FOR THE SHIFTED MESH
      IF(IR.LT.2) GO TO 122
C     AVERAGES RESULTS OVER SHIFTED AND UNSHIFTED MESHES
      DEN=5.668*(TEMC**4)*1.E-05
      DO 302 I=1,9
      DO 125 K=1,KR
  125 TRG(K)=(TRA(I,2*K-1)+TRA(I,2*K)+TRA(I,2*K+1))/3.
      WRITE(3,60) (TRG(K),K=1,KR)
   60 FORMAT(///(10F12.5/))
C     CALCULATES EMISSIVITY
      SUM=0.0
      DO 220 K=1,KR
      EM=1.-TRG(K)
  220 SUM=SUM+EM*PCK(K)
      BEMI=PI*SUM/DEN
      WRITE(3,221) BEMI,PL1(I)
  221 FORMAT(//10X,18HTHE EMISSIVITY IS ,E15.7,
     *       10X,18HTHE PATHLENGTH IS ,F10.2,7H ATM-CM)
  302 CONTINUE
      STOP
      END
```

APPENDIX C

COMPUTER PROGRAM TO CALCULATE NONHOMOGENEOUS BAND ABSORPTION AND BAND EMISSION

APPENDIX C

COMPUTER PROGRAM TO CALCULATE NONHOMOGENEOUS BAND ABSORPTION AND BAND EMISSION

```
C    MAIN PROGRAM TO CALCULATE NONHOMOGENEOUS TOTAL BAND ABSORPTANCE AND
C     BAND EMISSION
      DIMENSION PLCK(6,250),ABSO(6,250),BIN(6),BLP(6),BWP(6),HBIN(6),
     *         HBLP(6),HBWP(6),HIBIN(6),HIBLP(6),HIBWP(6),SUM(6),BC(6)
      T1(Y)=3.92*Y+1015.0
C     T2(Y)=-7.33*Y+1439.8
      DATA BC/140.0,500.0,1600.0,3760.0,5350.0,7250.0/
      A=0.0
      B=60.0
C     C=60.0
      XN1=120.0
C     XN2=60.0
      X1=(B-A)/XN1
C     X2=(C-B)/XN2
      PTOT=1.0
      PRE=0.786
      DO 50 I=1,6
      HBIN(I)=0.0
      HBLP(I)=0.0
   50 HBWP(I)=0.0
      PML=0.0
      M=1
  400 ARG=A+FLOAT(M)*X1-X1/2.
      IF(ARG.GT.B) GO TO 200
C     ARG=B+(FLOAT(M)-XN1)*X2-X2/2.
C     IF(ARG.GT.C) GO TO 200
C     DLTY=X2
C     TEMC=T2(ARG)
C     TEMC2=T2(ARG-X2/2.)
C     GO TO 300
  100 DLTY=X1
      TEMC=T1(ARG)
      TEMC2=T1(ARG-X1/2.)
C 300 PRE=PRESS(ARG)
  300 DENS=2193.115*PRE/TEMC
      CALL WATER(TEMC,BIN,BLP,BWP)
      PML=PML+DENS*DLTY
      BRO=6.6*SQRT(100.0/TEMC)+0.5
      PREC=PTOT+BRO*PRE
      DO 150 K=1,6
      HBIN(K)=HBIN(K)+BIN(K)*DENS*DLTY
      HBLP(K)=HBLP(K)+BLP(K)*PREC*BIN(K)*DENS*DLTY
      HBWP(K)=HBWP(K)+BWP(K)*BIN(K)*DENS*DLTY
      HIBIN(K)=HBIN(K)/PML
      HIBLP(K)=HBLP(K)/(PML*HIBIN(K))
      HIBWP(K)=HBWP(K)/(PML*HIBIN(K))
```

```
      ABSO(K,M)=EDWARD(PML,1.,HIBIN(K),HIBLP(K),HIBWP(K))
      PLCK(K,M)=PLANCK(TEMC2,BC(K))
  150 CONTINUE
      WRITE(3,10) (ABSO(I,M),I=1,6)
   10 FORMAT(/6F15.7)
      M=M+1
      GO TO 400
  200 DO 250 J=1,6
      HBIN(J)=HBIN(J)/PML
      HBLP(J)=HBLP(J)/(PML*HBIN(J))
      HBWP(J)=HBWP(J)/(PML*HBIN(J))
      ABSORP=EDWARD(PML,1.,HBIN(J),HBLP(J),HBWP(J))
      WRITE(3,20) PML,HBIN(J),HBLP(J),HBWP(J),ABSORP
   20 FORMAT(//,5F16.7)
  250 CONTINUE
      DO 500 N=1,6
  500 SUM(N)=0.0
      DO 600 L=1,M-2
      DO 700 I=1,6
  700 SUM(I)=SUM(I)+(ABSO(I,L+1)-ABSO(I,L))*PLCK(I,L+1)
      WRITE(3,30) (SUM(I),I=1,6)
   30 FORMAT(/6E15.7)
  600 CONTINUE
      STOP
      END
```

```
      SUBROUTINE WATER(TEMC,BIN,BLP,BWP)
      DIMENSION BETA(8),RTH(8),OMG(8),BIN(8),BLP(8),BWP(8),U(3),
     *          SUMI(3),HEX(3),EXM(3),F(6)
C     BAND ABSORPTION PARAMETERS
      DATA RTH/44205.0,5200.0,41.2,0.19,3.0,2.5,2.3,22.4/
      DATA BETA/0.14311,0.14311,0.09427,0.13219,0.08169,0.11628,
     *          0.13219,0.13219/
      DATA OMG/69.3,28.4,56.4,60.0,43.1,32.0,60.0,60.0/
C     CALCULATE TEMPERATURE DEPENDENT,FUNCTION FOR LINE WIDTH PARAMETER
      U(1)=5254.5/TEMC
      U(2)=2294.9/TEMC
      U(3)=5404.1/TEMC
      DO 100 I=1,3
      SUM=0.0
      V=0.0
    1 ADD=SQRT(V+1.)*EXP(-U(I)*V/2.)
      IF(ADD.LT.1.E-04) GO TO 2
      SUM=SUM+ADD
      V=V+1.
      GO TO 1
    2 SUMI(I)=SUM*SUM
  100 CONTINUE
      SUM=0.0
      V=0.0
    3 ADD=SQRT(V+1.)*SQRT(V+2.)*EXP(-U(2)*V/2.)
      IF(ADD.LT.1.E-04) GO TO 4
      SUM=SUM+ADD
      V=V+1.
      GO TO 3
    4 SUMII=SUM*SUM
      DO 200 I=1,3
      EXM(I)=1.-EXP(-U(I))
  200 HEX(I)=(1.-EXP(-U(I)/2.))*(1.-EXP(-U(I)/2.))
C
      F(1)=EXM(1)*EXM(2)*EXM(2)*EXM(3)*SUMI(2)/(HEX(1)*HEX(3))
      F(2)=EXM(1)*(EXM(2)**3)*EXM(3)*SUMII/(2.*HEX(1)*HEX(3))
      F(3)=EXM(1)*EXM(2)*EXM(2)*EXM(3)*EXM(3)*SUMI(2)*SUMI(3)/HEX(1)
      F(4)=EXM(1)*EXM(1)*EXM(2)*EXM(3)*EXM(3)*SUMI(1)*SUMI(3)/HEX(2)
      F(5)=EXM(1)*EXM(1)*EXM(2)*EXM(3)*SUMI(1)/(HEX(2)*HEX(3))
      F(6)=EXM(1)*EXM(2)*EXM(3)*EXM(3)*SUMI(3)/(HEX(1)*HEX(2))
C
      TEM=SQRT(TEMC/100.0)
C     CALCULATE BAND PARAMETER
      BIN(1)=RTH(1)*EXP(-9.0/TEM)
      BWP(1)=OMG(1)*TEM
      BLP(1)=BETA(1)/TEM
      BIN(2)=RTH(2)*EXP(-17.6/TEM)
      BWP(2)=OMG(2)*TEM
      BLP(2)=BETA(2)/TEM
C
      RTH(4)=0.19*(1.-EXP(-2.*U(2)))/(EXM(2)*EXM(2))
      RTH(5)=3.0*(1.-EXP(-(U(2)+U(3))))/(EXM(2)*EXM(3))
      RTH(6)=2.5*(1.-EXP(-(U(1)+U(3))))/(EXM(1)*EXM(3))
      DO 300 I=1,6
      BIN(I+2)=RTH(I+2)
```

```
      BWP(I+2)=OMG(I+2)*TEM
300   BLP(I+2)=BETA(I+2)*F(I)/TEM
      BIN(4)=BIN(4)+BIN(7)+BIN(8)
      XNUM=SQRT(RTH(4)*BLP(4))+SQRT(RTH(7)*BLP(7))+SQRT(RTH(8)*BLP(8))
      BLP(4)=XNUM*XNUM/BIN(4)
      RETURN
      END
```

```
      SUBROUTINE CARBON(TEMC,BIN,BLP,BWP)
      DIMENSION BETA(6),RTH(6),OMG(6),BIN(6),BLP(6),BWP(6),U(3),SUMI(3),
     *          SUMII(2),EXM(3),HEX(3),F(6),G(6),H(6)
      DATA RTH/19.0,2.47E-09,2.48E-09,110.0,4.0,0.66/
      DATA BETA/0.06157,0.04017,0.11888,0.24723,0.13341,0.39305/
      DATA OMG/12.7,13.4,10.1,11.2,23.5,34.5/
      U(1)=1943.82/TEMC
      U(2)=959.68/TEMC
      U(3)=3447.365/TEMC
      DO 100 I=1,3
      SUM=0.0
      V=0.0
    1 ADD=SQRT(V+1.)*EXP(-U(I)*V/2.)
      IF(ADD.LE.1.E-04) GO TO 2
      SUM=SUM+ADD
      V=V+1.
      GO TO 1
    2 SUMI(I)=SUM*SUM
  100 CONTINUE
      DO 200 I=1,2
      SUM=0.0
      V=0.0
    3 ADD=SQRT(V+1.)*SQRT(V+2.)*EXP(-U(I)*V/2.)
      IF(ADD.LE.1.E-04) GO TO 4
      SUM=SUM+ADD
      V=V+1.
      GO TO 3
    4 SUMII(I)=SUM*SUM
  200 CONTINUE
      SUI=0.0
      V=1.0
    5 ADD=SQRT(V+1.)*EXP(-U(1)*V/2.)
      IF(ADD.LE.1.E-04) GO TO 6
      SUI=SUI+ADD
      V=V+1.
      GO TO 5
    6 SUI=SUI*SUI
      DO 300 I=1,3
      EXM(I)=1.-EXP(-U(I))
  300 HEX(I)=(1.-EXP(-U(I)/2.))*(1.-EXP(-U(I)/2.))
      DENF=1./(EXM(1)*EXM(1))-1.
C
      F(1)=EXM(2)*EXM(2)*EXM(1)*EXM(2)*EXM(3)*SUMII(2)/(2.*HEX(1)*HEX(3)
     *)
      F(2)=EXM(2)*EXM(2)*EXM(3)*EXM(3)*EXM(3)*SUI*SUMI(2)*SUMI(3)/DENF
      F(3)=F(2)
      F(4)=EXM(1)*EXM(2)*EXM(2)*EXM(3)*EXM(3)*SUMI(2)*SUMI(3)/HEX(1)
      F(5)=EXM(1)*EXM(1)*EXM(2)*EXM(2)*EXM(3)*EXM(3)*SUMI(1)*SUMI(2)*SUM
     *I(3)
      F(6)=EXM(1)*EXM(1)*EXM(1)*EXM(2)*EXM(2)*EXM(3)*EXM(3)*SUMII(1)*SUM
     *I(2)*SUMI(3)/2.
C
      G(1)=1.0
      G(2)=1.383*(1.-EXP(U(1)-U(3)))*(2.-EXP(-U(1)))*EXP(-U(1))/(EXM(1)*
     *EXM(3))*1.E08
```

```
      G(3)=1.383*(1.-EXP(2.*U(2)-U(3)))*(2.-EXP(-U(1)))*EXP(-U(1))/(EXM(
     *1)*EXM(3))*1.E03
      G(4)=1.0
      G(5)=(1.-EXP(-U(1)-U(3)))/(EXM(1)*EXM(3))
      G(6)=(1.-EXP(-2.*U(1)-U(3)))/(EXM(1)*EXM(1)*EXM(3))
C
      H(1)=1.0291
      H(2)=1.0273
      H(3)=1.0273
      H(4)=1.0237
      H(5)=1.0238
      H(6)=1.0237
C
      TEM=SQRT(TEMC/100.0)
      DO 400 M=1,6
      BIN(M)=RTH(M)*G(M)
      bip(m)=beta(m)*f(m)/(tem*h(m))
  400 BWP(M)=OMG(M)*TEM
      RETURN
      END
```